Appendix G. Budd Inlet Recalibration Report

Appendix G.1. Budd Inlet Model Re-calibration

Introduction

The original Budd Inlet model was developed for Lacey, Olympia, Tumwater and Thurston County (LOTT) Partnership to support National Pollutant Discharge Elimination System (NPDES) permitting activities (Aura Nova Consultants et al., 1998). That work – generally referred to as the "LOTT model" and the "Budd Inlet Scientific Study" (BISS) – used the 3-D hydrodynamic and water quality model GLLVHT (Generalized, Longitudinal-Lateral-Vertical Hydrodynamics and Transport model), and calibrated to data collected between 1996 and 1998 during the BISS. Follow-up modeling work was conducted by Aura Nova and J.E. Edinger Associates, Inc. (JEEAI) in 1999 and 2000 (Aura Nova Consultants et al., 1999; JEEAI, 2000).

From 2003 through 2007, Ecology contracted with ERM Group, Inc. (ERM) to update the LOTT model to the latest version of the modeling framework (GEMSS; Generalized Environmental Modeling System for Surfacewaters) and to verify the goodness-of-fit of the calibration. Those tasks were documented in JEEAI (2005) and Kolluru (2006a), respectively. In 2006, ERM provided the latest calibrated model of Budd Inlet to Ecology, along with a comparison to previous model outputs (Kolluru, 2006b). ERM then extended the model domain south to encompass Capitol Lake; the resulting combined Budd Inlet/Capitol Lake (BI/CL) model was calibrated and submitted to Ecology in January 2008 (Prakash and Kolluru, 2008).

In the course of review of the BI/CL model the source code for the water quality modules were found to contain errors (Appendix K). After these issues were corrected by ERM, the calibration parameters were re-evaluated by Ecology to determine if calibration to the 1996-97 data was still acceptable. Because some differences were noted, Ecology re-calibrated the model. This appendix documents those re-evaluation and re-calibration efforts for the Budd Inlet regions of the model.

Data Quality Assurance (QA)

The source for Budd Inlet boundary condition and calibration data was the BISS conducted in 1996-97 (Aura Nova Consultants et al., 1998). Extensive review of all field data was performed to assess and assure the quality of the model inputs and calibration targets. Data QA generally involved the following:

- Compared original BISS data with field databases used for model calibration to confirm agreement.
- Ensured use of consistent units, reference time (Pacific Standard Time, PST), vertical datum (Mean Lower Low Water, MLLW), geographic coordinate system (NAD83, UTM Zone 10), and station identification.

- Verified derived values and intermediate calculations.
- Verified documented methods used to fill data gaps.

Water Quality Data

Water quality parameters monitored in 1996-97 for the BISS included dissolved oxygen (DO), chlorophyll *a*, ammonia, nitrate, nitrite, phosphate, filtered total nitrogen (FTN) and phosphorus (FTP), unfiltered total nitrogen (UTN) and phosphorus (UTP), dissolved organic nitrogen (DON) and phosphorus (DOP), total and dissolved forms of carbon, and 5-day biochemical oxygen demand (BOD_5). Data collection involved regular discrete and profile sampling throughout Budd Inlet.

Previous modeling efforts calibrated to a small subset of the BISS water quality data, utilizing data from only 7 of the 29 stations. Comparison of the field databases used for modeling and the original BISS data set further revealed that the calibration data were only a small fraction of the total data collected at those sites. Other issues included:

- Bottom layer (KB) data for DO, ammonia, and nitrate in the field databases consisted of measurements from variable depths; often the deepest measurement for a given day had been artificially assigned a near-bottom depth regardless of whether it was in fact from layer KB.
- The meaning of "nitrate" was not consistent in the field databases; at some stations "nitrate" values reflected nitrate (NO_3) measurements, but at other stations they represented nitrate *plus* nitrite ($NO_3 + NO_2$).
- The conditional formula used for calculating the average of a sample and its duplicate yielded incorrect results in some cases.
- Derived variables were often calculated incorrectly; as a rule calculations were to use the average of a sample and its duplicate when available, but often formulas were found to ignore the duplicate and simply used the sample value.
- Several profiles were absent from the field databases, while others contained incorrect date, time, and depth information.
- Field databases included 26 records of phytoplankton chlorophyll for which no source data could be found.

In light of these problems, the water quality field databases used for previous calibrations were abandoned, and a new field database was developed from the original BISS data. For the present re-calibration, water quality data from all of the BISS stations were used for goodness-of-fit statistics and 12 of the 29 stations were selected for plotting time series and profiles of predicted and observed data (see "Diagnostic Stations" section for locations). The new field database included as much available data as possible from the selected stations, omitting data only when justified (e.g., values clearly outside the plausible range, obvious problems with coincident measurements of other analytes, apparent problems with sensors, etc.). Problems discovered during data QA were corrected, and the following universal changes were made:

- Assigned non-detects the value of half the reporting limit (RL).
- Enforced a lower bound of zero for calculated values involving subtraction of variables.
- Used nitrate *plus* nitrite ($NO_3 + NO_2$) for model "nitrate" inputs and calibration data.

- Used *estimated* 5-day BOD results (BODEst) for model BOD inputs and calibration data. These data gave estimated values for measurements below the RL, whereas previous modeling used *reported* 5-day BOD values (BODRep) for which non-detects had been given at the RL.
- Converted all BOD_5 results to ultimate BOD (BOD_u) using the following relationship and assuming a decay rate *k* of 0.23/day (Chapra, 1997):

$$BOD_u/BOD_5 = 1 / (1 - e^{-5k})$$
$$BOD_u = BOD_5 \times 1.4634.$$

- Excluded 26 chlorophyll records for which no source data could be found.

Overall, these QA actions yielded an expanded set of water quality data for model re-calibration that better captured the variability of actual conditions and improved spatial coverage (both horizontally throughout Budd Inlet and vertically throughout the water column).

Hydrodynamic Data

Hydrodynamic and other physical measurements from 1996-97 included temperature, salinity, tides, currents, and flow rates from tributaries and wastewater treatment plants. Comparison of the original BISS data with field databases and model inputs used for previous calibration efforts found extensive problems (e.g., discrepancies, omissions, data smoothing errors) that warranted re-creation of these files.

Temperature and salinity profile data from 7 of the 29 BISS stations were used in previous calibration efforts. However, several profiles were found to have been omitted, and others were found to have flaws in date/time and depth records. Those errors and omissions were corrected for the present re-calibration, and profiles from five additional stations were added to provide improved spatial coverage to the re-calibration data set.

Records of current velocity and direction were available from six Anderaa current meters which had been moored intermittently at three sites in 1996-97. Previously a 9-point moving average was applied to 15-minute interval measurements of the X and Y velocity components of the current, and then velocity and direction were resolved from the smoothed X and Y components. The intent of that data smoothing technique was to average the values within 1-hour (+/-) of each record, but there was a failure to account for data gaps, across which averages were calculated as if the data set were continuous. For the re-calibration, a 1-hour (+/-) moving average was re-applied to the raw Anderaa data, with care taken to account for temporal gaps in the data.

Acoustic Doppler Current Profilers (ADCPs) were deployed at four locations in Budd Inlet in 1996-97, providing 2-minute averages of current speed and direction every 15 minutes in 1-meter depth intervals. As with the Anderaa data, a 9-point (1-hour +/-) moving average had been applied to the ADCP data for earlier calibration work. Similar errors were found in the smoothed ADCP data at temporal discontinuities, and the moving average was re-applied to the original raw data to fix these problems. Data from a depth of five meters below MLLW (model layer 11) at all four stations was used for re-calibration of the hydrodynamic model.

Continuous records of temperature and salinity were collected in 1996-97 by moored "in-situ" CTDs at two locations in Budd Inlet. The "in-situ" CTD field databases used for previous modeling was found to have widespread errors, mostly involving data mis-alignment in which segments of the time series had been shifted backwards or forwards in time (hours to days). Those databases were discarded and a new field database was created from the original records.

A tide gauge mounted at the Port of Olympia recorded sea level height during several months of 1996-97. The vertical datum of the measurements was verified, and a field database was constructed from the original data.

Modeling Framework

An overview of the modeling framework for the re-calibration is presented below. Various elements were influenced by updates to the GEMSS application, changes to the model source code, and corrections to the field data used for model inputs.

Grid and Layering of the Model Domain

During the BISS, two computational grids were developed for Budd Inlet using bathymetry data from the National Ocean Survey (NOS) digital elevation database and dredged channel depth data from a recent survey by Seattle District Corps of Engineers. The first grid, developed for hydrodynamic simulations, had 326 surface grid cells and a total of 4409 computational grid cells. The water quality grid had much lower resolution, with 168 surface grid cells and a total of 2219 computational grid cells. The two grids are shown side-by-side for comparison in Figure G-1. For previous calibrations, net transport was compared with the hydrodynamic grid at three locations; however, rigorous hydrodynamic calibration/verification was not conducted for the water quality grid.

In 2001, ERM converted the water quality grid to GEMSS format using a grid conversion utility (JEEAI, 2005). The grid points were slightly adjusted to make the grid orthogonal and conforming to the shoreline. The volume of the ERM water quality grid was compared with the volume estimated from the NOS digital elevation map for Budd Inlet below a horizontal plane of 6m MLLW. The ERM water quality grid used in the LOTT model and in Ecology's 2008 draft report was found to have a total volume that was 38% greater than the NOS-based volume. For the present report Ecology re-layered ERM's grid by re-scanning NOS bathymetry and dredged depths in Budd Inlet using the new Gridgen utility within GEMSS. The new grid used for the present re-calibration work had a total volume that is within 2% of the NOS-based volume. This grid was used for both hydrodynamic and water quality calibration (Figure G-2). The new grid had 19 layers below a horizontal datum of 6m MLLW. The top 10 layers each had a thickness of 1m, while the rest of the layers were 2m or 3m thick.

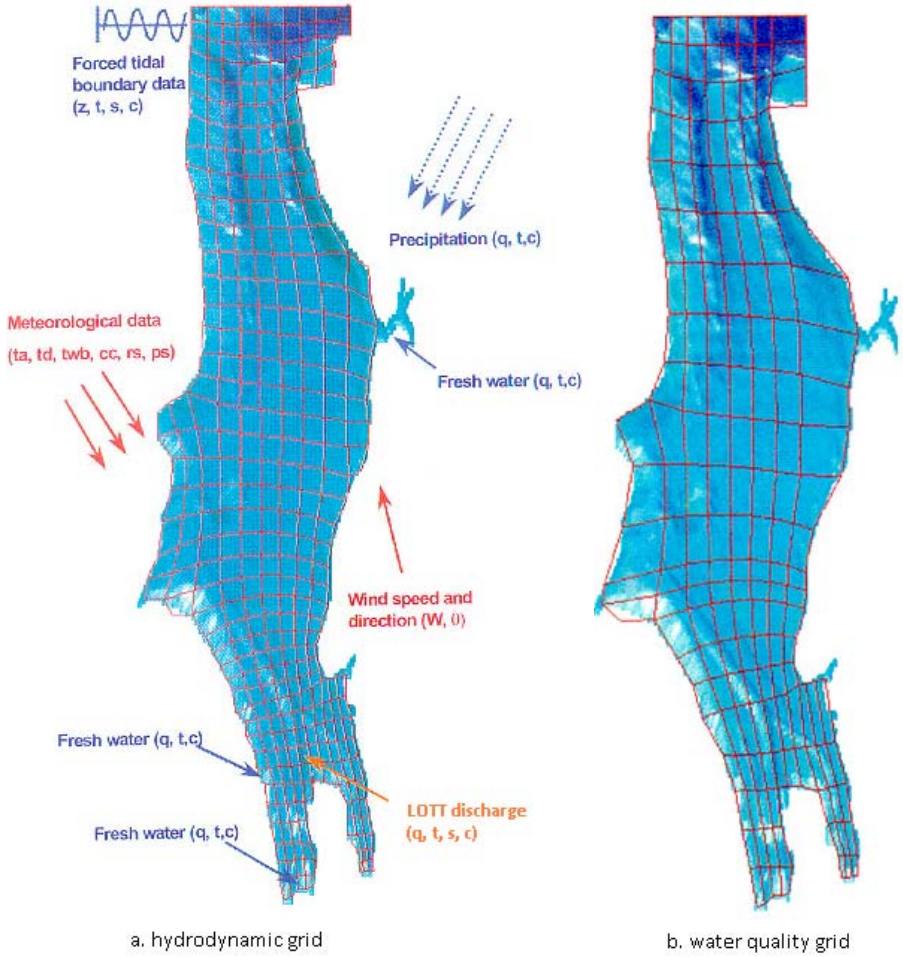

Figure G-1. Hydrodynamic (left) and water quality (right) computational grids in the Budd Inlet Scientific Study (Aura Nova Consultants et al., 1998).

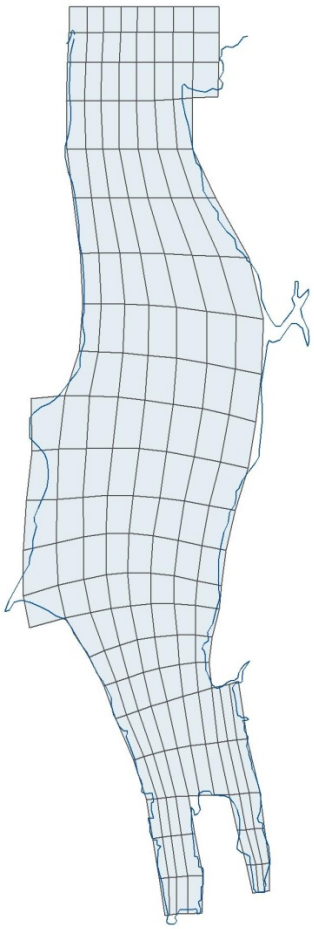

Figure G-2. Grid used for re-calibration of the Budd Inlet model (water quality and hydrodynamics).

Meteorology and Precipitation

Weather and wind records from the Olympia Airport station were downloaded from the University of Washington for the model simulation period (www-k12.atmos.washington.edu/k12/grayskies/nw_weather.html). Units were converted as appropriate for GEMSS meteorological data input.

A recent update to GEMSS placed input specifications for meteorological data in the boundary conditions section of the control file, allowing models to regionalize meteorological data (however, no regionalization was used for Budd Inlet modeling). Cloud-adjusted solar radiation was input directly via the meteorology file, and the control file was set to specify that cloud correction should not be performed internally in the model. Values of cloud-adjusted solar radiation in the meteorology file were calculated from records of clear-sky solar radiation (rs) and cloud cover (cc) using the Ryan-Stolzenbach equation (Ryan and Stolzenbach, 1972) and a cloud correction factor equal to 1 – 0.65 cc^2 (Brown and Barnwell, 1987).

No precipitation temperature records were available for the simulation period, and so values were estimated from the Olympia Airport meteorological records, with the precipitation temperature calculated as the average of the air and dew point temperatures (negative calculated

values were set to zero). Precipitation dissolved oxygen was calculated as the saturation DO at the estimated precipitation temperature. Aerial deposition of nutrients in rainfall was described in terms of concentration using values from the BISS.

Phytoplankton

Sampling in 1996-97 for the BISS found algal biomass maxima in early May and from mid-July through September, with a period of reduced abundance in late May through early July (Aura Nova Consultants et al., 1998). Phytoplankton species composition was also observed to vary seasonally, with diatoms, dinoflagellates, and "other" phytoplankton dominating at different times of the year. Spatial heterogeneity was apparent between the inner and central/outer areas of Budd Inlet, but these variations were less strong and less consistent.

To simulate the dynamics of the three major phytoplankton groups in Budd Inlet, three model algal groups were used in two GEMSS modules:

- **WQCBM module:** The DFP phytoplankton variable was used to represent dinoflagellates, a motile group capable of vertical movement in the water column in response to changing light. The DAP phytoplankton variable was not used in the present application; instead, Ecology chose to represent other phytoplankton groups using the GEMSS General Algae (GAM) module, which contained a more sophisticated temperature limitation function. Kinetic rate parameters for DFP were specified in the WQCBM module. The WQCBM module was also used to simulate the concentrations and transformations of dissolved oxygen, ammonia, nitrate, dissolved and particulate organic N, dissolved and particulate organic P, and dissolved organic C (CBOD), as well as the influence of phytoplankton variables in the WQCBM (DFP) and GAM modules.
- **GAM module:** Two phytoplankton groups in the GAM module were used (GAM1 and GAM2) to represent phytoplankton. GAM1 was used to represent early growing season phytoplankton and GAM2 represented late growing season phytoplankton. The GAM1 kinetics were expected to be influenced by diatoms. The GAM2 kinetics were expected to be influenced more by dinoflagellates and other species. Kinetic rate parameters for GAM1 and GAM2 were specified in the GAM module.

The model algal groups were given unique ratios of carbon to chlorophyll *a*, light/temperature/ nutrient limitation parameters, and other various kinetic rates. The ratio of nitrogen to carbon for all phytoplankton groups was assumed to be constant as specified in the WQCBM module. Light and temperature limitation parameters facilitated calibration to seasonal variations in both the total algal biomass and species composition. For example, defining low and high temperature optima for GAM1 and GAM2, respectively, corresponded to simulation of early and late biomass peaks. Other kinetic parameters such as the maximum growth rates, respiration rates, death rates, settling velocities, and carbon-to-chlorophyll ratios were used to optimize the model skill for the prediction of the magnitude of the biomass and the influence of phytoplankton on the nutrient concentration variables.

Further, all three algal groups were regionalized to improve simulation of differences between inner and central/outer Budd Inlet (Figure G-3A). When varying regional kinetics of any of the three groups, all parameters "inherent" to a group (such as carbon-to-chlorophyll ratio, optimum

temperature, saturating light constant, etc.) were held constant between regions. Other kinetics such as growth and death rates were regionally varied to achieve the strongest calibration to the observed data.

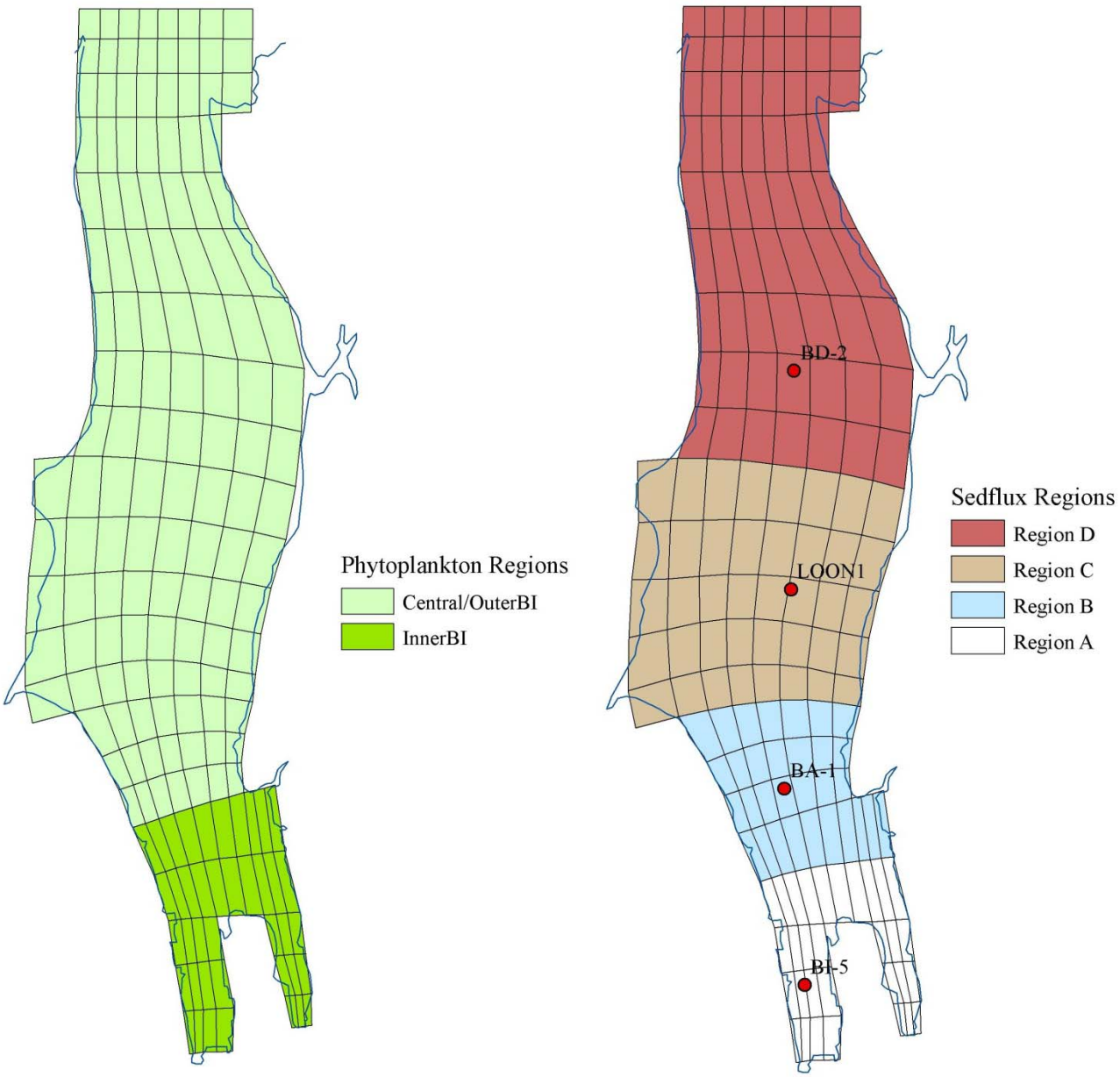

Figure G-3. **A** (left): Phytoplankton regions used in the model. **B** (right): Stations where sediment fluxes were measured (dots) and sediment regions used in the model.

Boundary Conditions (BC)

Sediment Flux

Sampling conducted at four sites in Budd Inlet in 1996-97 yielded estimates for sediment fluxes of DO, ammonia, nitrate, and phosphate. Sampling locations were distributed along an approximately north-south line over the length of the inlet with the intent of characterizing fluxes within segments of the inlet. Model sediment flux regions were defined in relation to the original BISS sampling locations, as shown in Figure G-3B.

Previous modeling efforts found that the BISS measurements greatly underestimated the sediment oxygen demand (SOD) required to calibrate the water quality model. To compensate, multipliers were applied regionally (based on bathymetry) to scale up the time-varying SOD values. The magnitude of those multipliers was large in the original LOTT model – generally between 2 and 3 times the observed SOD – and suggested that temporal differences may not be as important as relative regional differences. For the present work, constant regional SOD values were assumed throughout the model simulation period. Those constants were varied to re-calibrate the model, but relative regional differences of the observed data were preserved (e.g., D<A<B~=C). Final SOD rates are presented in Table G-5 of the "Final Kinetic Rates and Constants" section of this appendix. The observed sediment fluxes of nutrients were used without adjustment.

Discharge

The discharge boundary conditions described loads contributed by the major freshwater flows to Budd Inlet, including nine tributaries, Capitol Lake, and five wastewater treatment plants. The source of this data was BISS sampling conducted in 1996-97 at a frequency of approximately 2-3 weeks. The model control file was set to linear interpolate (in time) between input values for both hydrodynamics and water quality.

Data QA was performed on the water quality input files (GEMSS file format .wdg) used for previous calibration work. As detailed earlier in this appendix, source data and derived variables were checked, methods for filling data gaps were verified, non-detects were assigned at half the reporting limit, and so on. Other notable changes that affected all discharges included:

- *Estimated* BOD results (BODEst) were substituted for *reported* BOD (BODRep) data. The 5-day BODEst values were converted to ultimate BOD (as presented earlier) prior to being entered in the discharge BC input files.
- Ultimate BODEst values were specified as input values for CBOD_F ("fast-reacting"), and CBOD_S ("slow-reacting") was set to zero.
- Particulate organic carbon inputs were apportioned equally between slow, fast, and refractory pools by assigning scalars of 0.3333, 0.3334, and 0.3333, respectively.

The discharges of Moxlie, Mission, Ellis, and Little Tykle Creeks were set to enter Budd Inlet in more than one grid cell, effectively mapping the channel followed by those tributaries during

wetting and drying of tidally varying conditions. During the model simulation, the first wet cell (of those specified cells) encountered at a given time was the discharge location for the tributary.

Flow data for North Creek Gull Harbor ("GullNE") was available for the entire simulation period, but only a single month of water quality data was collected by the BISS. The full water quality data set from South Creek Gull Harbor ("GullSE") was substituted in place of the limited GullNE data set, and was used in conjunction with GullNE hydrodynamics.

Discharge from Capitol Lake was unlike other tributary sources in that flows were controlled by the lake's outlet dam. Dam operations were dynamic and the tide gates opened and closed in response to tides to maintain the lake at a desired level (the "set point"). For periods with low tides when the dam gates were open, Capitol Lake discharged to Budd Inlet as if it were a major river; with the gates closed at high tides, no flow was discharged. In 1997 flows were not monitored at the dam, and so a numerical model was developed to estimate flows on a continuous basis (Aura Nova Consultants et al., 1998). Inputs to the model included Budd Inlet tides, Deschutes River and Percival Creek flows, dam set points, and temperature and salinity measurements from the lake and the inlet. The model time series (15-minute intervals) of estimated flows out of the dam were used for the hydrodynamic input file (.hdg) of the Capitol Lake discharge BC.

The water quality and hydrodynamic data for Capitol Lake included a drawdown event during which the lake level was lowered (via discharge to Budd Inlet's West Bay) over a four-day period, then re-filled with seawater from West Bay to eradicate the non-native macrophyte Eurasian watermilfoil (*Myriophyllum spicatum*). The dam gates remained closed for five days while the lake was refilled by the Deschutes River to its usual level, at which time operation resumed. The input files had 15-minute records of temperature, salinity, DO, and flow from the beginning of the drawdown on 7/22/97 through 8/7/97.

Due to sampling errors during the BISS, measurements of BOD at the following wastewater treatment plants were not usable: Beverly Beach, Boston Harbor, Seashore, and Tamoshan. For those sampling dates, values of BOD_5 reported by the treatment plants were obtained. Non-detect results were assigned half the reporting limit, and all measurements were converted to ultimate BOD as described earlier.

Discharge BC input files for LOTT contained bi-weekly measurements from the BISS and daily measurements reported by the treatment plant. Apart from the aforementioned changes applied to all discharge data, LOTT input data files used for previous modeling were not altered.

Head Boundary

The head boundary defined time-varying inputs at the northern boundary of the model domain where Budd Inlet is open to southern Puget Sound. Available water quality data from the BISS included discrete and profile samples at four locations across the boundary: stations BF-4, BF-3, BF-2, and BF-1 (from west to east). In the model domain the width of the head boundary was eight grid cells; the data from each station was assigned to two grid cells (i.e., the station grid cell and the adjacent cell) to provide inputs across the entire boundary.

Water quality data at each station were binned to the model layers (i.e., for a given variable, the average of the measurements within a layer was specified at the layer mid-depth), and layers for which no data existed were assigned values using nearest-neighbor interpolation. In this way, all layers (from surface KT to bottom KB) at each of the four stations contained input values for water quality parameters.

To be consistent with the "Discharge" boundary conditions, particulate organic carbon inputs at each of the head boundary stations were apportioned equally between slow, fast, and refractory pools using scalars. Likewise, ultimate BODEst values were specified as input values for CBOD_F ("fast-reacting"), and CBOD_S ("slow") was set to zero. The conversion from 5-day to ultimate BOD, however, was accomplished using a scalar of 1.4634 in the time-varying data (TVD) file, as opposed to the method employed for the "Discharge" BC which used already-converted values in the TVD file and specified a scalar of 1.0. Since BOD data was only available from one western and one eastern station at the head boundary, those data were applied to the four western and eastern grid cells, respectively.

The source for temperature and salinity data was two "in-situ" CTDs moored at station 3C near the westernmost head boundary station BF-4. One CTD had been moored in the upper water column and one near the bottom, recording measurements every 15 minutes. Data QA was performed on the input files (.wdg) used for previous modeling work, and these files were found to be acceptable for use in the present re-calibration. However, previously the input files incorrectly specified the depth ranges of the upper and lower water column, resulting in data collected by the top CTD being attributed to the upper water column when the actual deployment depth of that CTD had been deeper than the upper zone (as defined). The depth of the division between upper and lower layers was therefore re-defined based on temperature profiles at the four head boundary stations and the deployment depths of the "in-situ" CTDs, extending the upper layer from the surface (KT) to -11m MLLW (model layer K13).

The same "in-situ" CTDs provided dissolved oxygen and chlorophyll data for the head boundary. For previous modeling work, the high-resolution (15-minute intervals) data had been smoothed to approximately twice daily measurements and data gaps had been filled. No changes were made to these existing chlorophyll and DO input files, but the upper and lower water columns were re-defined as surface layer (KT) to K13, and K14 to the bottom (KB), respectively. Scalars were applied to apportion the chlorophyll values between the three algal groups as follows: DFP scalar of 0.25, GAM1 scalar of 0.38, and GAM2 scalar of 0.37.

To incorporate tidal forcing at the head boundary, the time series of water surface elevation from Boston Harbor tide gauge measurements during the BISS were used as a hydrodynamic input file (.hdg) for the head boundary.

Re-evaluation of the Original Calibration

After the correction of model code errors, and in light of major changes to the modeling framework (grid and layering), to model inputs (meteorology and boundary conditions), and to the calibration data, it was not expected that the parameter values calibrated in the Budd Inlet Scientific Study would still be appropriate. For re-evaluation of that calibration parameter set, a

control file containing the previous BISS calibration parameters was built for the updated GEMSS model. Output from that model run clearly demonstrated that the BISS parameters no longer predicted the system water quality trends. For example, Figure G-4 shows that model predictions of DO in the surface and bottom layers at station BI-6 substantially overestimated the field observations in the second half of the simulation period. As such, the BISS calibration parameters were deemed invalid, and re-calibration was undertaken.

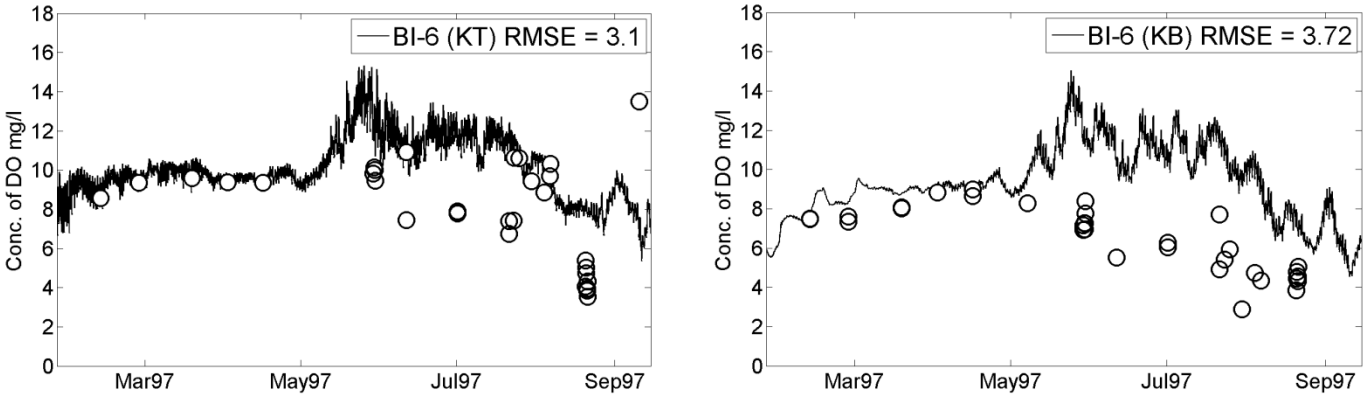

Figure G-4. Time series of DO predicted using the previous calibration parameters with the updated GLLVHT. Model-predicted values (solid line) are shown relative to the field data (circles); the left plot is the surface layer (KT) and the right plot shows the bottom layer (KB).

Water Quality Model Re-calibration

The water quality parameter of primary concern to Ecology and the focus of the re-calibration effort was dissolved oxygen. In particular, re-calibration of the Budd Inlet model sought to accurately predict the low DO conditions observed in the lower water column of the Inner Inlet.

The original calibration period was from 6/25 to 9/15/97, with model verification conducted for the period 1/25 to 9/15/97. For the present re-calibration, only the verification period was considered since it was inclusive of the calibration period.

The root mean square error (RMSE) statistic was used to describe the unbiased goodness-of-fit of the predicted to the observed values. The RMSE is defined as follows:

$$RMSE = \sqrt{\frac{1}{N}\sum (X_f - X_m)^2}$$

where X_f is the field-observed value, X_m is the model-predicted value, and N is the number of paired model and field data. The model bias was quantified using the mean standard deviation of the residuals (difference between predicted and observed values).

Parameter Estimation

The process of calibrating a water quality model involves selection of values for the many parameters that represent various kinetic processes. Calibration of the model for this project

involved running batches of typically about 100 model runs at a time with a matrix of critical parameter estimates varying around a base model run that had the best skill from the previous batch. The parameter estimates were constrained to be within the ranges of prior distributions of expected reasonable values. The results of each batch of runs were examined to compare the relative model skill with different combinations of parameter values. Information about which combinations of parameters improved the model skill was used to guide the selection of parameter values for the base model run of the next batch and for the development of new parameter combinations for sensitivity analysis in the batch. This process was repeated for 15 batches of runs in this project for a total of about 1500 model runs, and resulted in continuous improvement of the skill of the best model run from one batch to the next.

Earlier batches tended to focus on sensitivity of optimal parameters for the light and temperature limitation parameters to optimize the timing of phytoplankton blooms. Later batches focused on sensitivity to other parameters to optimize model skill for prediction of the magnitude of phytoplankton biomass and other water quality variables.

Two approaches were used to assess model skill for each batch during the parameter estimation process and to guide the selection of the base parameter set for the next batch of runs for sensitivity analysis:

- Graphical comparison of predicted and observed values using charts of time series and profiles of concentrations;
- Ranking of model runs based on a weighted average RMSE statistic that combined the skill for prediction of bottom DO, entire water column DO, DIN, and chlorophyll *a* to describe the overall goodness-of-fit.

In general, both of these approaches tended to reinforce each other and indicate that the same parameter sets had the best overall skill for predicting the observed data. Usually one of the model runs within the top 5% ranking of the overall goodness-of-fit statistics for a batch also appeared to visually be the best match at representing major features of the observed data in charts of time series and profiles (e.g., timing and magnitude of blooms and trends in nutrient and DO concentrations).

The entire process of parameter optimization – including the selected base parameter values in each batch and the matrix of parameter variations that were used for sensitivity analysis in each batch, as well as the corresponding charts of model output comparing predicted and observed conditions and goodness-of-fit statistics for all 1500 model runs – is documented in a Web-based model output browser (https://fortress.wa.gov/ecy/spsdos/bicl/index.html). The use of a Web-based model output browser facilitated rapid comparison of model skill for various combinations of parameter values. The final re-calibration parameter set was the model run with the overall best skill in the last batch of runs, and is presented at the end of this appendix.

Diagnostic Stations

The diagnostic stations where model-predicted time series and profiles were compared with observed water quality data included the same seven stations used for previous model calibration and verification, plus five additional stations to increase the rigor of the final re-calibration.

Table G-1 gives the model grid cell associated with each of the diagnostic stations. Several stations located near the border of cells were shifted to an adjacent model grid cell based on evaluation of observed versus predicted depths:

- BI-6 was located at the border of grid cells (3,1) and (4,1), where bottom elevations were -3m and -4m, respectively (relative to MLLW). Observed depths at BI-6 were usually deeper than model depth predictions at (3,1), but were comparable to model depth predictions at (4,1). Thus, BI-6 was shifted to cell (4,1).
- BI-5 was located at the border of grid cells (4,2) and (5,2). The bottom elevations of these cells were -3m and -11m MLLW, respectively. Model-predicted depths for the deeper cell better reflected the observed depths; as such, BI-5 was placed in (5,2).

Table G-1. Model grid cell coordinates (i, j) and number of layers (k) for the diagnostic stations used for water quality re-calibration.

Station	i	j	k
BF-3	6	21	16
BE-2	6	18	12
BD-2	6	15	13
BC-2	6	13	12
LOON1	7	11	11
BB-2	5	9	11
BA-2	5	6	12
BI-1	10	2	9
BI-2	10	4	10
BI-4	6	4	12
BI-5	5	2	12
BI-6	4	1	10

Water Quality Re-calibration Results: Time Series

Figures G-5 through G-10 show model-predicted time series of bottom layer DO, surface layer total chlorophyll, and surface layer DIN at each diagnostic station. The RMSE statistic presented on each plot indicates the goodness-of-fit of the predictions to the field data for the specified layer at that specific location. Time series comparisons from the bottom, middle, and surface layers at these locations are presented for all diagnostic variables in Appendix G.2.

The seasonal pattern of dissolved oxygen in the bottom layer involved a gradual increase of DO into May, peaking with the spring phytoplankton bloom and then decreasing through summer and into autumn. The re-calibrated model was able to reproduce the long-term temporal trends quite well throughout Budd Inlet (Figures G-5 and G-6), with reasonably low RMSE values at all stations (average RMSE of 1.2 mg/L), indicating good agreement between model predictions and field observations. The RMSE at some locations would have been significantly lower were it not for a few anomalous field measurements that clearly increased the RMSE statistic. For example, the bottom layer DO of 13.53 mg/L measured at BI-1 on 9/10/97 was higher than any other DO record from that station (from any depth) during 1996-97. Exclusion of this outlier value would

drop the RMSE from 2.4 mg/L to 1.45 mg/L for layer KB at BI-1. If real[1], those data appear to represent an abrupt event; while the model did not predict such extreme short-term variability, it nonetheless proved capable of capturing the long-term trends in bottom DO.

Surface layer DO was accurately predicted during the first half of the simulation period, but the model generally under-predicted surface DO during the late growing season (Appendix G.2). Late season surface DO measurements were typically very super-saturated and highly variable, in part due to the dinoflagellates which may have consumed DO in the bottom waters at night and produced DO near the surface during the day. Predicted surface DO during the late growing season was also typically super-saturated, but closer to DO saturation than the observed DO. Although the model had difficulty reproducing all of the variability of the field data, the predicted surface DO was within the range of the measured data (at the low end of the super-saturation range).

Time series plots of chlorophyll observations showed considerably more variation than DO time series (Figures G-7 and G-8 and Appendix G.2). Even so, the model was able to reproduce both the long-term patterns and short-term variability reasonably well. The model accurately predicted low early-season chlorophyll and the slight increase in concentrations observed in April preceding the major spring bloom at all stations and depths. The high chlorophyll spike associated with the spring bloom was simulated fairly well by the model, which predicted a rapid increase in the GAM1 group in response to favorable temperature, light, and nutrient conditions in May. Although the field data was too coarse (i.e., sampling frequency was insufficient) to precisely resolve the timing and magnitude of bloom, the model appeared to lag slightly behind the onset of the bloom at most locations. The latter half of the simulation period was characterized by a marked increase in short-term variability of chlorophyll; during that time the model simulated succession of the phytoplankton species, with GAM1 dominance giving way to the GAM2 and DFP groups. The motility of the DFP group, with daily migrations between the surface and bottom waters, helped to reproduce some of the variability seen in the field data, and overall the model did an adequate job of capturing the general late season chlorophyll trend.

The re-calibrated model was able to describe the seasonal variability of DIN concentrations (Figures G-9 and G-10 and Appendix G.2). The model reproduced the seasonal pattern of lower ammonia in the winter and spring followed by increasing concentrations coincident with and following the spring phytoplankton bloom. The ammonia field data showed substantial variability (possibly due to the low measured concentrations) which was not always reproduced by the model, especially in the bottom waters of several central Budd Inlet stations (e.g., BA-2, BB-2, and BD-2). Nonetheless, the model generally predicted within the range of the measured ammonia and captured the long-term trends. The time series of nitrate measurements for both the surface and bottom layers were simulated quite well by the model, matching the progressive decrease and then precipitous decline in the early spring, as well as the near-zero concentrations observed in August and September. In contrast to the ammonia under-predictions in KB at the central stations, model-predicted nitrate concentrations at those stations were in excellent agreement with measured values.

[1] DO and chlorophyll data from 9/10/97 were likewise problematic for previous modeling work (Aura Nova Consultants et al., 1999). Discrepancies between discrete and profile (CTD) measurements were large at some Inner Inlet stations on this date, and there remains uncertainty as to the quality of those data.

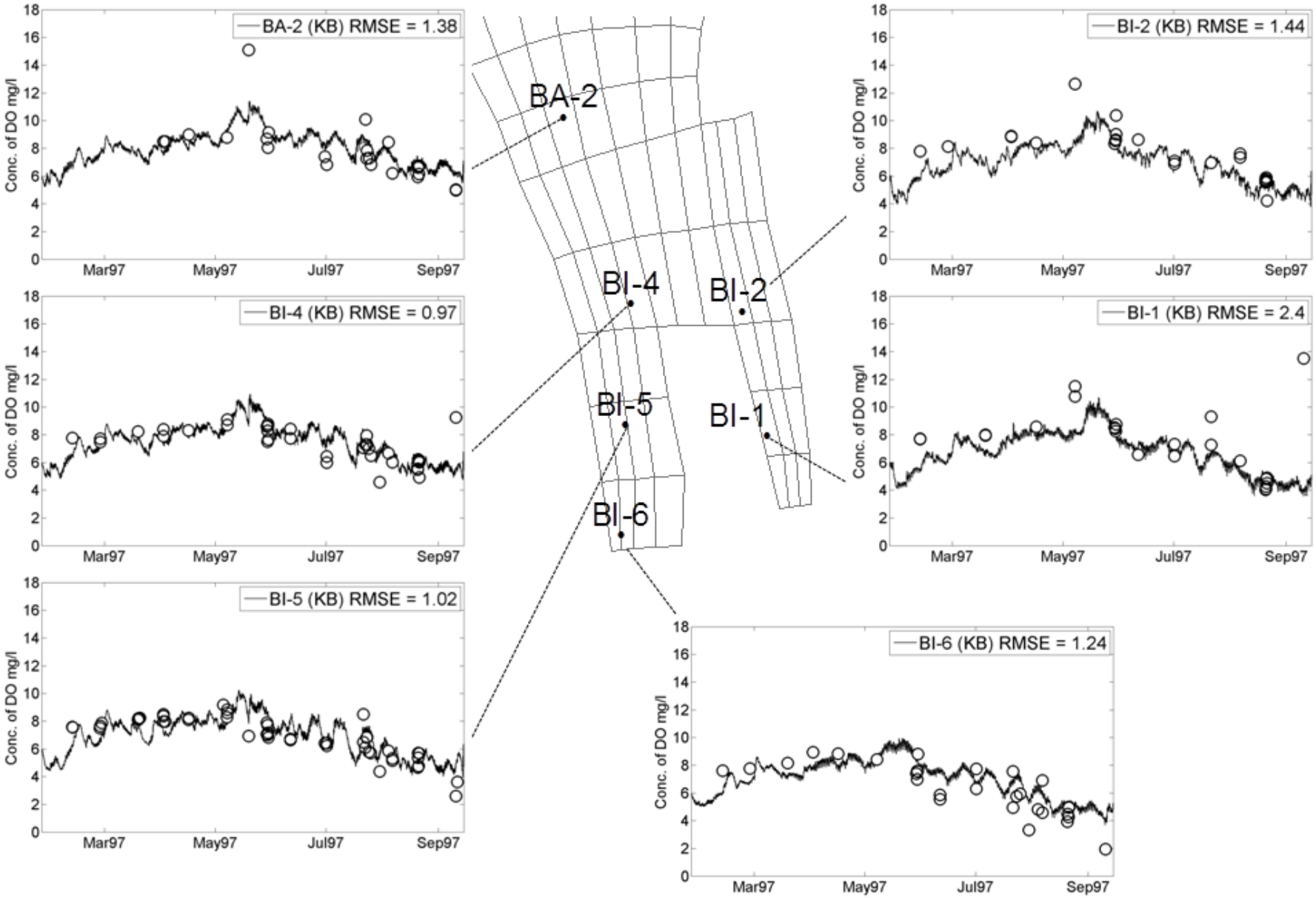

Figure G-5. Predicted and observed bottom layer (KB) dissolved oxygen in inner Budd Inlet.

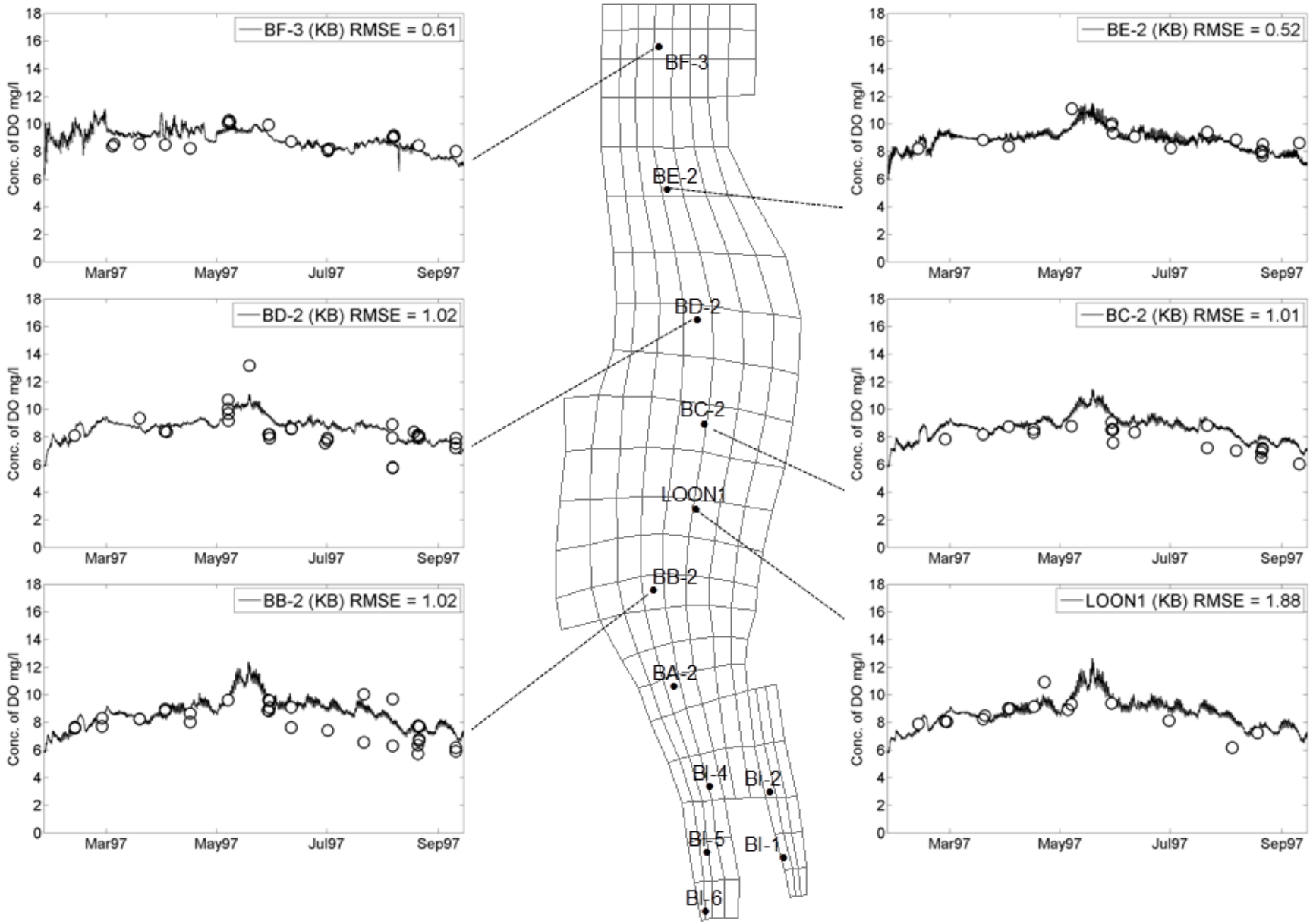

Figure G-6. Predicted and observed bottom layer (KB) dissolved oxygen in central and outer Budd Inlet.

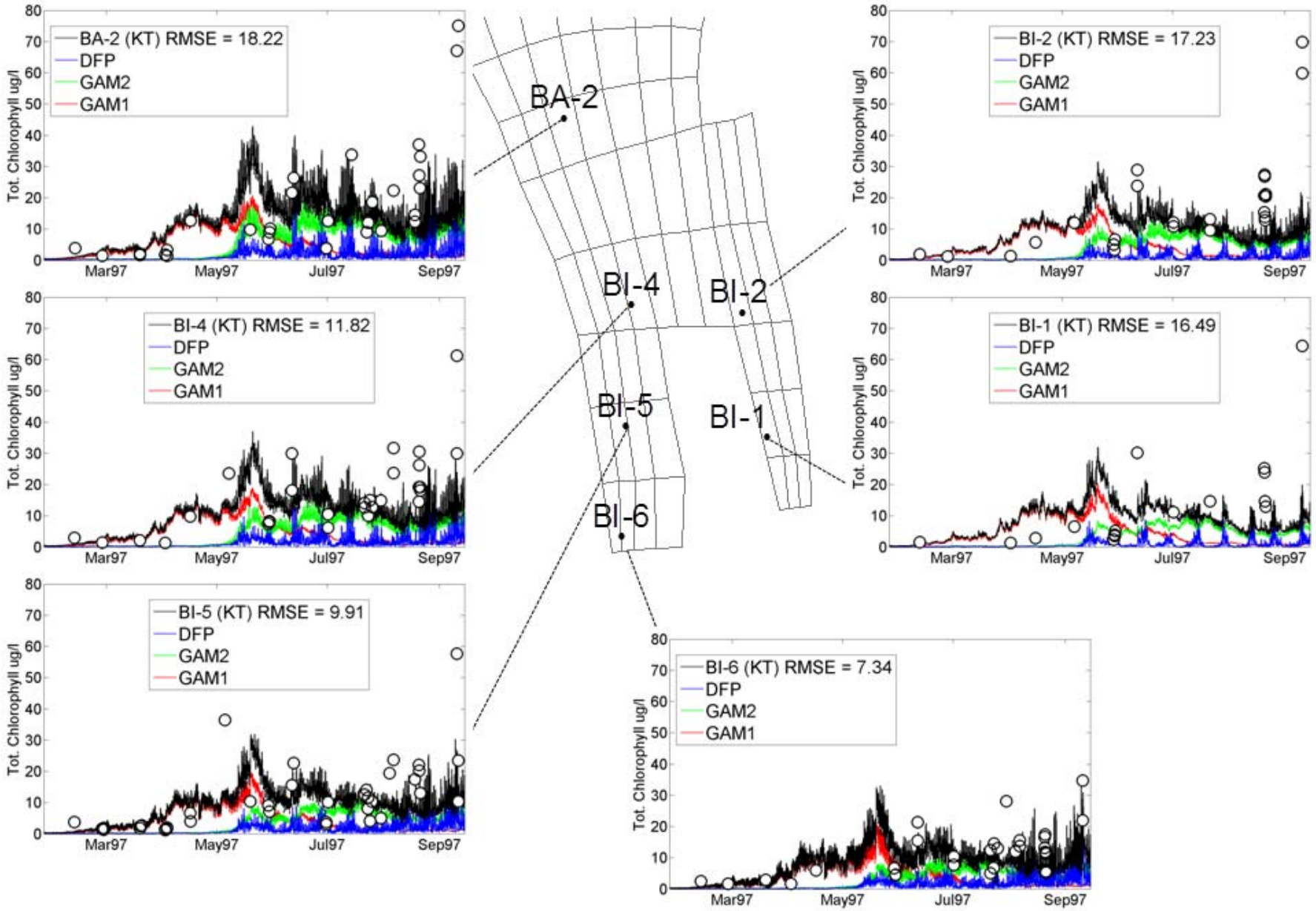

Figure G-7. Predicted and observed surface layer (KT) chlorophyll in inner Budd Inlet.

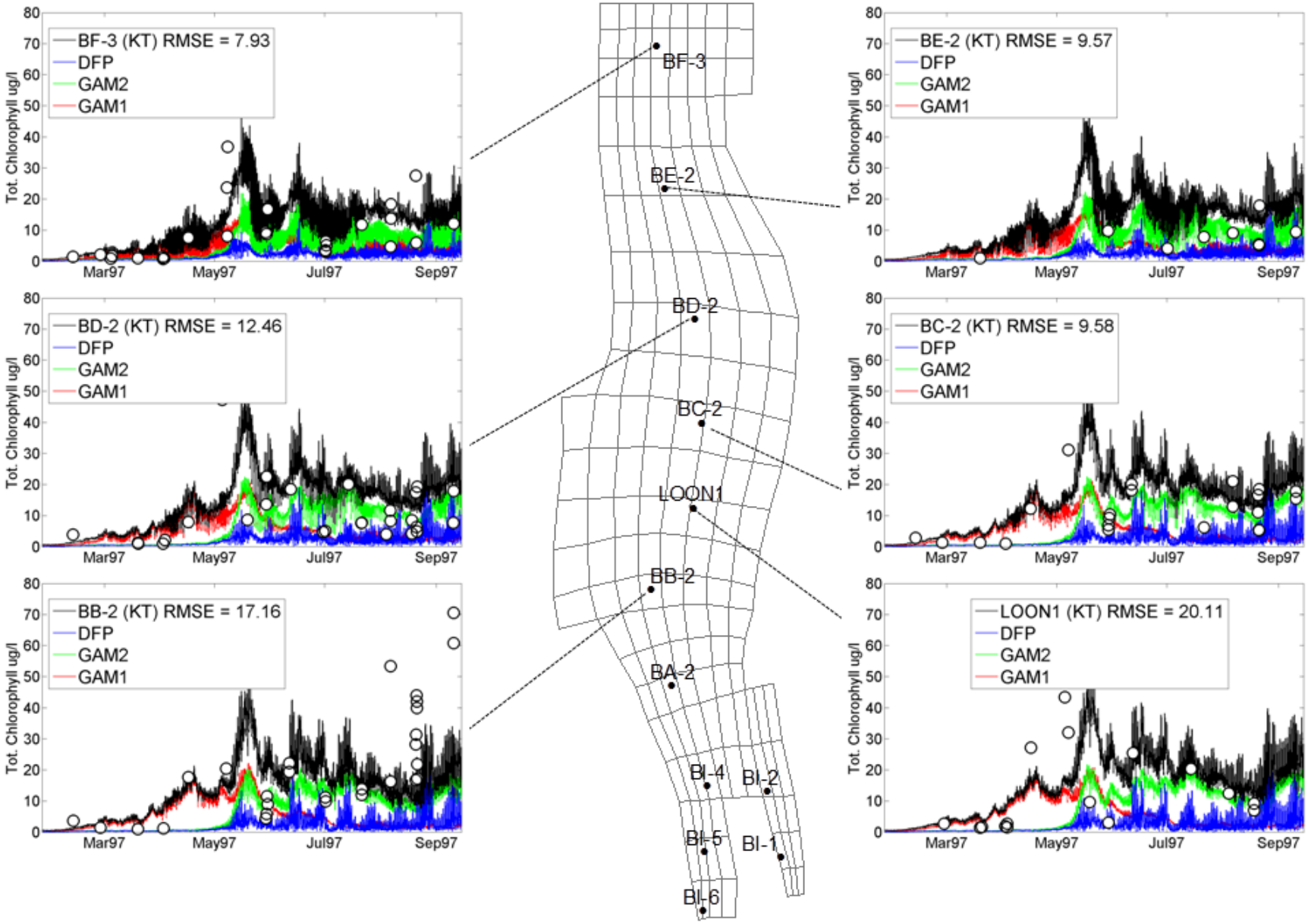

Figure G-8. Predicted and observed surface layer (KT) chlorophyll in central and outer Budd Inlet.

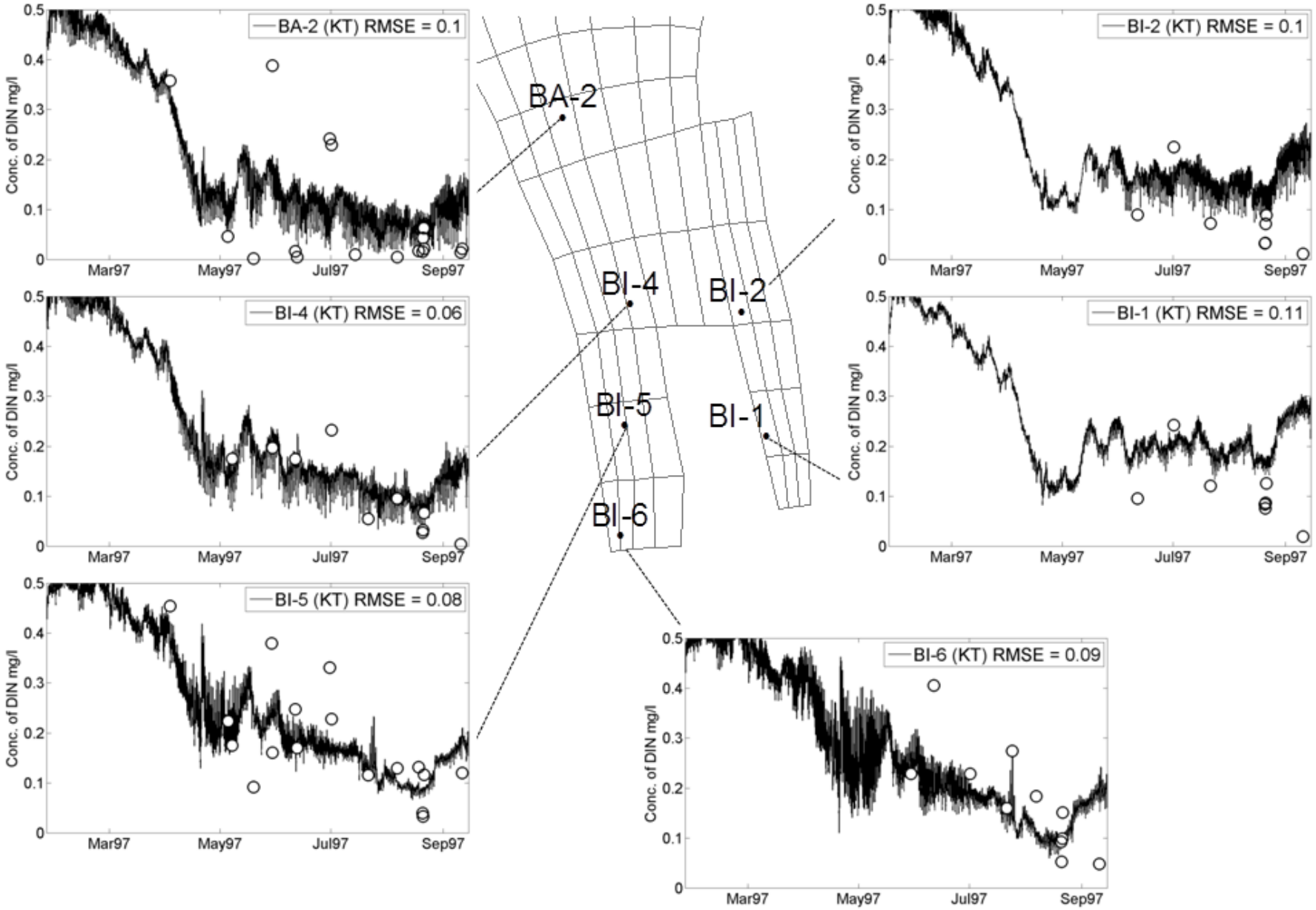

Figure G-9. Predicted and observed surface layer (KT) dissolved inorganic nitrogen in inner Budd Inlet.

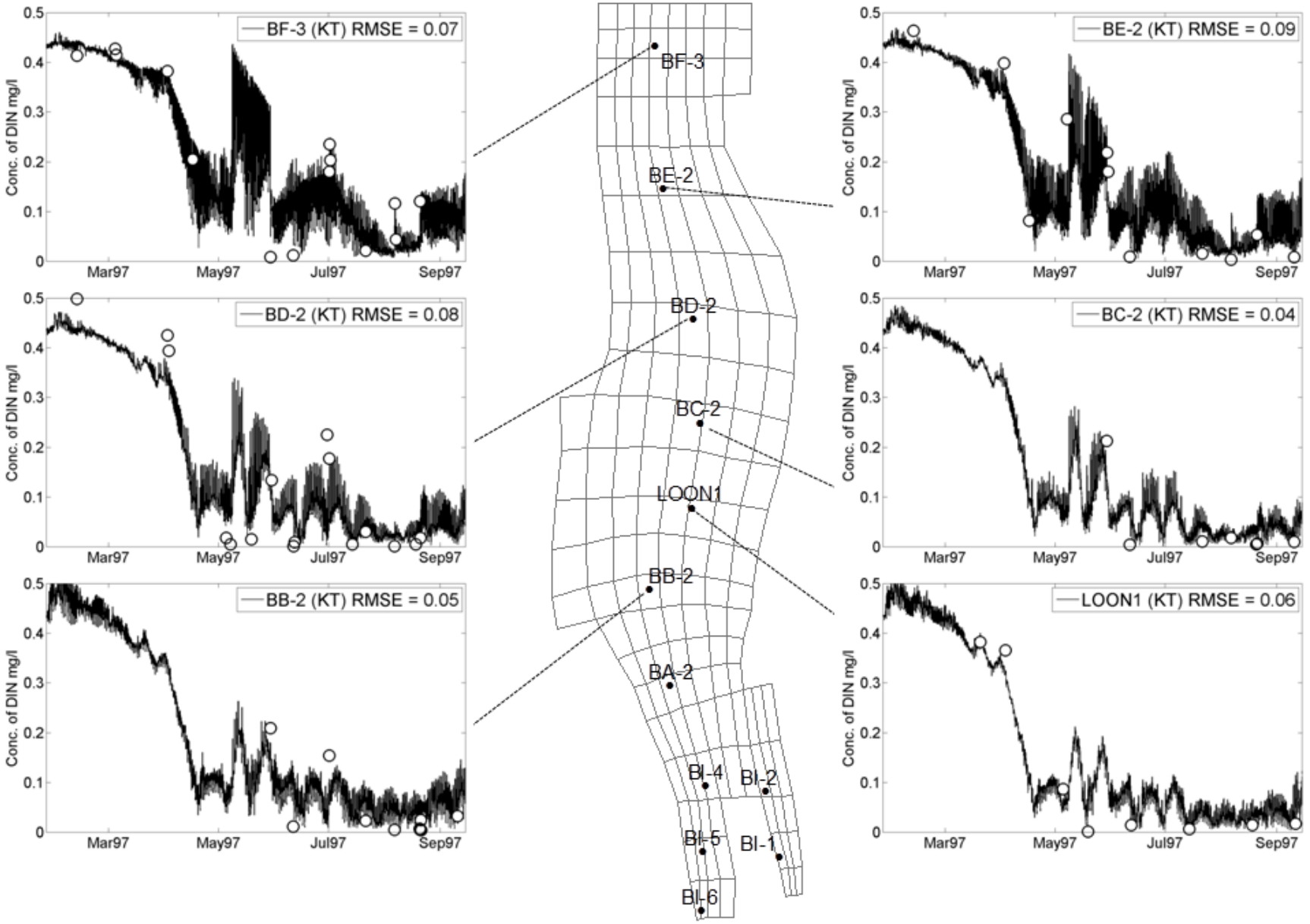

Figure G-10. Predicted and observed surface layer (KT) dissolved inorganic nitrogen in central and outer Budd Inlet.

Water Quality Re-calibration Results: Profiles

Appendix G.3 presents water column profiles of model-predicted DO, total chlorophyll, and DIN compared to field measurements at each diagnostic station. Four profiles from throughout the simulation period are presented for each variable, providing an indication of how well the model predicted seasonal vertical structure.

All profile plots in Appendix G.3 give depths in meters relative to MLLW, with depths *above* MLLW given as negative values and depths *below* MLLW given as positive values. The depth of the water surface varied with time due to tidal action, and so the top of the profiles may not be consistent between plots. Additionally, the deepest field measurement does not necessarily coincide with the bottom of the model profile because field sampling may have been conducted in a deeper- or shallower-than-average location within the grid cell.

Mid-March

Late winter was characterized by an absence of vertical structure in the DO, chlorophyll, and DIN at all diagnostic stations and the model generally did an excellent job of replicating the observed data. Differences between the field data and model predictions were minor, but included the following: DO was slightly under-predicted at Inner Budd Inlet stations; chlorophyll was very slightly over-predicted at all stations; and DIN was generally under-predicted by the model (although only a few DIN records existed for comparison).

Early May

By May the water column had developed more structure and the spring phytoplankton bloom was apparent throughout Budd Inlet. Model-predicted DO profiles matched the field data reasonably well in West Bay, but profiles in East Bay were not as good, substantially under-predicting the observed DO. In the central and outer areas, the model did not reproduce the very super-saturated surface DO present in the upper water column. Chlorophyll data showed elevated concentrations below the surface layer and throughout the water column; while the model sometimes predicted slight increases in the mid-waters, in general the model profiles had less vertical structure than the observed data. However, as noted earlier for the time series comparisons, the model results appeared to lag slightly behind the onset of the observed bloom; these early May profiles coincided with that lag period, just prior to the model bloom, and so the strong chlorophyll signal was not yet developed in the model results. DIN profiles predicted by the model tended to have lower concentrations than the few available field measurements.

Early July

In early July there was little or no vertical structure in the DO data, and the re-calibrated model was quite successful at matching the observed values. The RMSE statistic for the model-predicted DO profiles was low at all stations, averaging 0.75 (maximum RMSE was 1.22). The model was also able to accurately reproduce the chlorophyll profiles at most stations, which likewise had minimal vertical structure. The DIN during this period was in transition, with nitrate levels low and declining while ammonia concentrations were increasing. The model tended to slightly under-estimate both the measured nitrate and ammonia at this time (see time

series charts in Appendix G.2), and this was reflected in the DIN profiles in which model-predicted concentrations were uniformly lower than measured values.

Late August

There was no vertical DO structure at Inner Inlet stations in late August. The model was able to match the field data reasonably well at those locations, but tended to slightly over-predict the observed values. At stations in the central and outer areas model-predicted DO profiles were consistently within the range of the field measurements. Chlorophyll measurements were approximately constant through the water column in West Bay, and the model reproduced the data well. An at-depth chlorophyll peak was observed at many of the central and outer stations; model profiles generally did not predict those peaks, but agreed well with field data in the lower water column. Nitrate and ammonia concentrations had declined to very low levels by late August. DIN profiles showed little structure in the water column, and the model predictions were in closer agreement with the field data than at any other time in the simulation period.

Summary of Model Skill and Goodness-of-Fit Statistics

Model predictions using the re-calibrated rates and constants were able to reproduce the long-term trends and much of the short-term variability seen in the field data. At diagnostic stations throughout Budd Inlet the model predictions showed strong agreement with observed values.

Table G-2 presents summary statistics for comparison of observed and predicted values at all stations and layers of the water column for important water quality variables. Figure G-11 shows spatial patterns for the RMSE and mean bias for prediction of DO in the bottom layer. Model predictions were not biased compared with observed data considering that the confidence interval for the residuals (e.g., mean +/- 2 standard deviations of the residual differences between predicted and observed concentrations) was not significantly different from zero.

Overall, the model is considered to be suitable for the main purpose of this project to predict the response of critical bottom DO concentrations in inner Budd Inlet to variations in nutrient loadings and concentrations.

Table G-2. Summary of overall goodness-of-fit statistics.

Parameter	N[1]	RMSE	RMSE relative to the mean observed value (% of mean)	Mean residual (bias)	Standard deviation of residual (bias)
Bottom DO (mg/L)[2]	678	1.3	16%	-0.02	1.3
Surface DO (mg/L)[2]	1994	2.2	23%	-0.86	2.0
All DO (mg/L)	2672	2.0	22%	-0.65	1.9
Total chlorophyll a (µg/L)	2562	12.7	88%	-1.92	12.6
DIN (mgN/L)	916	0.086	48%	-0.005	0.086
Nitrate+Nitrite (mgN/L)	916	0.067	50%	-0.004	0.067
Ammonium (mgN/L)	916	0.040	97%	0.002	0.040

[1] Number of comparisons.
[2] Bottom and surface DO statistics were calculated for lower half and upper half of the water column, respectively.

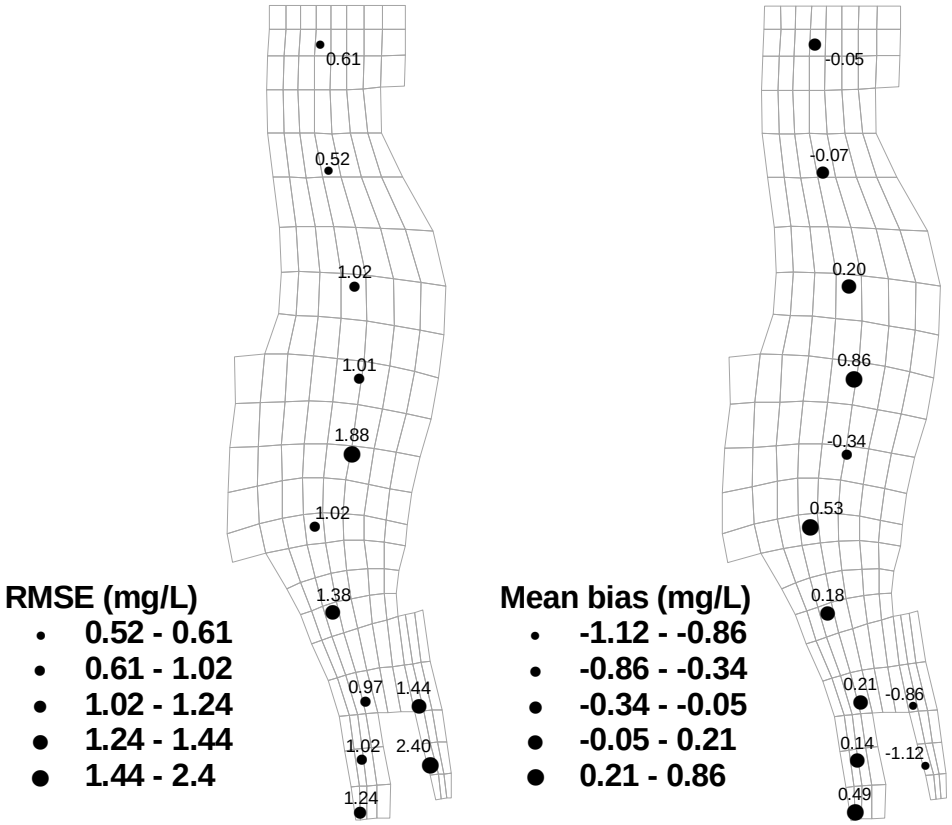

Figure G-11. Goodness-of-fit for predicted to observed bottom layer (KB) dissolved oxygen.

Hydrodynamic Model Re-calibration

Re-calibration of the hydrodynamic model followed an iterative procedure similar to the water quality re-calibration. The model was executed using an initial parameter set based on previous calibration work, and the output was compared to various field measurements collected during the BISS in 1997. For successive model runs hydrodynamic parameters were varied to obtain the best agreement between model predictions and the field data. These parameters included the Chezy friction coefficient, wind sheltering coefficient, wind speed function, transport scheme, and momentum dispersion functions, as well as minor adjustments to the model bathymetry. The RMSE statistic was used to evaluate the goodness-of-fit of the predicted to observed values. A summary of the final parameter values for hydrodynamic components is given in Table G-5.

The figures presented in the following sub-sections show comparisons of the model output (solid black line) and the various field observations (magenta dotted line). These figures replicate many of the graphics presented in the original BISS report (Aura Nova Consultants et al., 1998).

Hydrodynamic Re-calibration Results: Tidal Elevation

Water surface elevation measurements were recorded during the BISS using a tide gauge mounted to a dock piling in Olympia Harbor (at the southeast end of the ship turning basin in West Bay). Figure G-12 shows a comparison of the measured to model-predicted tidal elevation for February 1997. The model was able to predict tidal elevations with accuracy, and the model time series was practically indistinguishable from the observed data.

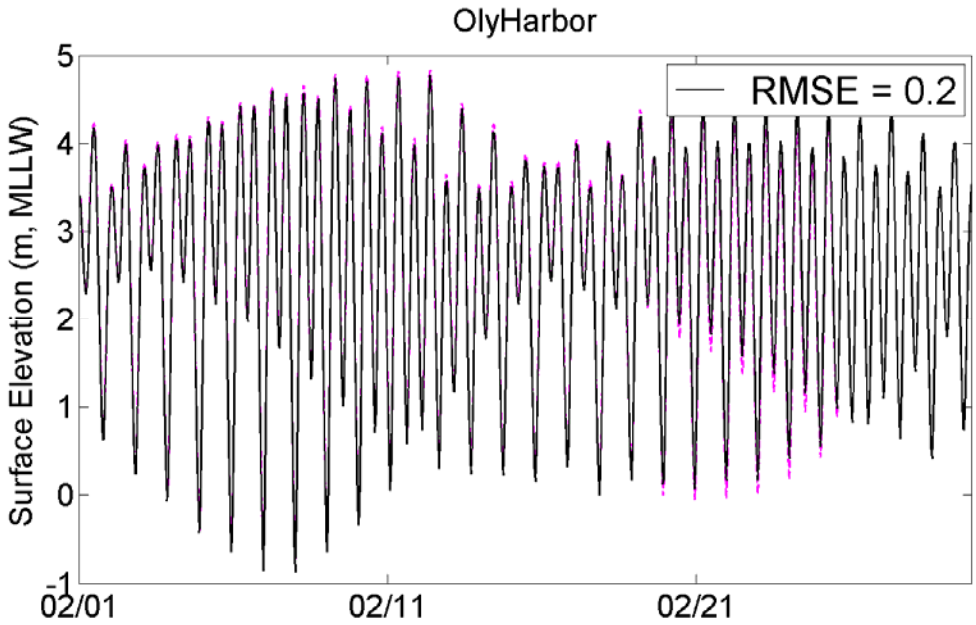

Figure G-12. Comparison of model-predicted (black line) tidal elevation and records from the Olympia Harbor tide gauge station (magenta dotted line).

Hydrodynamic Re-calibration Results: Currents

Current speed and direction were measured in 1997 using Anderaa current meters moored at fixed depths. At three Anderaa stations (Figure G-13), time series of the predicted and measured east-west (U) and north-south (V) components of the current velocities were compared. Figure G-14 presents time series for May 1997 deployments, and Figure G-15 shows late-May through July deployments. During both deployments the current meters were positioned as follows: 2.6 m below MLLW at station 1A (i=6, j=6, layer=9); 3.4 m below MLLW at station 2A (i=7, j=13, layer=10); and 5.8 m below MLLW at station 3A (i=8, j=18, layer=11).

Acoustic Doppler Current Profiler (ADCP) data from 1997 deployments was also used to verify the model re-calibration. Current velocity data from four ADCPs (Figure G-13) were compared to model predictions for a one-month period in Figures G-16 and G-17. To avoid boundary effects at the surface and bottom, the ADCP measurements selected for comparison were from 5 m below MLLW, which corresponded to model layer 11.

Model predictions of both U and V velocity components did a good job of capturing the range of magnitudes measured by the Anderaa current meters and ADCPs. The RMSE statistics for the time series comparisons were generally low, but a few values were possibly exaggerated due to a slight phase shift between the model and observed data. The model slightly under-predicted north-south velocities in the Inner Inlet (Anderaa station 1A and ADCP mooring M5) during flood tides, and had difficulty reproducing the highly-variable spikes in the east-west velocities at Anderaa station 2A. Nonetheless, the re-calibration time series was generally in strong agreement with the phase and velocity ranges of the field data at all stations, and was comparable to that achieved by previous calibration work.

Figure G-13. Anderaa current meter stations (left) and ADCP sites (right) in Budd Inlet in 1997.

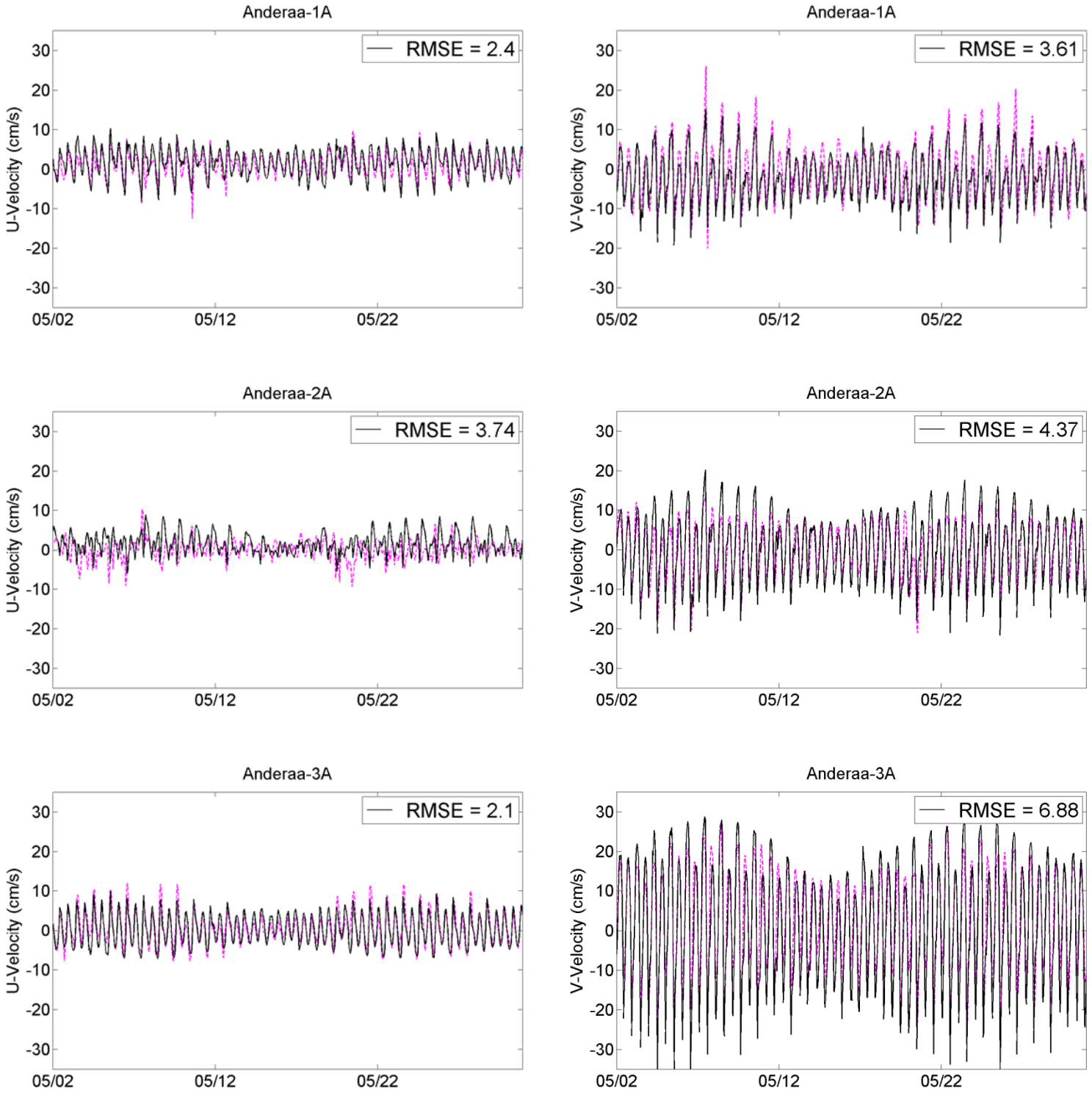

Figure G-14. Time series comparison of model-predicted East-West (left) and North-South (right) current velocities and Anderaa current meter observations for the May 1997 deployment. The black line is model-predicted, and the magenta dotted line is measured values.

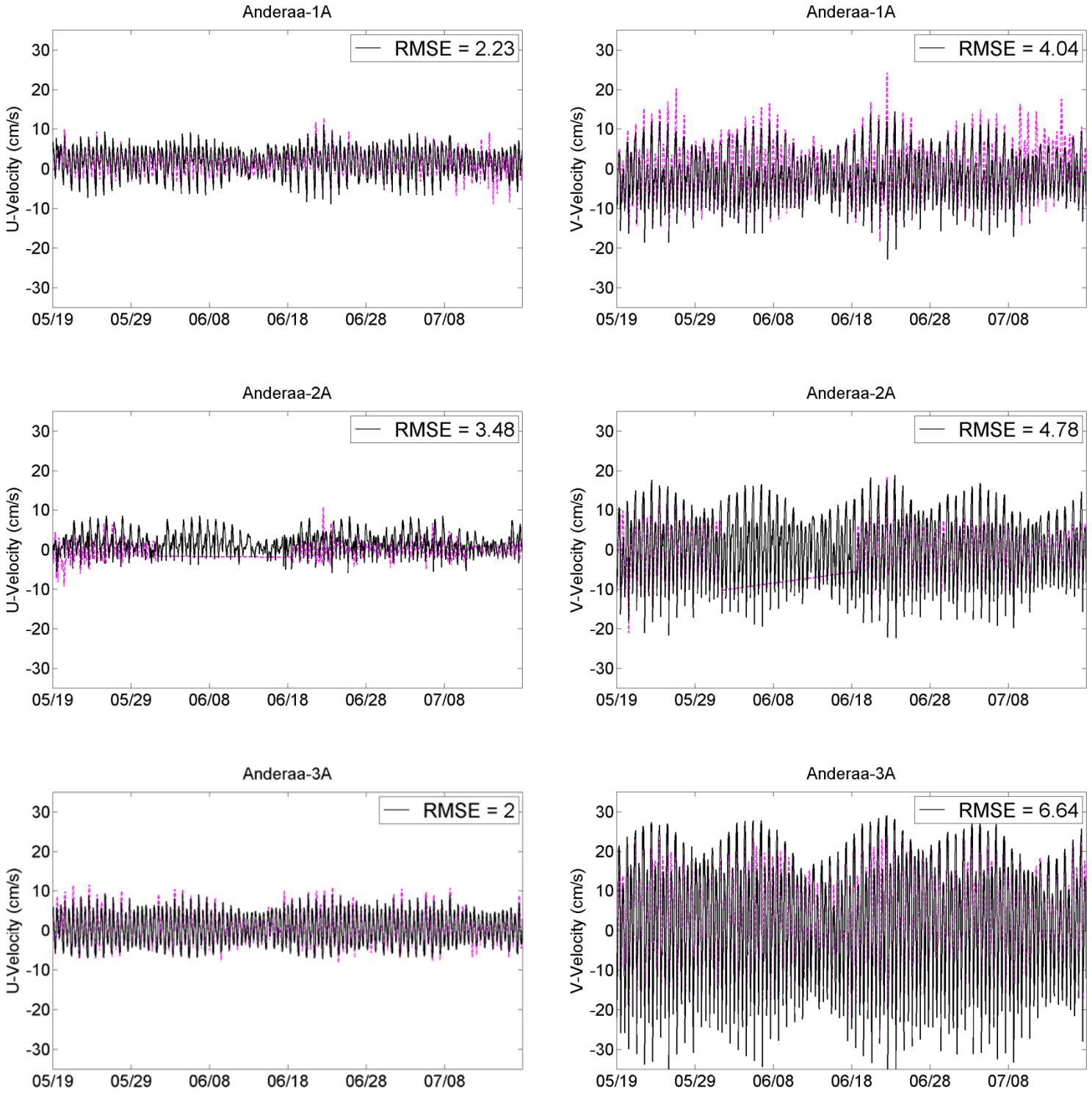

Figure G-15. Time series comparison of model-predicted East-West (left) and North-South (right) current velocities and Anderaa current meter observations for the May through July 1997 deployment. The black line is model-predicted, and the magenta dotted line is measured values.

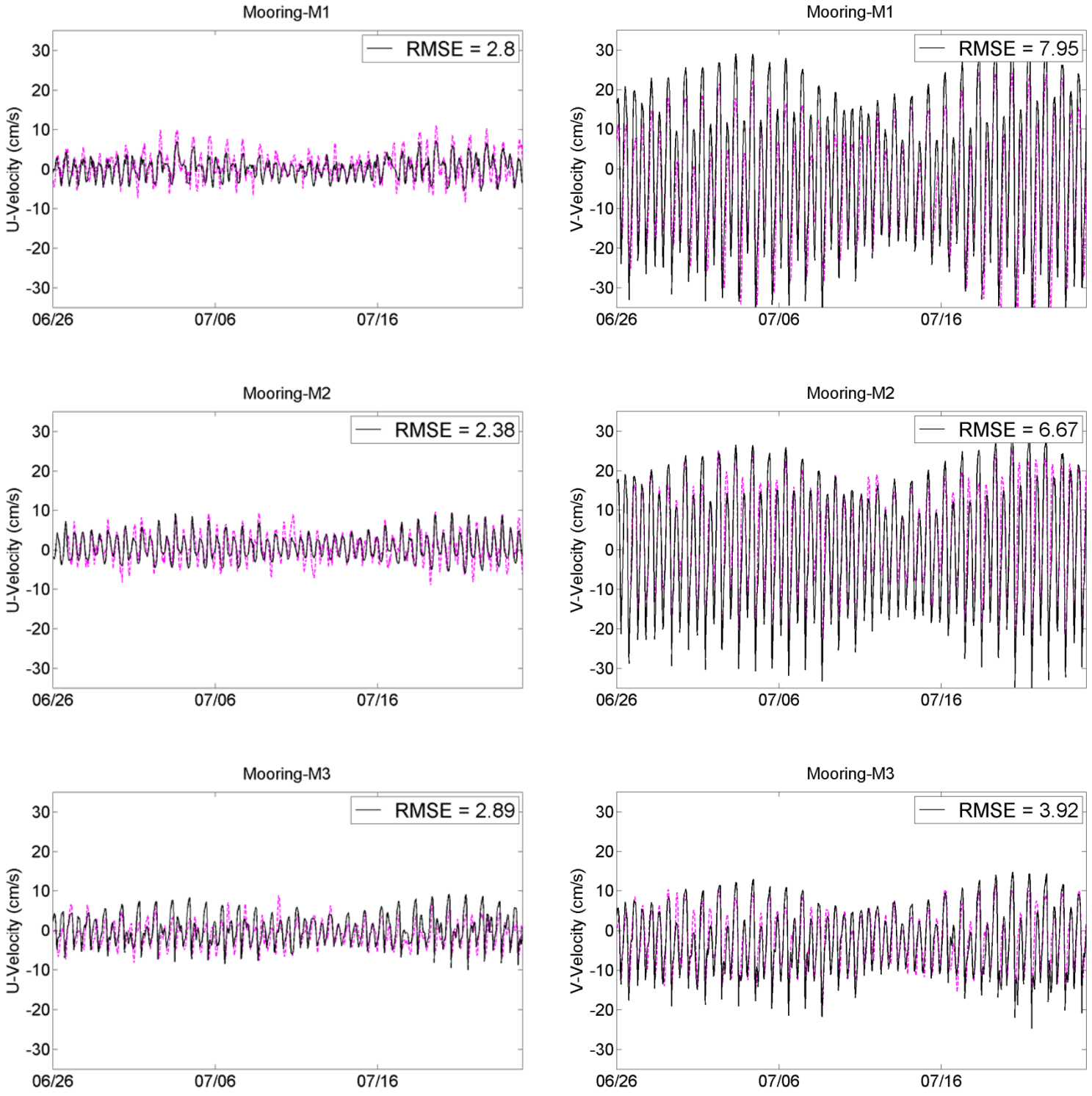

Figure G-16. Time series comparison of model-predicted East-West (left) and North-South (right) current velocities and ADCP measurements for the June to July 1997 deployment at 5 m below MLLW. The black line is model-predicted, and the magenta dotted line is measured values.

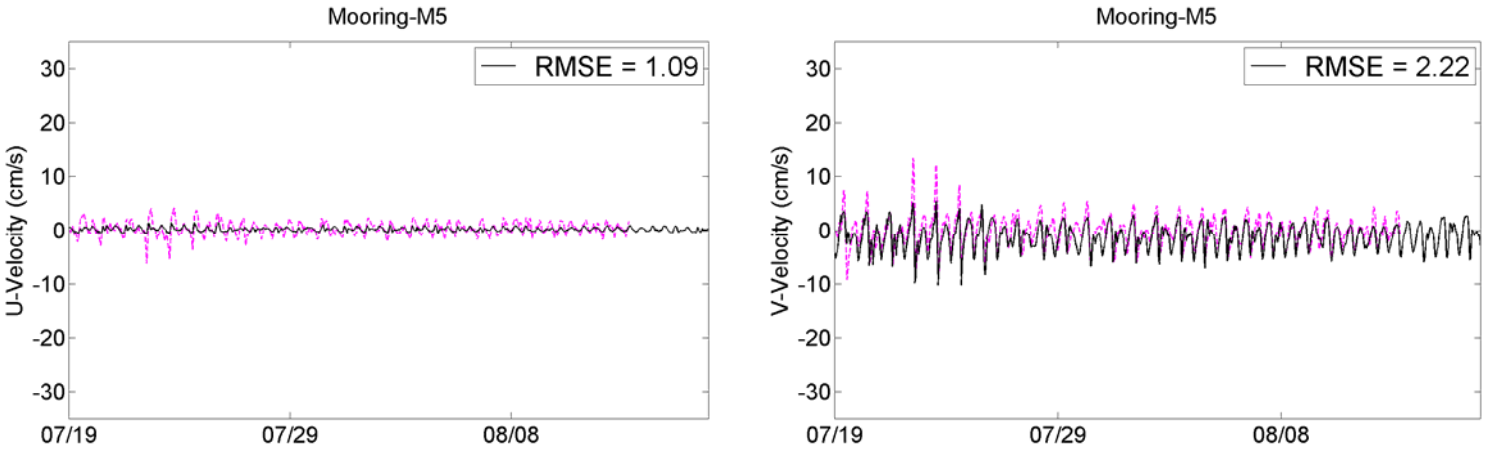

Figure G-17. Time series comparison of model-predicted East-West (left) and North-South (right) current velocities and ADCP measurements at Mooring M-5 for the July to August 1997 deployment at 5 m below MLLW. The black line is model-predicted, and the magenta dotted line is measured values.

Hydrodynamic Re-calibration Results: "In-situ" CTD Time Series

CTDs moored continuously at two locations in Budd Inlet in 1997 (Figure G-18) provided long-term, high resolution (15-minute records) time series of temperature and salinity for comparison with model output. Model predictions were evaluated for two deployment periods, the first in June (Figure G-19) and the second in late August of 1997 (Figure G-20). The CTD at station 1C was positioned at 1.65 m below MLLW for the first deployment period and at 1.99 m below MLLW for the second period. At station 2C the deployment depths were 1.61 m and 2.0 m below MLLW for the first and second evaluation periods, respectively. Time series comparisons involved model predictions from layer 8 at grid cells (6,6) and (7,11), corresponding to CTD stations 1C and 2C, respectively.

Model predictions of temperature showed excellent agreement with the "in-situ" CTD data from both stations. While the predicted temperatures consistently over-estimated the observed data, the low RMSE statistics (maximum of 1.21 degrees C) indicated that the over-prediction was quite small. Salinity predictions tended to slightly exaggerate the magnitude of short-term (i.e., tidal) fluctuations, and generally under-predicted the field observations. Still, RMSE statistics for salinity comparisons were very low (maximum of 1.63 ppt), and the model did a good job of capturing the long-term trends.

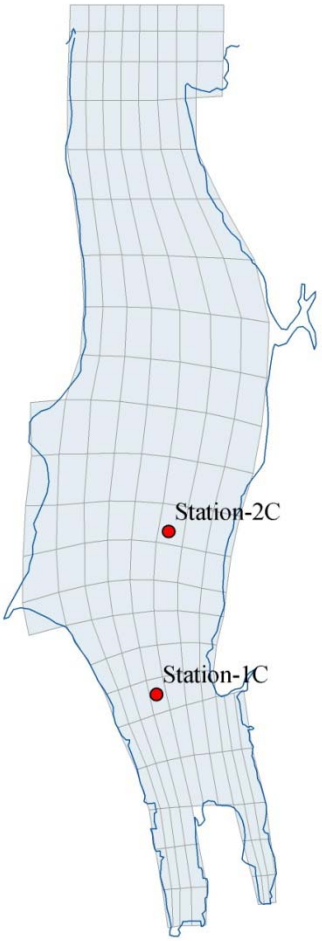

Figure G-18. Locations of "in-situ" CTD deployments in Budd Inlet in 1997.

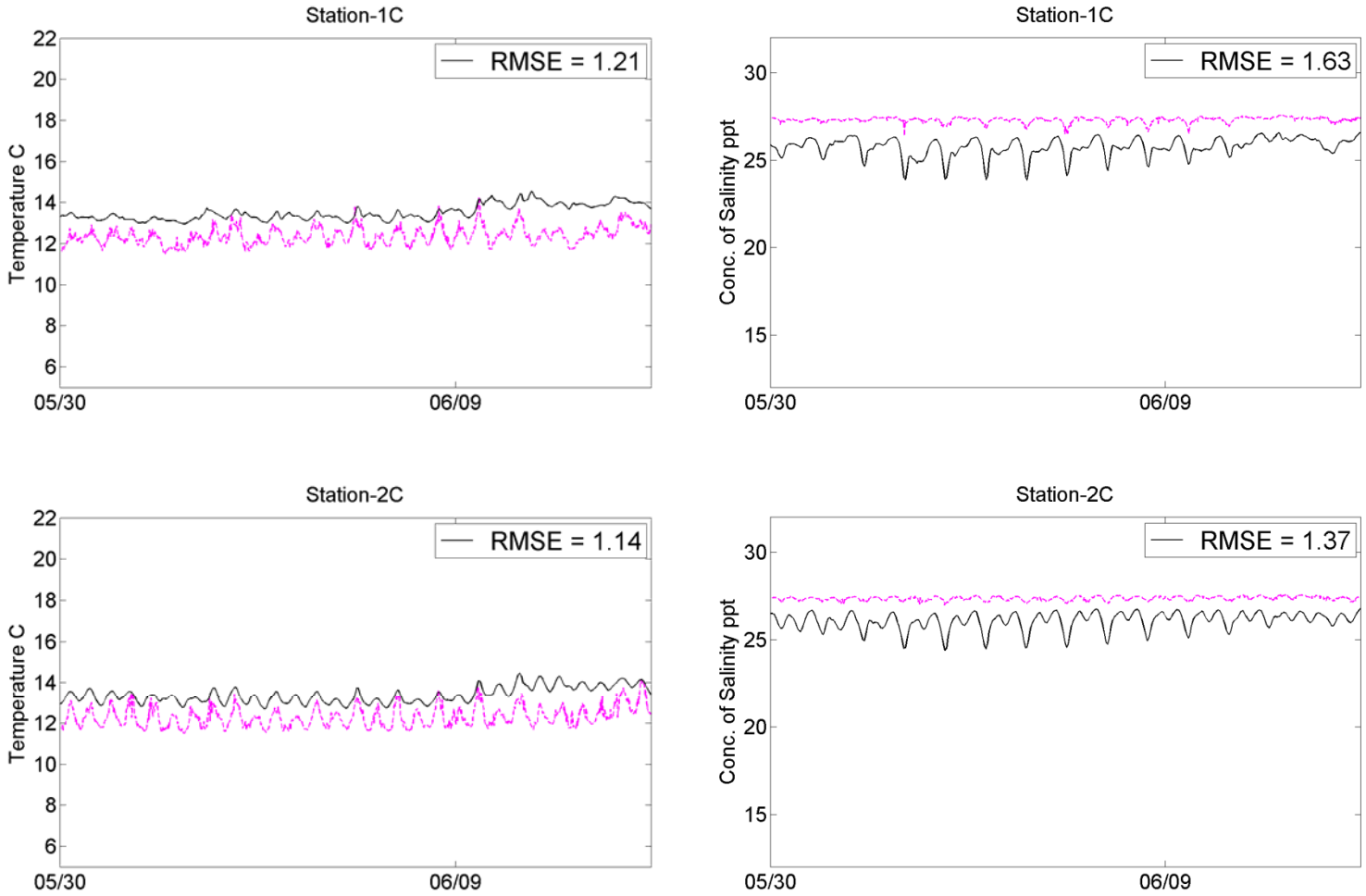

Figure G-19. Time series comparison of model-predicted and "in-situ" CTD measurements of temperature (left) and salinity (right) in June 1997. The black line is model-predicted, and the magenta dotted line is measured values.

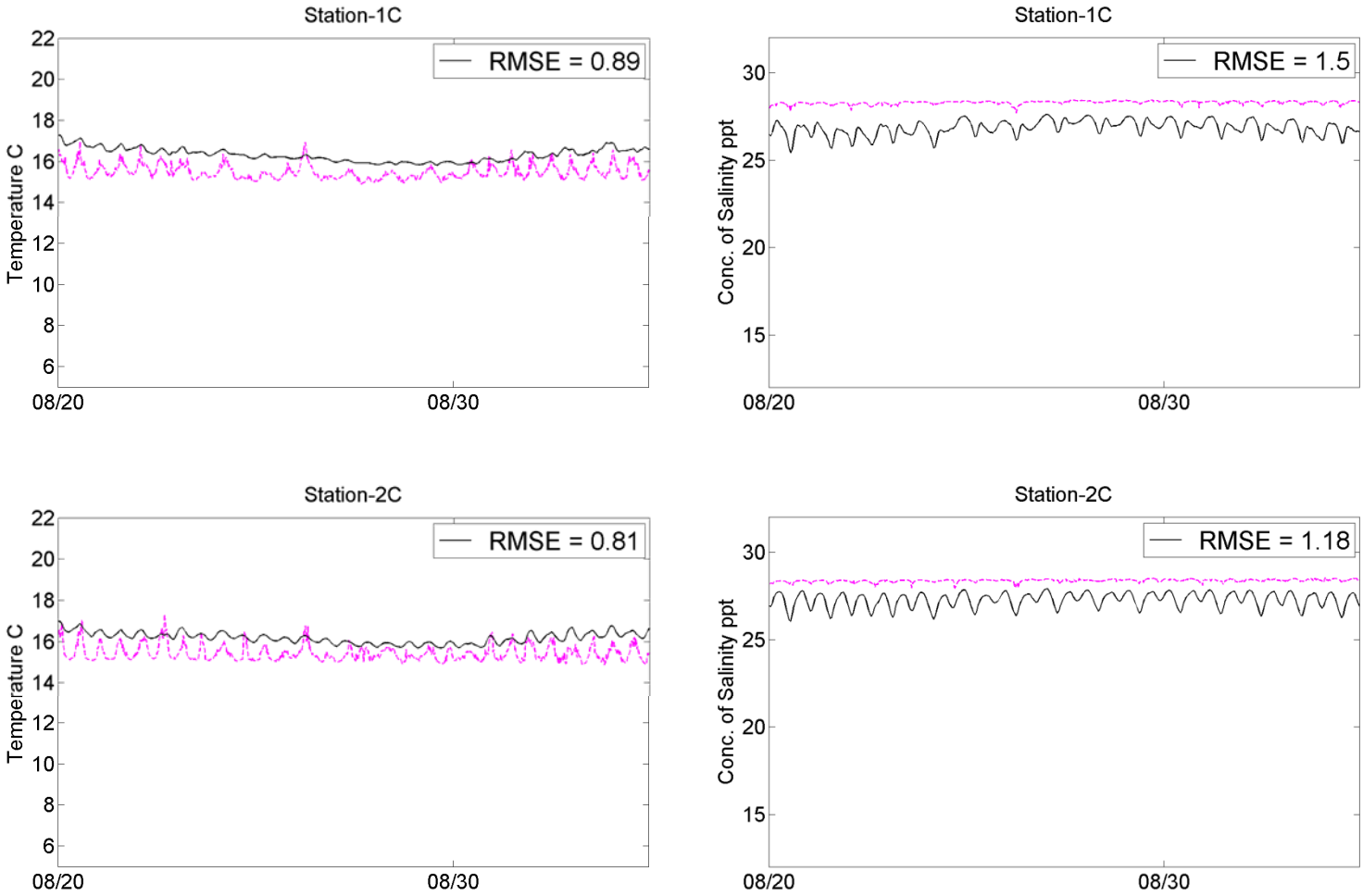

Figure G-20. Time series comparison of model-predicted and "in-situ" CTD measurements of temperature (left) and salinity (right) in August 1997. The black line is model-predicted, and the magenta dotted line is measured values.

Hydrodynamic Re-calibration Results: On-station CTD Profiles and Time Series

Temperature and salinity measurements from CTD profiles at the nine stations shown in Figure G-21 were used to evaluate the ability of the model to reproduce the vertical structure observed throughout Budd Inlet during the simulation period. Predicted and measured profiles were compared in Figures G-22 through G-30. The model matched the observed temperatures well in all seasons, accurately predicting the thermal structure of the water column during times of stratification and also when stratification was absent. The RMSE of temperature profiles was generally at or below 1 degree C, indicating excellent agreement. Salinity profiles likewise showed that the model was capable of reproducing vertical structure stemming from freshwater inputs, tides, and precipitation. Salinity predictions were very good at stations in the central and outer areas of Budd Inlet, with RMSE statistics at or below 2 ppt. More variable structure was seen at the Inner Inlet stations due to the Capitol Lake discharge, but the model made accurate salinity predictions there, too, with RMSEs generally less than 3 ppt.

Time series of temperature and salinity were created from the CTD profile data for further evaluation of the model re-calibration. Specifically, measurements from the surface and bottom layers throughout the simulation period were compared to model-predicted time series (Figures G-31 through G-34). The model was able to accurately reproduce both the long-term trend and much of the short-term variability of the observed temperature time series in both layers, with an average RMSE of 1.3 degrees C for the nine stations (both depths included). Although the model tended to slightly over-predict bottom layer temperatures late in the simulation period, the average bottom layer RMSE of 0.9 degrees C signified that these model predictions were nonetheless excellent. Salinity time series plots showed extremely high surface variability at the southern stations due to the intermittent freshwater discharge from Capitol Lake. The model had some difficulty precisely reproducing the observed salinities at the three Inner Inlet stations, but was able to capture the high variability and general trends. Surface layer salinity predictions were much more accurate in the central and outer surface waters, and RMSEs were very low except when exaggerated by occasional anomalous field measurements (possibly due to heavy, short-duration precipitation events). Bottom layer salinities very slightly under-predicted observed values, but generally were in excellent agreement (average RMSE of 0.8 ppt).

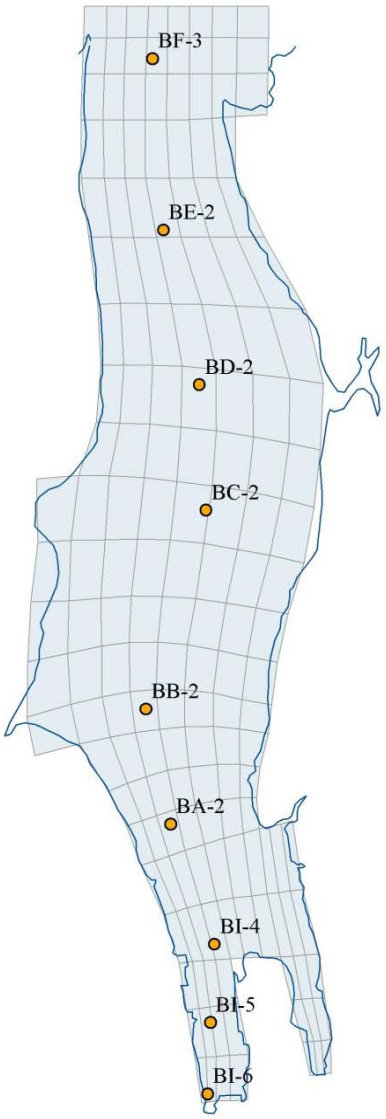

Figure G-21. Diagnostic stations used for evaluation of temperature and salinity profiles and time series.

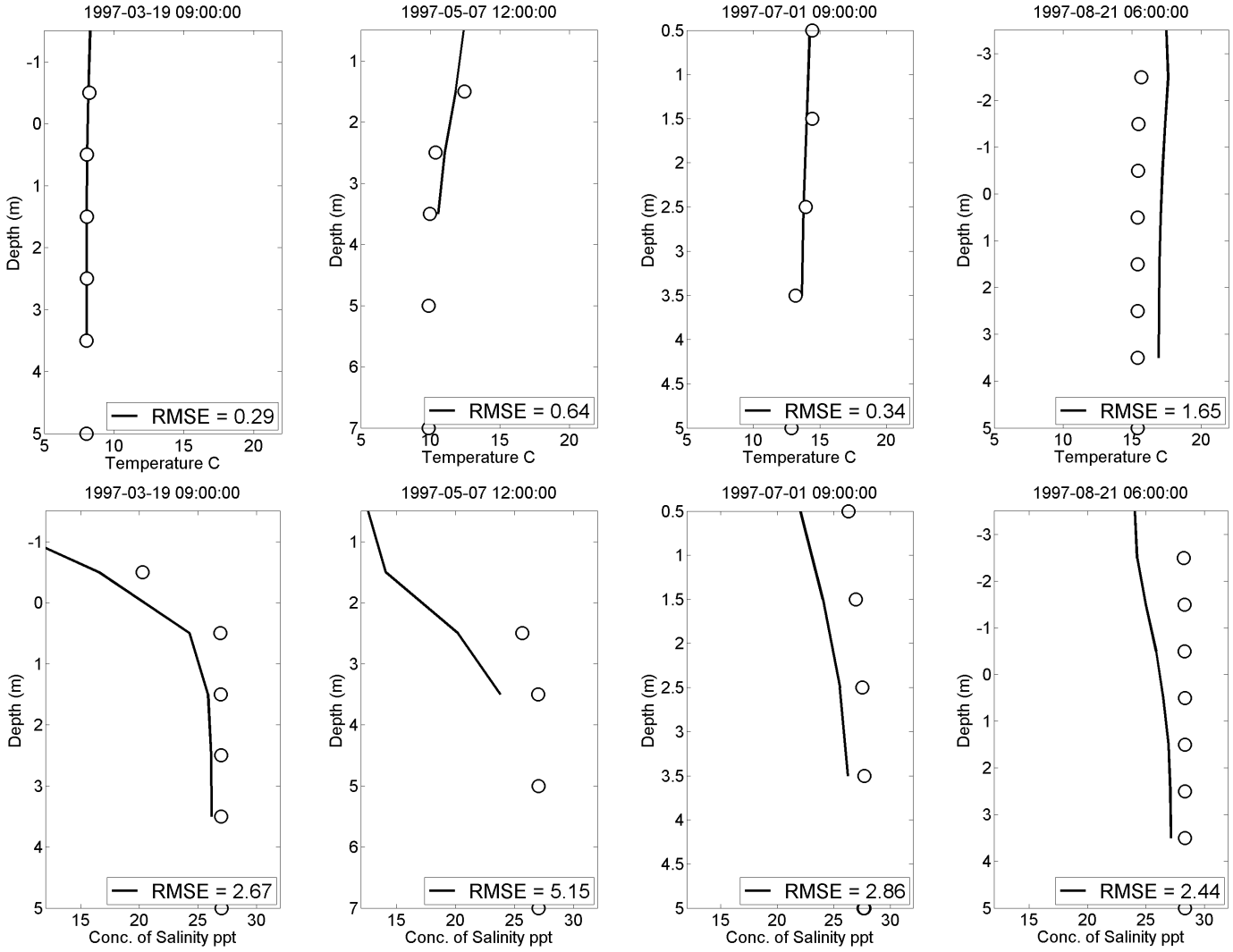

Figure G-22. Station BI-6 profile plots of model-predicted and observed temperature and salinity.

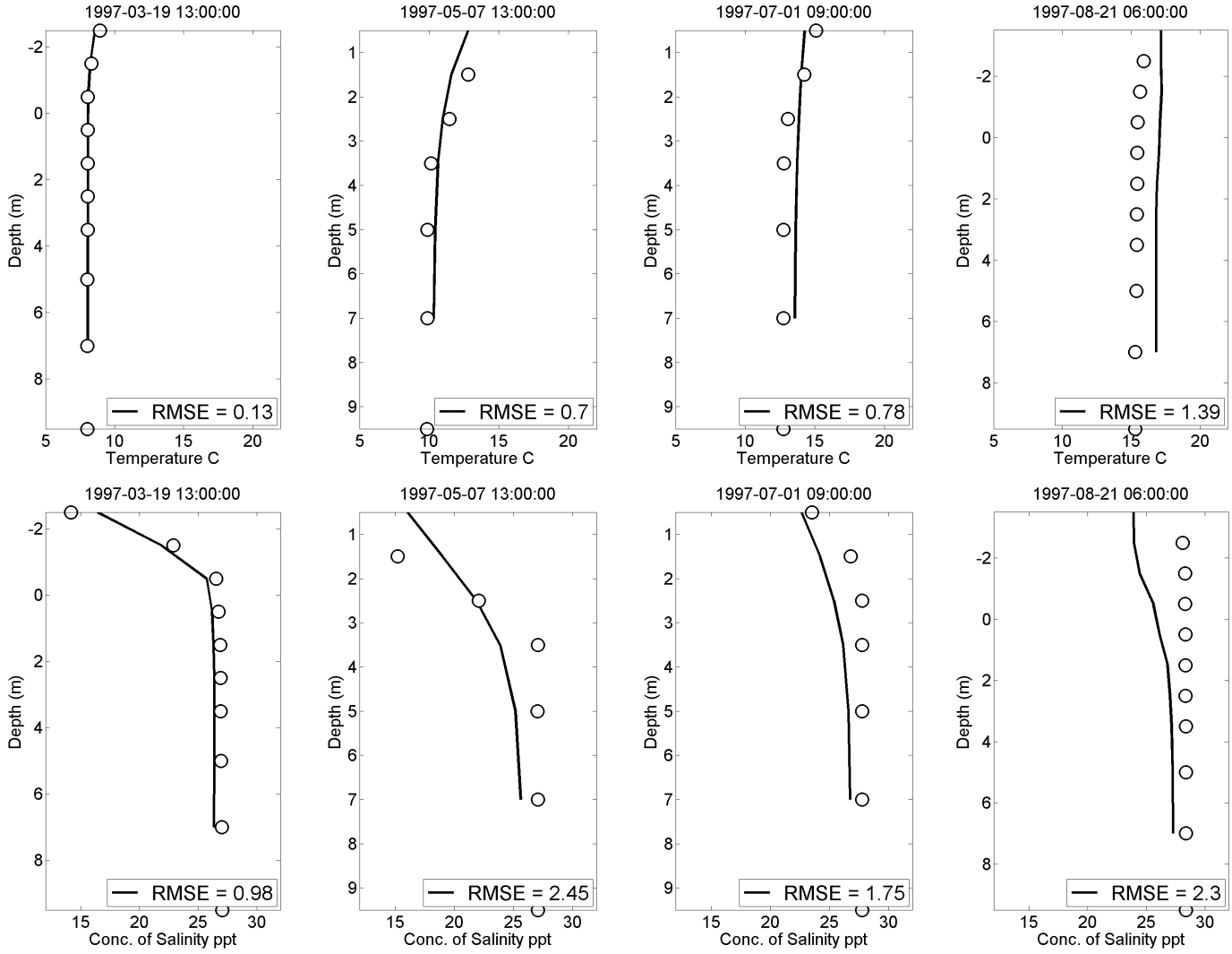

Figure G-23. Station BI-5 profile plots of model-predicted and observed temperature and salinity.

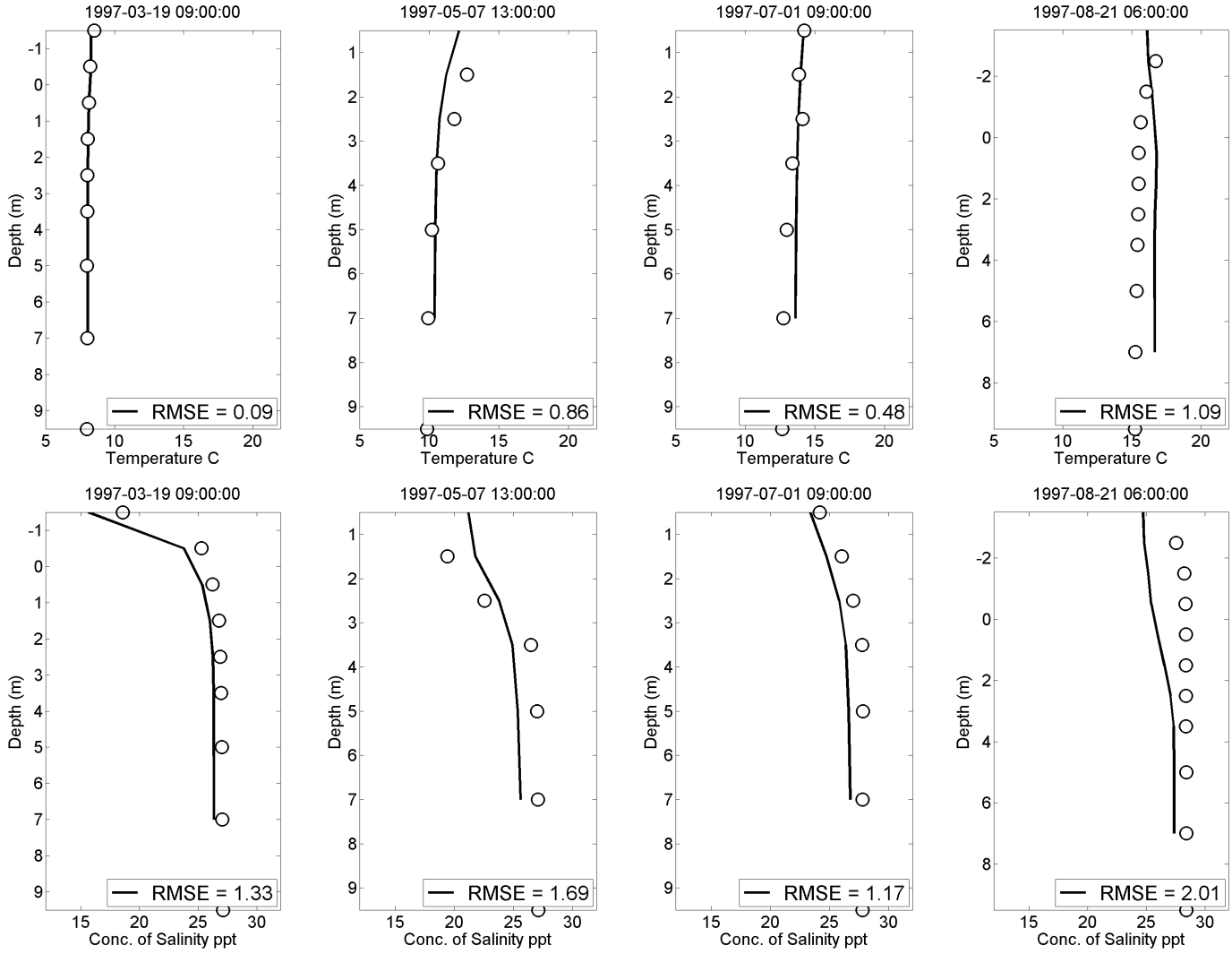

Figure G-24. Station BI-4 profile plots of model-predicted and observed temperature and salinity.

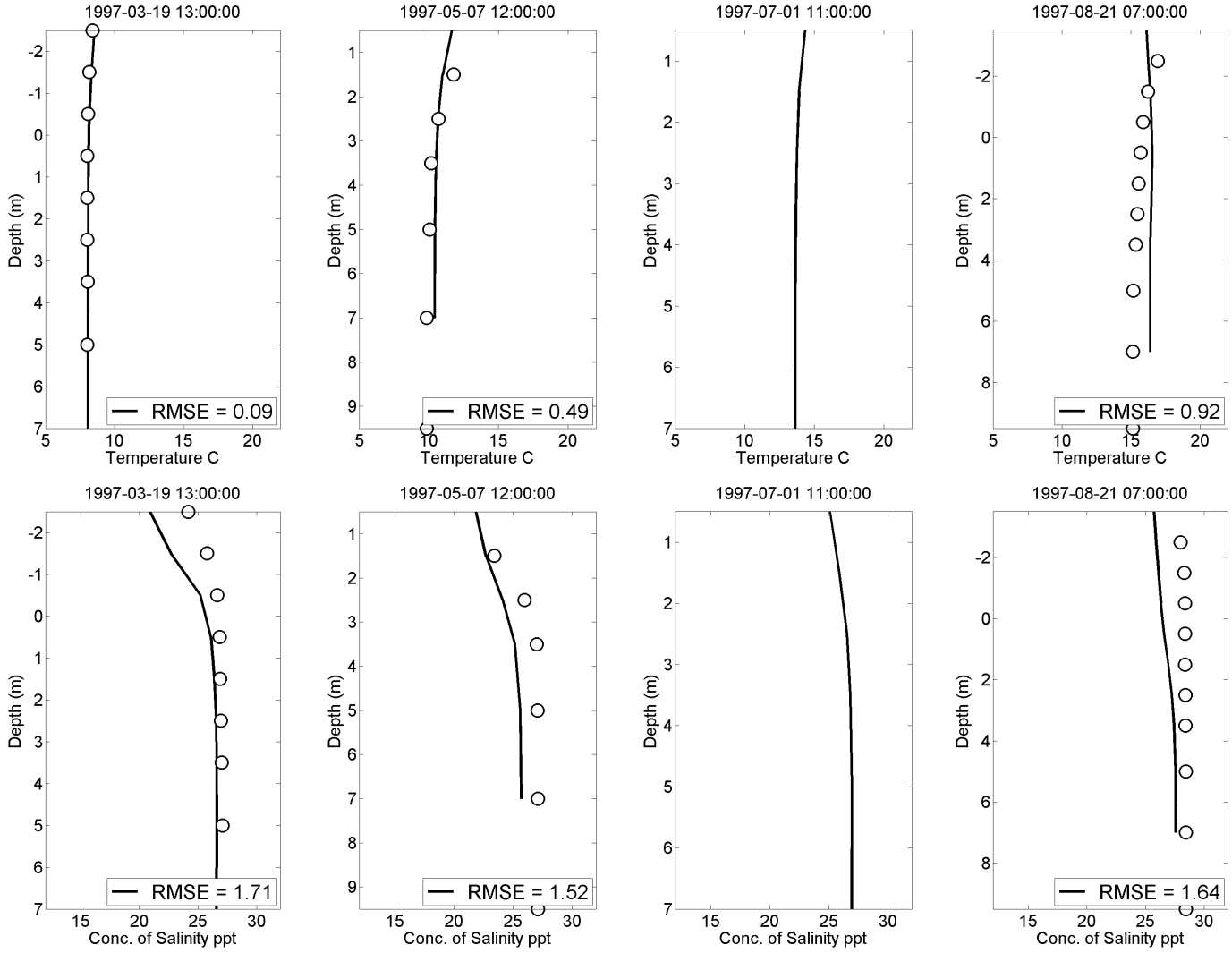

Figure G-25. Station BA-2 profile plots of model-predicted and observed temperature and salinity.

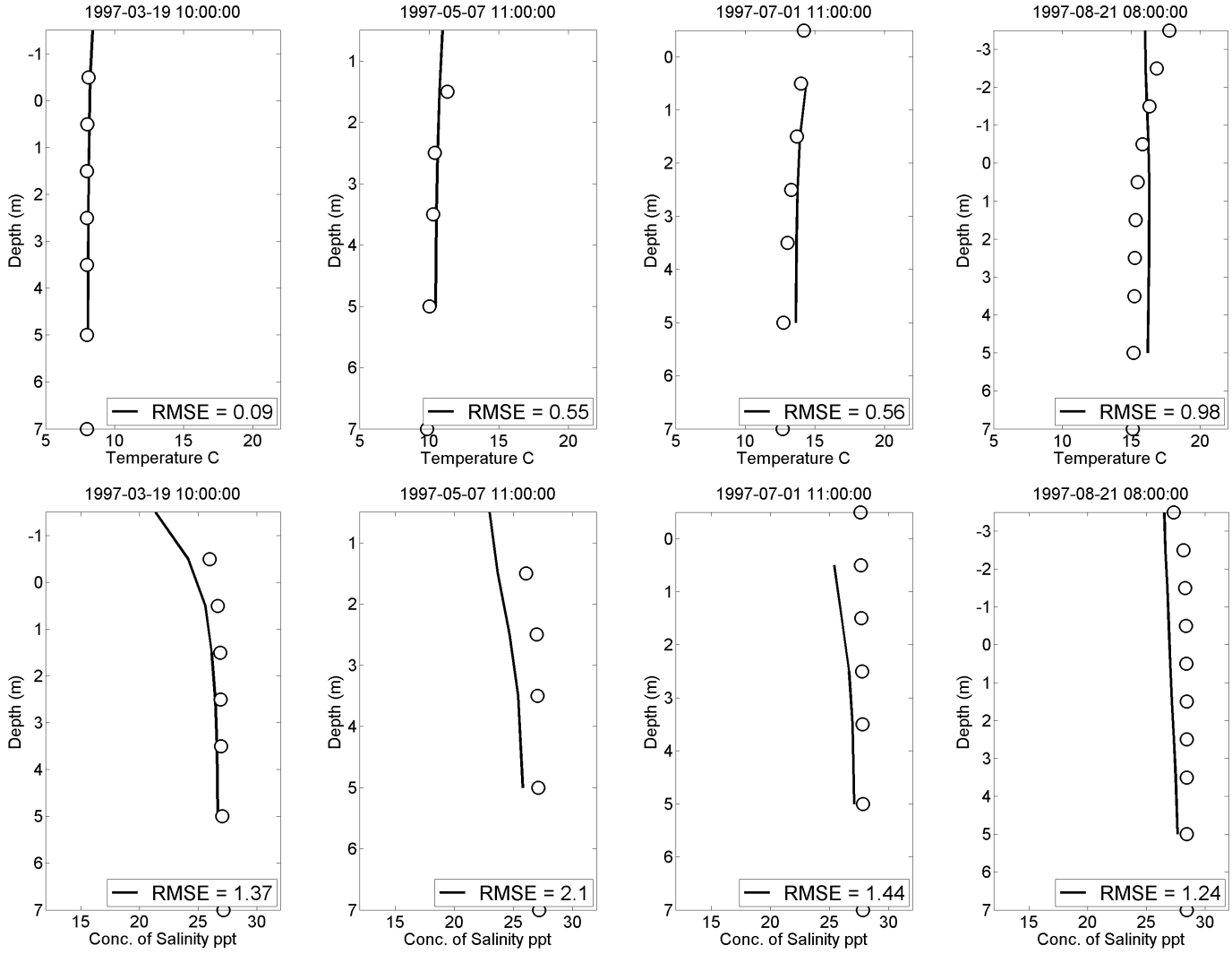

Figure G-26. Station BB-2 profile plots of model-predicted and observed temperature and salinity.

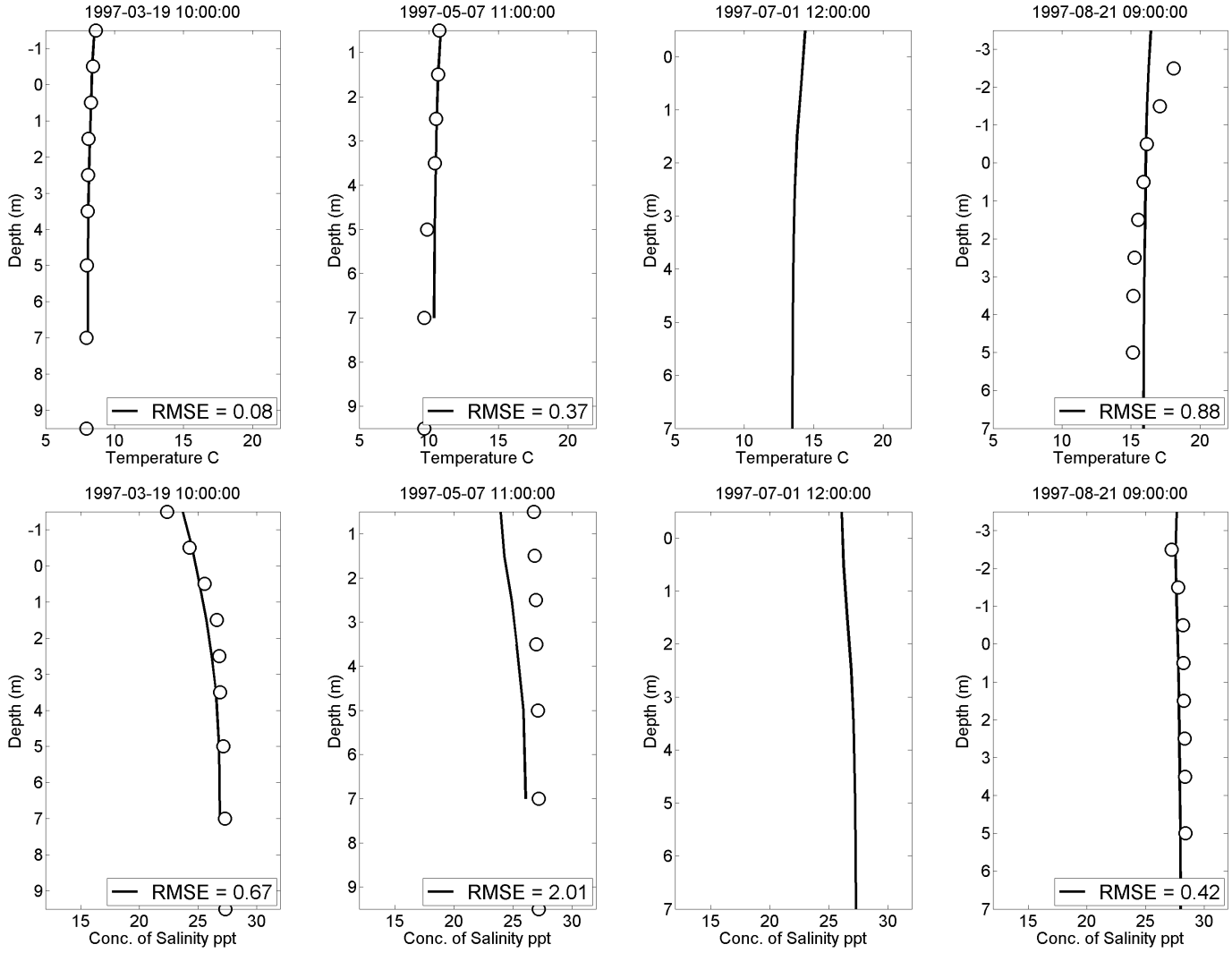

Figure G-27. Station BC-2 profile plots of model-predicted and observed temperature and salinity.

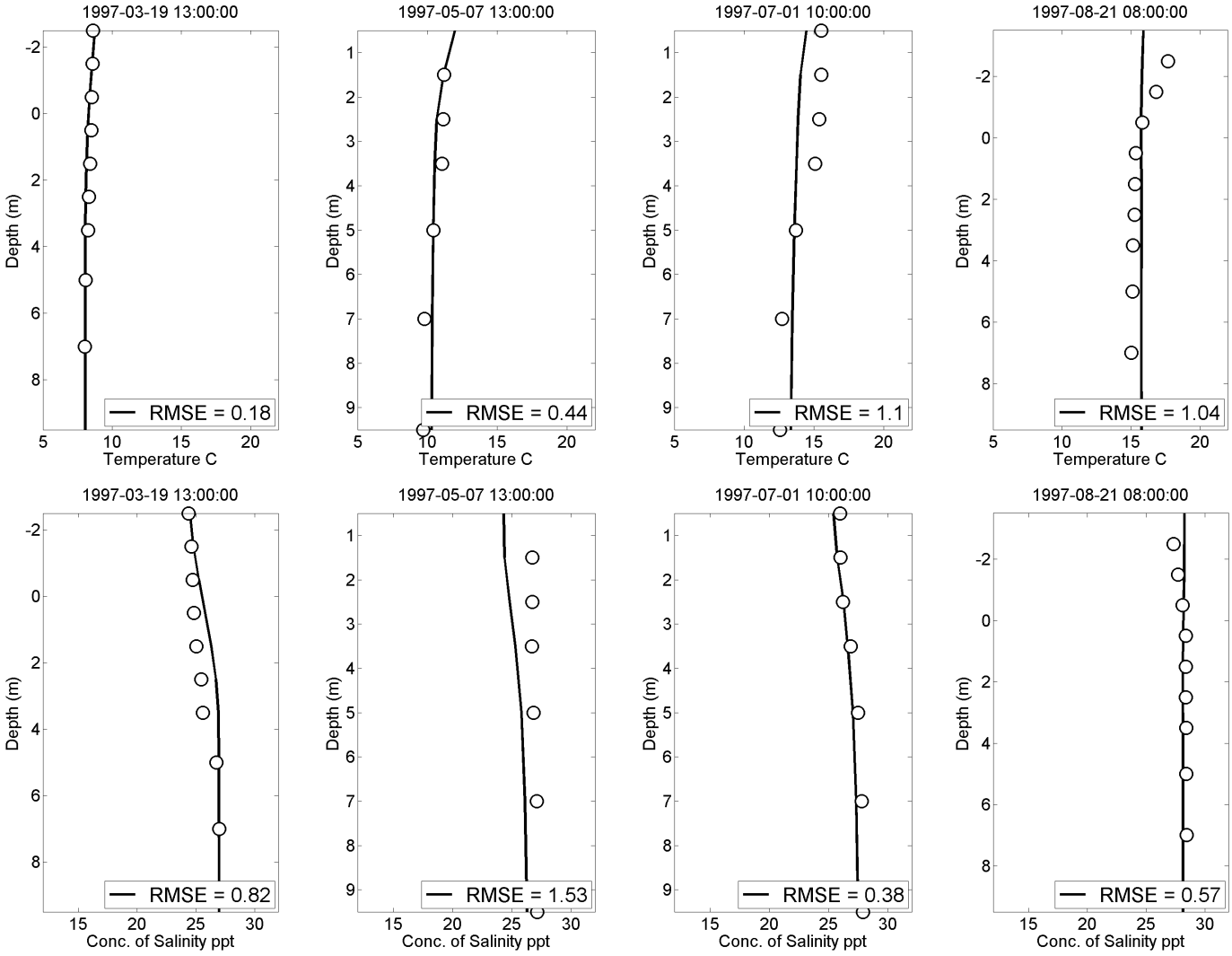

Figure G-28. Station BD-2 profile plots of model-predicted and observed temperature and salinity.

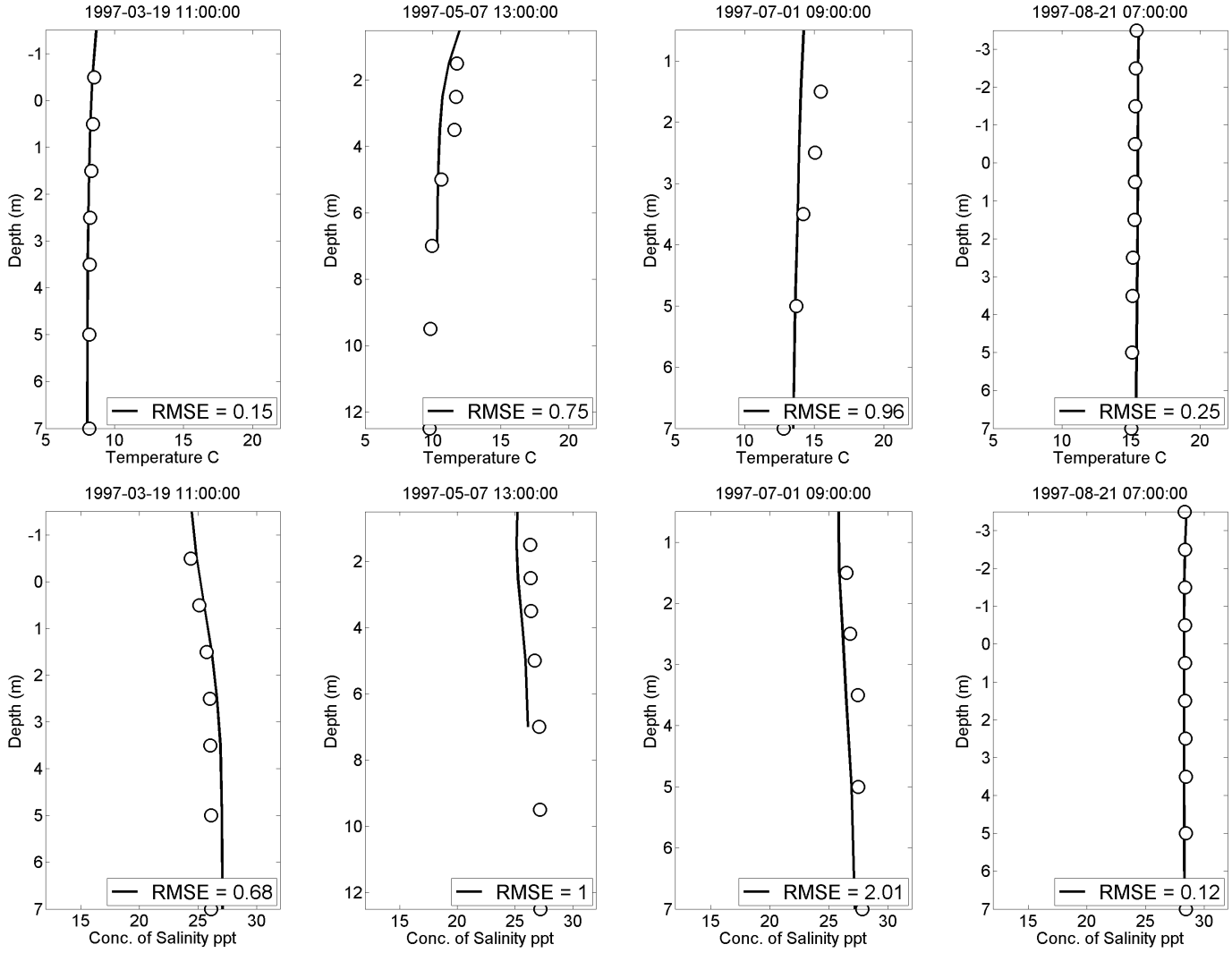

Figure G-29. Station BE-2 profile plots of model-predicted and observed temperature and salinity.

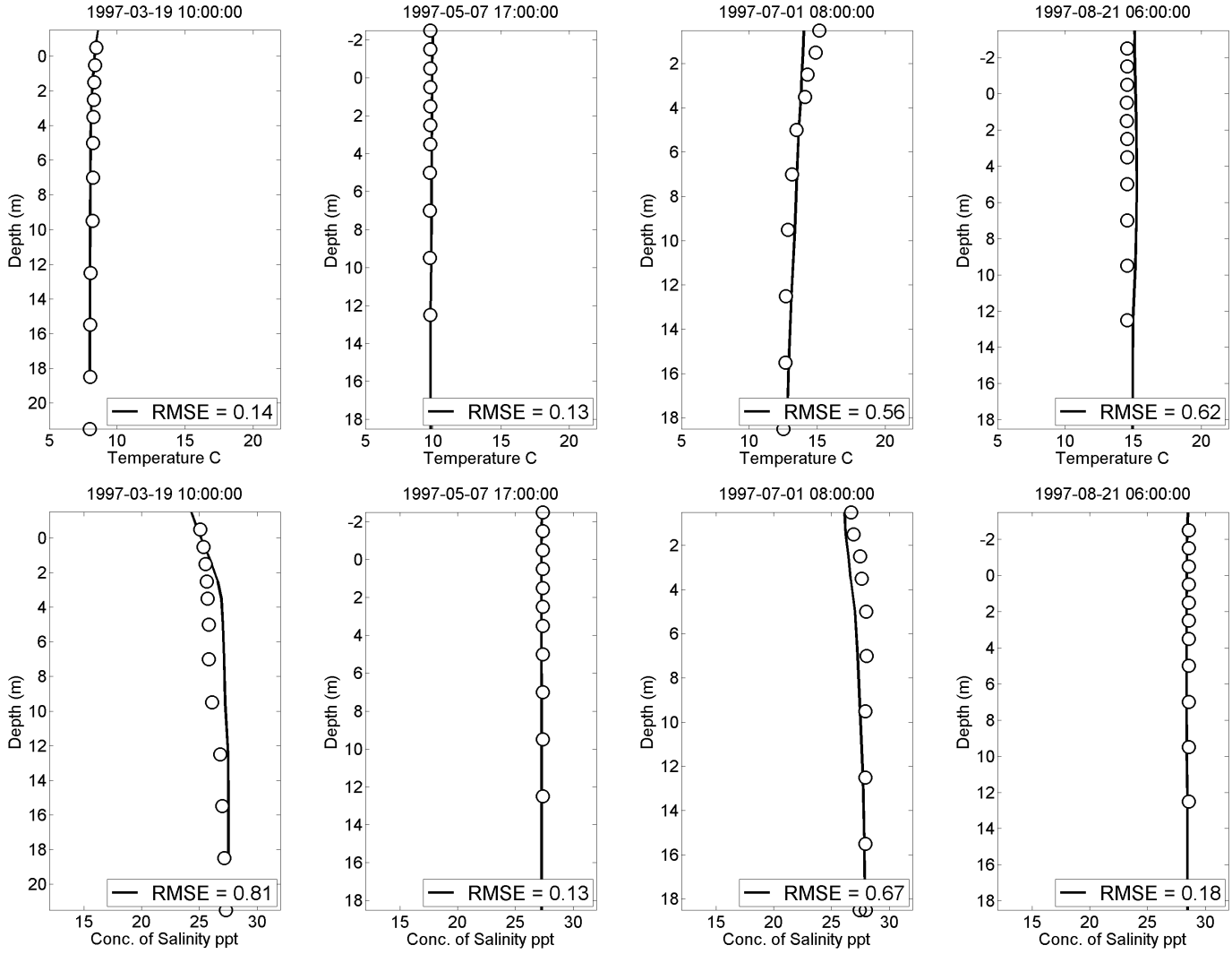

Figure G-30. Station BF-3 profile plots of model-predicted and observed temperature and salinity.

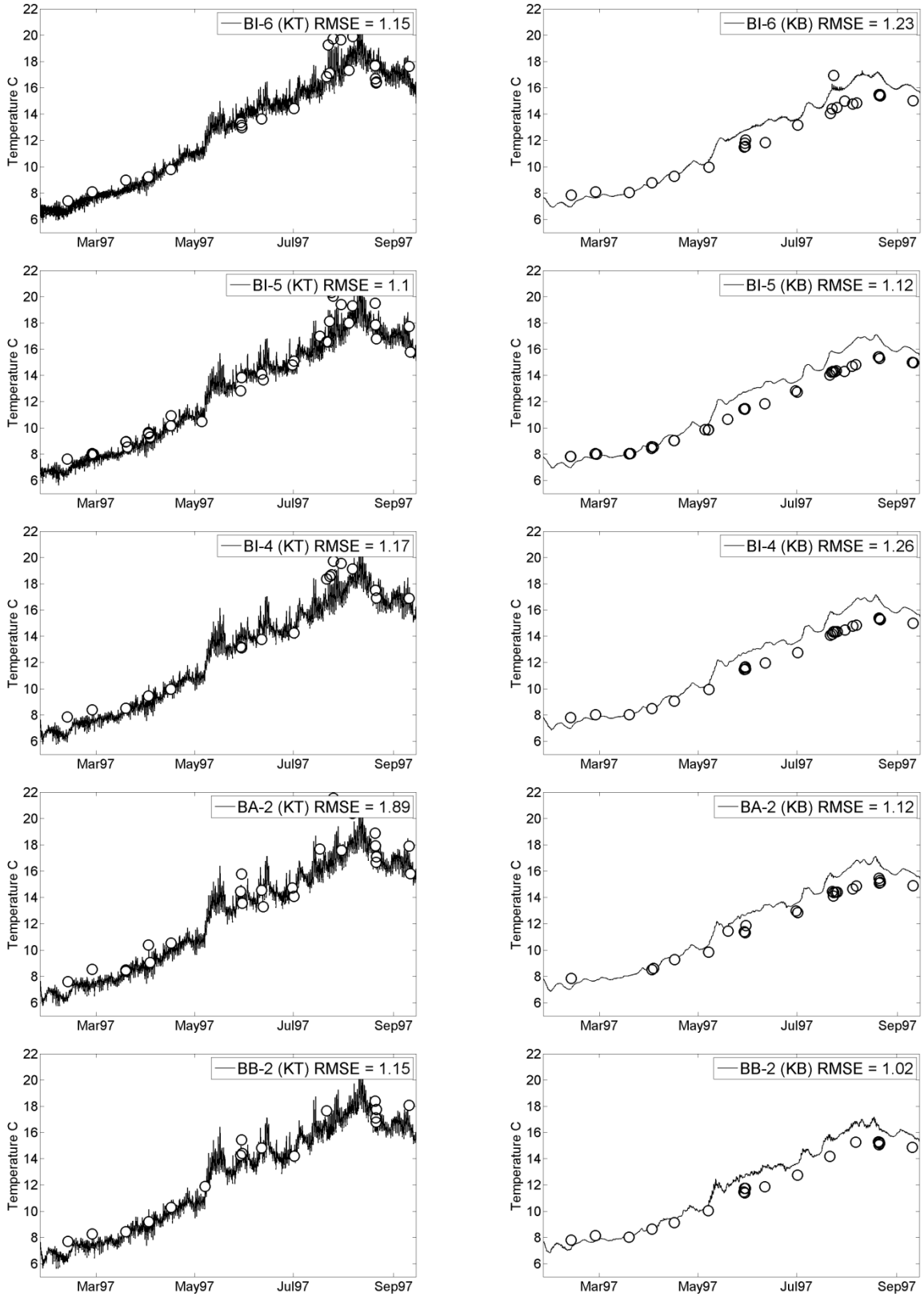

Figure G-31. Time series plots of model-predicted and observed temperature in the surface layer (KT; left plots) and bottom layer (KB; right plots) at stations BI-6, BI-5, BI-4, BA-2, and BB-2.

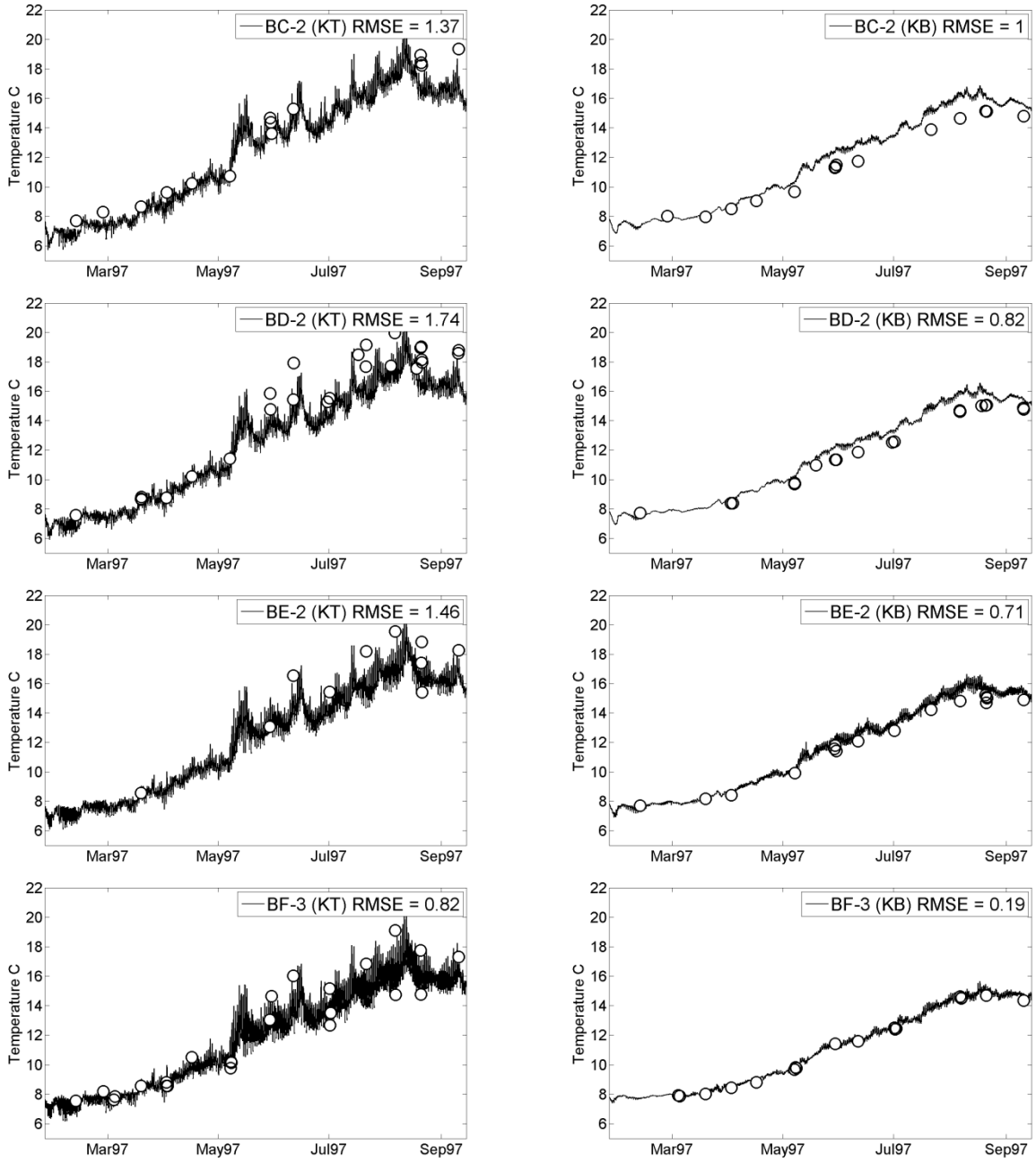

Figure G-32. Time series plots of model-predicted and observed temperature in the surface layer (KT; left plots) and bottom layer (KB; right plots) at stations BC-2, BD-2, BE-2, and BF-3.

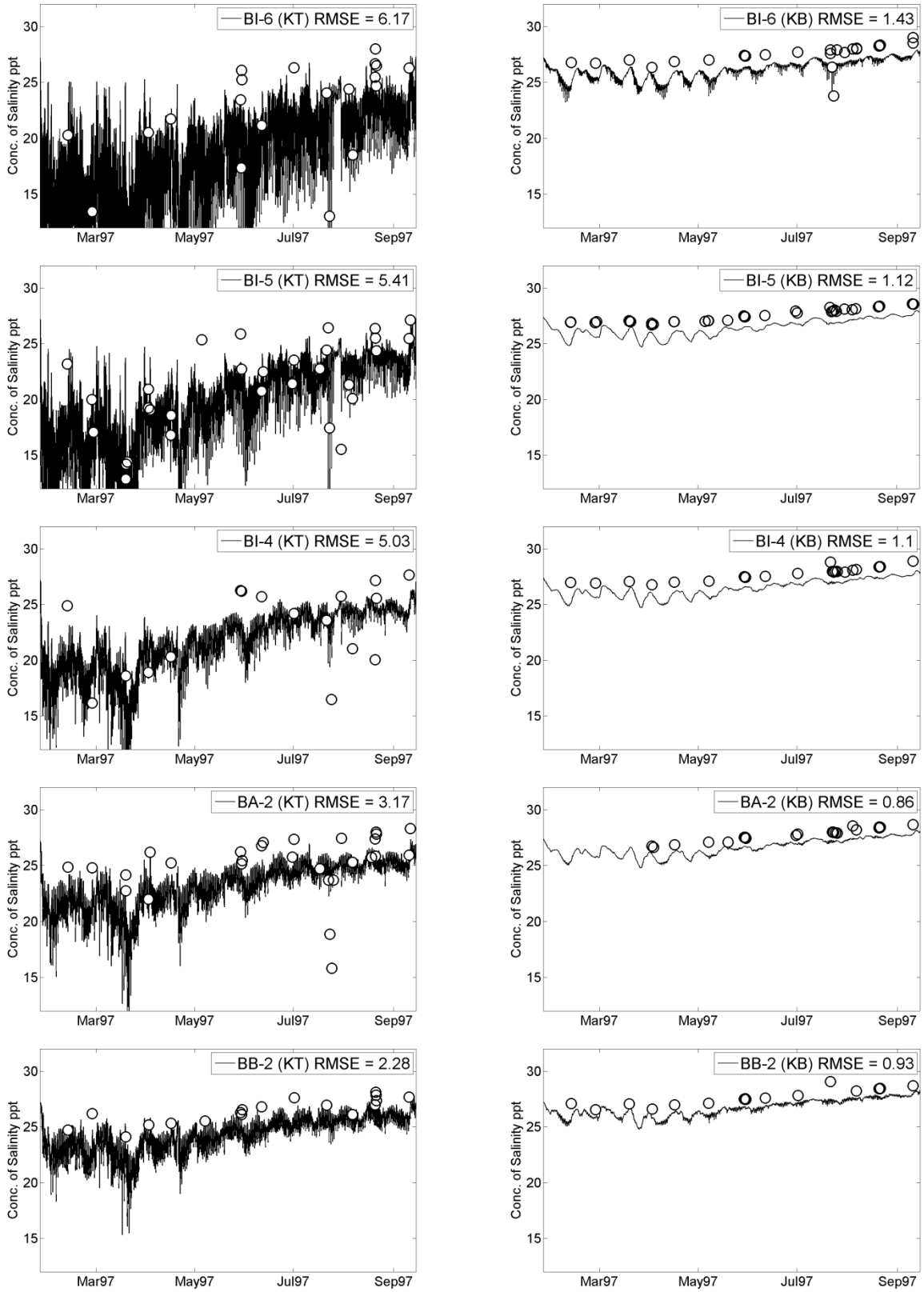

Figure G-33. Time series plots of model-predicted and observed salinity in the surface layer (KT; left plots) and bottom layer (KB; right plots) at stations BI-6, BI-5, BI-4, BA-2, and BB-2.

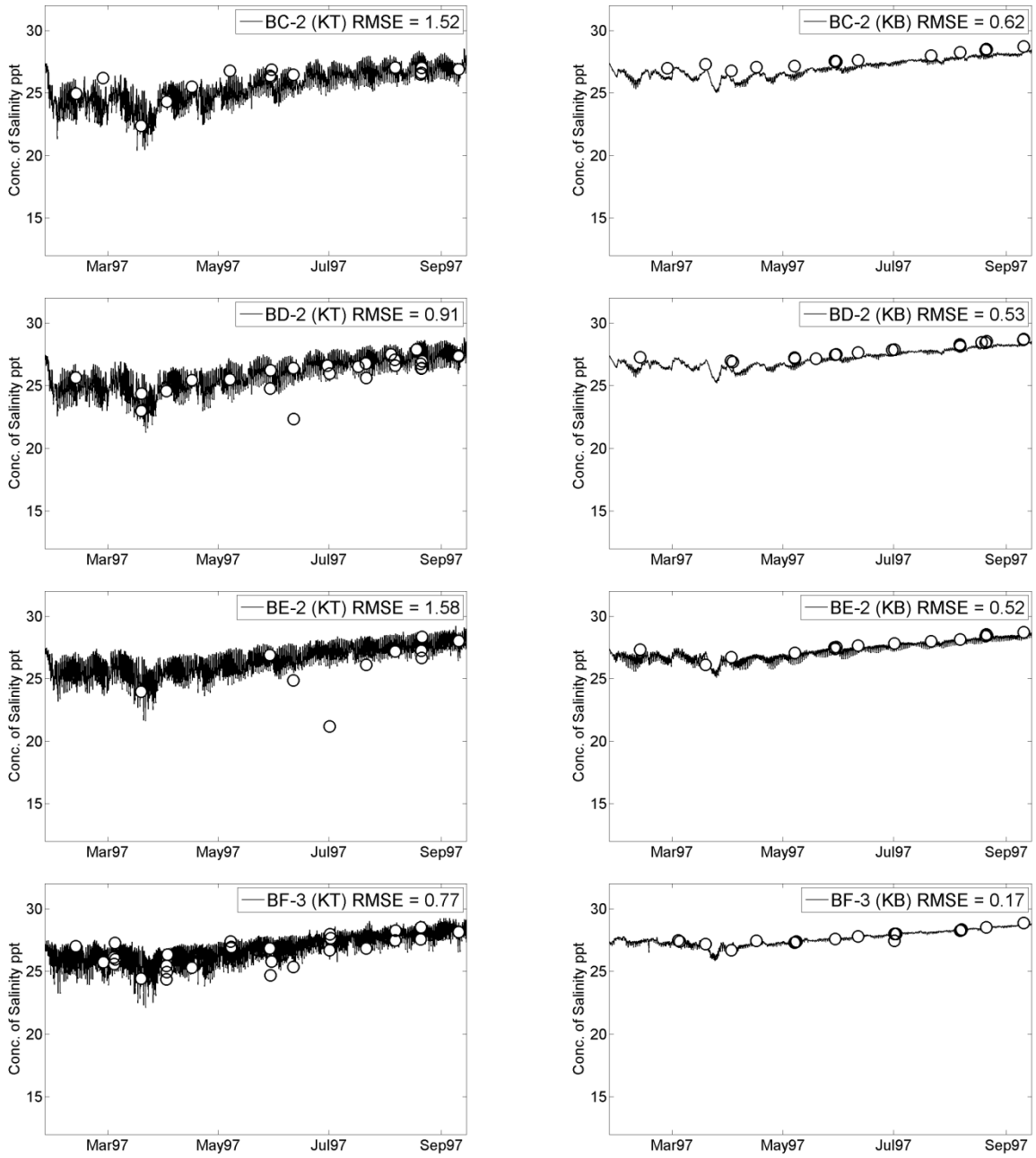

Figure G-34. Time series plots of model-predicted and observed salinity in the surface layer (KT; left plots) and bottom layer (KB; right plots) at stations BC-2, BD-2, BE-2, and BF-3.

Subtidal Estuarine Exchange Flows

The subtidal exchange flow in an estuary is the long-term average flow across a transect such as the open boundary. In a typical estuary the subtidal exchange flow is a positive flow of fresher water out of the estuary on the surface and a negative flow of saltier water into the estuary on the bottom. The interface between the two opposing flows is called the depth of no motion. The outflow on the surface is typically greater than the inflow on the bottom, with the difference representing the net inflow of freshwater from tributaries and precipitation less evaporation. The surface and bottom exchange flows are typically many times greater than the flow of freshwater from tributaries (MacCready and Banas, 2012); in Puget Sound as a whole the ratio of exchange flow to river flow is about 20 (i.e., exchange flow into and out of Puget Sound from/to the ocean is about 20 times greater than the total of all river flows).

The April-September 1997 exchange flow ranged from about 100 m^3/sec for inner Budd Inlet across a transect at Priest Point (station transect BA) to about 500 m^3/sec for all of Budd Inlet across the open boundary transect (station transect BF). The exchange outflows on the surface were greater than the exchange inflows on the bottom by an amount that corresponds to the total tributary flow of about 10 m^3/sec. The range of exchange flows of 100 to 500 m^3/sec corresponds to about 10 to 50 times the total tributary flow of about 10 m^3/sec. The magnitudes of the estuarine exchange flows relative to tributary flows are comparable to findings of previous studies in Budd Inlet and Puget Sound (Aura Nova Consultants et al., 1998).

Final Kinetic Rates and Constants

Tables G-3 through G-5 document the kinetic rates and constants used for the final model re-calibration run. These parameter values were selected from the model run in the final batch of calibration runs with the best overall skill for prediction of observed conditions.

Table G-3 presents final parameter values for the WQCBM module of GEMSS, which includes transformation rates for the various nutrient forms, as well as kinetic rates of the dinoflagellate (DFP) phytoplankton group. The WQCBM module was regionalized during the re-calibration to vary characteristics of DFP in the inner and outer regions of Budd Inlet. However, the strongest calibration was achieved using the same parameter values in each region, and so the parameter values for DFP kinetics in the table are identical for InnerBI and Central/OuterBI.

Rates and constants for the two GAM phytoplankton groups were specified in the GAM, as shown in Table G-4. These values were also regionalized between Inner and Central/OuterBI.

Finally, Table G-5 presents the re-calibration values for other model components, including hydrodynamic and transport processes, dispersion, meteorology, and sediment fluxes.

Table G-3. WQCBM rates for the final re-calibration (from the GEMSS control file).

Parameter	Description	InnerBI	Central/ OuterBI	Unit
General Variables				
Ke_a	Background non-algal light extinction	0.336	0.336	0 : 1/m
Ke_b	Coefficient for chlorophyll for light extinction	0.0365	0.0365	0 : 1/m/ (ugA/L)^Ke_c)
Ke_c	Exponent for chlorophyll for light extinction	0.64	0.64	0 : No Units
NH3	Ammonia			
anc	Nitrogen to Carbon Ratio	0.14	0.14	0 : g N/g C
k71	Organic Nitrogen Mineralization Rate	0.15	0.15	0 : 1/day
th71	Temperature Coefficient	1.07	1.07	No Units
k12	Nitrification Rate	0.12	0.12	0 : 1/day
th12	Temperature Coefficient	1.08	1.08	No Units
knit	Half Saturation Constant for Oxygen Limitation of Nitrification	1	1	0 : g O2/m^3
kmnc	Half Saturation Constant for Nitrogen Mineralization	0.9	0.9	0 : g C/m^3
NO3	Nitrate			
k2d	Denitrification Rate @ 20 °C	0.15	0.15	0 : 1/day
th2d	Temperature Coefficient	1.05	1.05	No Units
DO	Dissolved Oxygen			
SDOEMethod	Surface DO Reaeration Formulation	2 : Chen & Kanwisher	2 : Chen & Kanwisher	
kdf	Deoxygenation Rate @ 20°C for Fast CBOD	0.5	0.5	0 : 1/day
kds	Deoxygenation Rate @ 20°C for Slow CBOD	0.05	0.05	0 : 1/day
ReaerationFactor	Factor to Increase the Reaeration Rate	1	1	No Units
Thtk2	Temperature Correction for Reaeration	1.024	1.024	No Units
CBOD_F	Fast Reacting Dissolved Carbonaceous BOD			
aoc	Oxygen to Carbon Ratio	2.67	2.67	0 : g O2/g C
thd	Temperature Coefficient	1.06	1.06	No Units
kbod	Half Saturation Constant for Oxygen Limitation	0.5	0.5	0 : g O2/m^3
foc	Oxygen from Dead Algae	0.5	0.5	No Units
r_CBODP	Stoichiometric Equivalent Between CBOD and Phosphorous	0.004	0.004	No Units
r_CBODN	Stoichiometric Equivalent Between CBOD and Nitrogen	0.006	0.006	No Units
r_CBODC	Stoichiometric Equivalent Between CBOD and Carbon	0.32	0.32	No Units
CBOD_S	Slow Reacting Dissolved Carbonaceous BOD			
fd5	Fraction of Dead Phyto Recycled to Fast Reacting CBOD	0.75	0.75	No Units
ON_D and ON_P	Dissolved and Particulate Organic Nitrogen			
kh7p	Hydrolysis Rate for Particulate Organic Nitrogen	0.086	0.086	0 : 1/day
thh7p	Temperature Coefficient	1.047	1.047	No Units
fon	Organic Nitrogen from Dead Algae	0.5	0.5	No Units
vs7	Organic Matter Settling Velocity	0.2	0.2	5 : m/day
ancp	Particulate Organic Nitrogen to Carbon Ratio	0.25	0.25	No Units
OP_D and OP_P	Dissolved and Particulate Organic Phosphorus			
kh8p	Hydrolysis Rate for Particulate Organic Phosphorus	0.086	0.086	0 : 1/day
thh8p	Temperature Coefficient	1.047	1.047	No Units
fop	Organic P from Dead Algae; Fraction to Dissolved Component	0.5	0.5	No Units
vs8	Organic Matter Settling Velocity	0.2	0.2	5 : m/day
apcp	Particulate Organic Phosphorus to Carbon Ratio	0.75	0.75	No Units
OC_P_F	Fast Reacting Particulate Organic Carbon			
fd9f	Fraction of Dead Phytoplankton Recycled to Fast Reacting POC	0.4	0.4	No Units

Parameter	Description	InnerBI	Central/ OuterBI	Unit
fg9f	Fraction of Micro-Grazing to Fast Reacting POC	0.4	0.4	No Units
kpd9f	Hydrolysis Rate for Fast Reacting POC	0.08	0.08	0 : 1/day
thpd9p	Temperature Coefficient for the Hydrolysis Rate	1.04	1.04	No Units
vs9	Settling Velocity of Particulate Organic Carbon	0.2	0.2	5 : m/day
OC_P_S	Slow Reacting Particulate Organic Carbon			
fd9s	Fraction of Dead Phytoplankton Recycled to Slow Reacting POC	0.4	0.4	No Units
fg9s	Fraction of Micro-Grazing to Slow Reacting POC	0.4	0.4	No Units
kpd9s	Hydrolysis Rate for Slow Reacting POC	0.02	0.02	0 : 1/day
thpd9s	Temperature Coefficient for the Hydrolysis Rate	1.04	1.04	No Units
OC_P_R	Refractory Particulate Organic Carbon			
fd9r	Fraction of Dead Phytoplankton Recycled to Refractory POC	0.2	0.2	No Units
fg9r	Fraction of Micro-Grazing to Refractory POC	0.2	0.2	No Units
DFP	Dynoflagellates - Phytoplankton	1	1	
c2chla_f	Ratio of Carbon to Chlorophyll a	70	70	No Units
rins_f	Saturating Light Intensity	75	75	0 : cal/m^2-day
kmn_f	Half Saturation Constant for Nitrogen	0.01	0.01	0 : g N/m^3
ZPGMode_f	Zooplankton Grazing Mode	1 : LinearGrazing	1 : LinearGrazing	No Units
kgmicro_f	Grazing Rate due to Microzooplankton	0.04	0.04	0 : 1/day
kgmacro_f	Grazing Rate due to Macrozooplankton	0.0100224	0.0100224	0 : 1/day
thkt_f	Temperature Coefficient	1.04	1.04	No Units
k1d_f	Death Rate	0.02	0.02	0 : 1/day
k1c_f	Maximum Growth Rate	1.5	1.5	0 : 1/day
th1c_f	Temperature Coefficient	1.07	1.07	No Units
kmp_f	Half Saturation Constant for Phosphorus	0.001	0.001	0 : g P/m^3
k1r_f	Endogenous Respiration Rate @ 20 °C	0.1	0.1	0 : 1/day
th1r_f	Temperature Coefficient	1.05	1.05	No Units
vs4_f	Settling Velocity	0.1	0.1	5 : m/day
fe_f	Excretion Fraction of Phytoplankton	0.15	0.15	No Units
as_f	Assimilation Efficiency of Zooplankton Grazing	0.5	0.5	No Units
UseVtemp	Use Temperature Dependent Velocity	1	1	
Vtmax	Maximum Temperature Dependent Velocity	0.000145	0.000145	0 : m/sec
b	Empirical Constant	0.632	0.632	No Units
c	Empirical Constant	2	2	No Units
tL	Lower Temperature Constant °C	11.68	11.68	0 : C
tH	Higher Temperature Constant °C	33	33	0 : C
Voff	Swim Speed Enhancement due to Light During Experiments	0.000035	0.000035	No Units
UseVlight	Use Light Dependent Velocity	1	1	
Vlmax	Maximum Light Dependent Velocity	0.000035	0.000035	0 : m/sec
Alpha	Empirical Constant	10	10	0 : um m^2/uEinst

Table G-4. GAM rates for the final re-calibration (from the GEMSS control file).

Parameter	Description	InnerBI	Central/ OuterBI	Unit
I_GAM1				
UseNutrientLimit	Use Nutrient Limit Function in Growth Computations	1	1	No Units
UseTempLimit	Use Temperature Limit Function in Growth Computations	1	1	No Units
UseSalineToxicLimit	Use Saline Toxicity Limit Function in Growth Computations	0	0	No Units
UseLightLimit	Use Light Limit Function in Growth Computations	1	1	No Units
k1r	Respiration Rate @t 20 °C	0.24	0.075	0 : 1/day
Tht_k1r	Temperature Coefficient	1.05	1.05	No Units
k1c	Growth Rate @ 20 °C	1.5	2.5	0 : 1/day
Tht_k1c	Temperature Coefficient	1	1	No Units
k1d	Death Rate @ 20 °C	0.03	0.03	0 : 1/day
fe	Excretion Fraction	0.08	0.05	No Units
as	Assimilation Efficiency of Zooplankton Grazing	0.5	0.5	No Units
ws	Settling Velocity	0.5	0.5	5 : m/day
ZPGMode	Zooplankton Grazing Mode	1 : LinearGrazing	1 : LinearGrazing	No Units
kgmicro	Grazing Rate due to Micro Zooplankton	0.11	0.11	0 : 1/day
Tht_kgmicro	Temperature Coefficient	1.04	1.04	No Units
kgmacro	Grazing Rate due to Macro Zooplankton	0.01	0.01	0 : 1/day
Tht_kgmacro	Temperature Coefficient	1.04	1.04	No Units
cchl	Carbon to Chlorophyll Ratio	50	50	0 : gC/gChl-a
LightModel	Light Model	3 : Steele Equation	3 : Steele Equation	No Units
kke	Light Extinction Coefficient	1	1	No Units
kechl	Light Attenuation Coefficient	17	17	0 : m^2/mg
lsat	Light Constant	40	40	0 : langleys/day
khn	Constant for Algae Nitrogen Uptake	0.024	0.024	0 : gm N/m^3
khp	Constant for Algae Phosphorous Uptake	0.00001	0.00001	0 : gm P/m^3
stMethod	Salinity Toxicity Method	1 : Equation_1	1 : Equation_1	
stf	Maximum Mortality due to Salinity Toxicity	0.01	0.01	0 : 1/day
khst	Salinity at which Toxicity is Half the Maximum Value	0.5	0.5	0 : ppt
tm	Optimum Temperature for Algae Growth	9.5	9.5	0 : C
ktg1	Suboptimal Temperature Effect for Algae Growth	0.035	0.035	No Units
ktg2	Superoptimal Temperature Effect for Algae Growth	0.024	0.024	No Units
fd5	Fraction of Dead Phytoplankton Recycled to Fast CBOD	0.75	0.75	No Units
fon	Organic Nitrogen from Dead Algae	0.5	0.5	No Units
fop	Organic Phosphorous from Dead Algae	0.5	0.5	No Units
foc	Organic carbon from dead algae	0.5	0.5	No Units
I_GAM2				
UseNutrientLimit	Use Nutrient Limit Function in Growth Computations	1	1	No Units
UseTempLimit	Use Temperature Limit Function in Growth Computations	1	1	No Units
UseSalineToxicLimit	Use Saline Toxicity Limit Function in Growth Computations	0	0	No Units
UseLightLimit	Use Light Limit Function in Growth Computations	1	1	No Units
k1r	Respiration Rate @t 20 °C	0.6	0.05	0 : 1/day
Tht_k1r	Temperature Coefficient	1.05	1.05	No Units
k1c	Growth Rate @ 20 °C	1.5	3	0 : 1/day
Tht_k1c	Temperature Coefficient	1	1	No Units
k1d	Death Rate @ 20 °C	0.03	0.03	0 : 1/day
fe	Excretion Fraction	0.08	0.05	No Units
as	Assimilation Efficiency of Zooplankton Grazing	0.5	0.5	No Units
ws	Settling Velocity	0.2	0.2	5 : m/day

Parameter	Description	InnerBI	Central/ OuterBI	Unit
ZPGMode	Zooplankton Grazing Mode	1 : LinearGrazing	1 : LinearGrazing	No Units
kgmicro	Grazing Rate due to Micro Zooplankton	0.04	0.04	0 : 1/day
Tht_kgmicro	Temperature Coefficient	1.04	1.04	No Units
kgmacro	Grazing Rate due to Macro Zooplankton	0.01	0.01	0 : 1/day
Tht_kgmacro	Temperature Coefficient	1.04	1.04	No Units
cchl	Carbon to Chlorophyll Ratio	50	50	0 : gC/gChl-a
LightModel	Light Model	3 : Steele Equation	3 : Steele Equation	No Units
kke	Light Extinction Coefficient	1	1	No Units
kechl	Light Attenuation Coefficient	17	17	0 : m^2/mg
lsat	Light Constant	70	70	0 : langleys/day
khn	Constant for Algae Nitrogen Uptake	0.028	0.028	0 : gm N/m^3
khp	Constant for Algae Phosphorous Uptake	0.00001	0.00001	0 : gm P/m^3
stMethod	Salinity Toxicity Method	1 : Equation_1	1 : Equation_1	
stf	Maximum Mortality due to Salinity Toxicity	0.01	0.01	0 : 1/day
khst	Salinity at which Toxicity is Half the Maximum Value	0.5	0.5	0 : ppt
tm	Optimum Temperature for Algae Growth	16.5	16.5	0 : C
ktg1	Suboptimal Temperature Effect for Algae Growth	0.03	0.03	No Units
ktg2	Superoptimal Temperature Effect for Algae Growth	0.03	0.03	No Units
fd5	Fraction of Dead Phytoplankton Recycled to Fast CBOD	0.75	0.75	No Units
fon	Organic Nitrogen from Dead Algae	0.5	0.5	No Units
fop	Organic Phosphorous from Dead Algae	0.5	0.5	No Units
foc	Organic Carbon from Dead Algae	0.5	0.5	No Units

Table G-5. Other constants and settings for the final re-calibration.

Parameter	Description	Value
Hydrodynamic and Transport		
Coriolis Forcing Term	Reference Latitude (degrees)	47.5
Wind Stress Coefficient	Method	Wu (1983)
Bottom Friction	Method	Chezy
	Chezy Coefficient	Constant
	Limiting Chezy Selector	0
	Czo = (units m^1/2/sec)	20
Transport Modeling Scheme	Scheme	Upwind First Order
	Advection Theta in Z-Direction	0
	Diffusion Theta in Z-Direction	0
Wetting and Drying of Layers	Wetting Limiting Thickness Factor	0.85
	Drying Limiting Thickness Factor	0.8
Density	Density Function	Gill (1982)
Dispersion		
Vertical Momentum Dispersion	Scheme	0-Equation
	Mixing Length	Von Karman
Momentum Dispersion Coef. (m^2/sec)	X-Direction	Okubo
	Axo =	0.00584
	n(x) =	1.1
	Y-Direction	Okubo
	Ayo =	0.0054
	n(y) =	1.1
Transport Diffusion Coef. (m^2/sec)	X-Direction	Prandtl
	Y-Direction	Prandtl
	Prandtl Number	10
Meteorology		
	Input Data Type for Meteorology	2 : Time Varying Data
	Time Varying Input Data Interpolation Scheme for M	1 : Linear Interpolation Between Time t1 and t2
wsc_v	Wind Sheltering Coefficient wsc Value	0.8
sd_v	Secchi Depth sd Value	1
rscc	Compute Solar Radiation Using Cloud Cover	0
rsts_v	Vegetative and Topographic Shading Factor rsts Value	0
ishe	Surface Heat Exchange Method	2 : Term by Term
KEMethod	Compute K & E in the Model	0
cshe	Surface Heat Exchange Coefficient Unit	0 : w/m2/C
cshe_v	Surface Heat Exchange Coefficient	30
te	Equilibrium Temperature Unit	0 : C
te_v	Equilibrium Temperature Value	21
PAR	Fraction of Solar Radiation in the Range of 400 to 700 nm	0.43
Albedo	Fraction of Solar Radiation Reflected from the Water Surface	0.07
iwsf	Wind Speed Function	1 : Brady
BetaMethod	Method to Compute Fraction of Solar Energy Absorbed at Sfc	1 : Linear Relation
Beta	Fraction of Solar Energy Absorbed at the Surface	0.43
Gamma_A	Light Attenuation Parameter a	1.2
Gamma_B	Light Attenuation Parameter b	0.6
Sediment Flux of DO		
	Region A	-2.0 g/m^2/day
	Region B	-2.5 g/m^2/day
	Region C	-2.5 g/m^2/day
	Region D	-1.0 g/m^2/day

Conclusion

The calibrated Budd Inlet model obtained from ERM (Kolluru, 2006a) was evaluated following amendment and testing of the model code (Appendix K), improvements to the model framework, and extensive review of the model inputs and target calibration data. It was determined that ERM calibration was no longer appropriate, and a rigorous re-calibration effort was carried out to improve the capability of the model to simulate observed water quality and hydrodynamic conditions in Budd Inlet.

The water quality parameter of primary concern to Ecology and the focus of the re-calibration effort was dissolved oxygen. In particular, the main purpose of the re-calibration of the model was to provide a tool to accurately predict the response of critical bottom DO concentrations in inner Budd Inlet in response to variations in nutrient loading and phytoplankton kinetics. The model is considered to be adequate for this purpose.

References

Aura Nova Consultants, Inc. and J.E. Edinger Associates, Inc. 1998. Budd Inlet Scientific Study Final Report. August, 1998.

Aura Nova Consultants, Inc. and J.E. Edinger Associates, Inc. 1999. LOTT NPDES Permit Modifications Modeling Revised Interim Report. November 24, 1999.

Brown, L.C., and T.O. Barnwell. 1987. The enhanced stream water quality models QUAL2E and QUAL2E-UNCAS: documentation and user manual. EPA/600/3-87/007.

Chapra, S.C. 1997. Surface Water Quality Modeling. McGraw-Hill Publishers.

J.E. Edinger Associates, Inc. 2000. Budd Inlet Water Quality Modeling – Correction Report. April 25, 2000.

J.E. Edinger Associates, Inc. 2005. Budd Inlet & Capitol Lake Hydrodynamic & Water Quality Modeling, Task 1: First Phase Interim Report. June 24, 2005.

Kolluru, Venkat. 2006a. Appendix A: Comparison of GEMSS Results and Field Data. Personal communication (email) to Greg Pelletier, Washington State Department of Ecology. January 18, 2006. Environmental Resources Management, Inc.

Kolluru, Venkat. 2006b. Appendix B: Results from Previous Modeling Results. Personal communication (email) to Greg Pelletier, Washington State Department of Ecology. January 18, 2006. Environmental Resources Management, Inc.

MacCready, P. and N.S. Banas. 2012. Residual circulation, mixing, and dispersion. Estuary Treatise Chapter 2.5. University of Washington, Department of Oceanography. Elsevier ESCO 00205.
http://faculty.washington.edu/pmacc/PM_Papers/MacCready_Banas_2011_Treatise_Galleys.pdf

Prakash, S., and V.S. Kolluru. 2008. Capitol Lake Water Quality Calibration and Verification. Memorandum to Greg Pelletier, Washington State Department of Ecology. February 28, 2008. Environmental Resources Management, Inc.

Ryan, P.J. and K.D. Stolzenbach. 1972. Engineering aspects of heat dispersal from power generation, (D.R.F. Harleman, ed.). R.M. Parson Laboratory for Water Resources and Hydrodynamics, Department of Civil Engineering, Massachusetts Institute of Technology, Cambridge, MA.

Appendix G.2. Budd Inlet Model: Water Quality Time Series

XPI_BI_GAMDFP_base016_000_newGLLVHT.nc, BI−6 (K = KB)

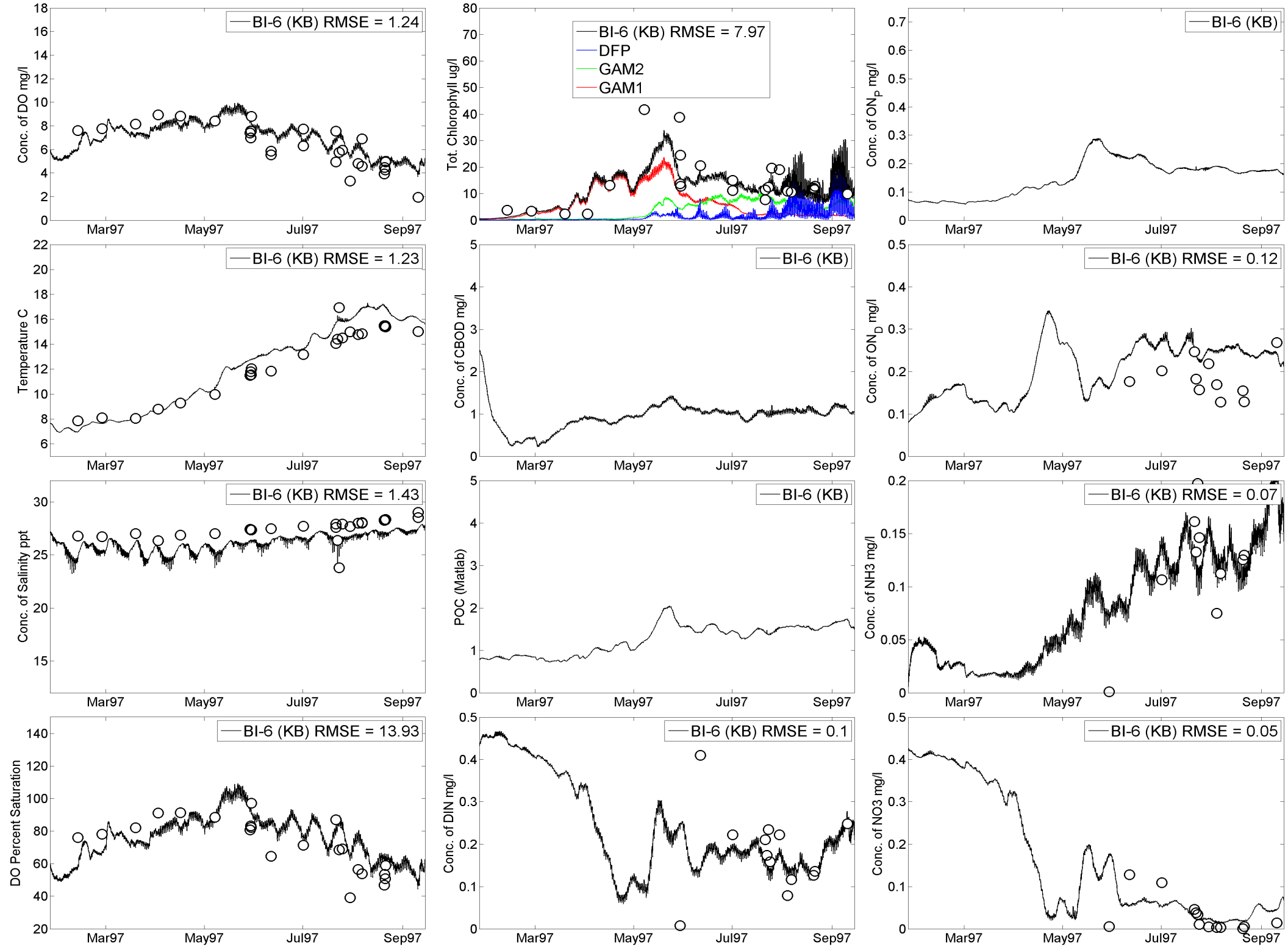

XPI_BI_GAMDFP_base016_000_newGLLVHT.nc, BI−6 (K = 8)

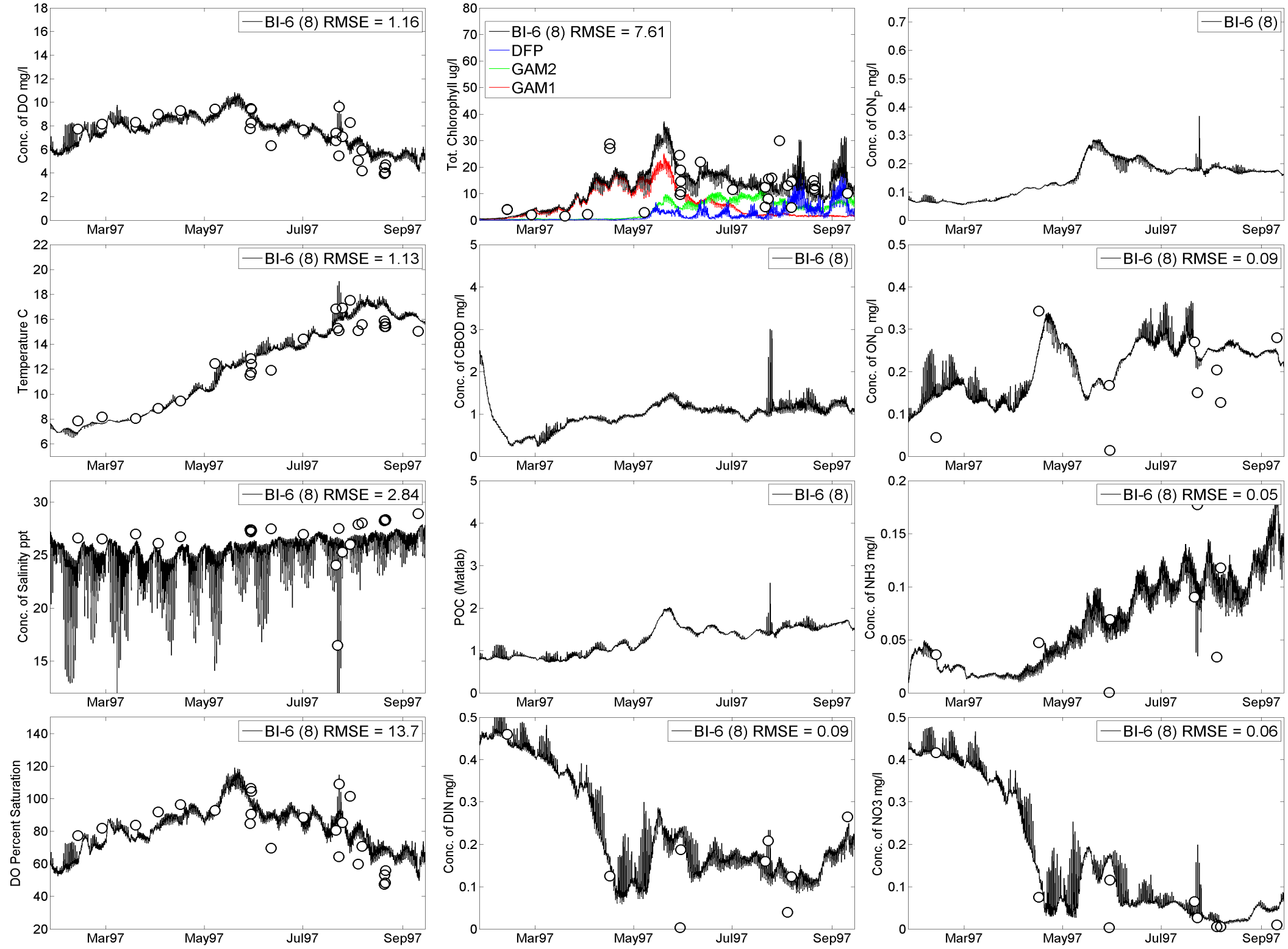

XPI_BI_GAMDFP_base016_000_newGLLVHT.nc, BI−6 (K = KT)

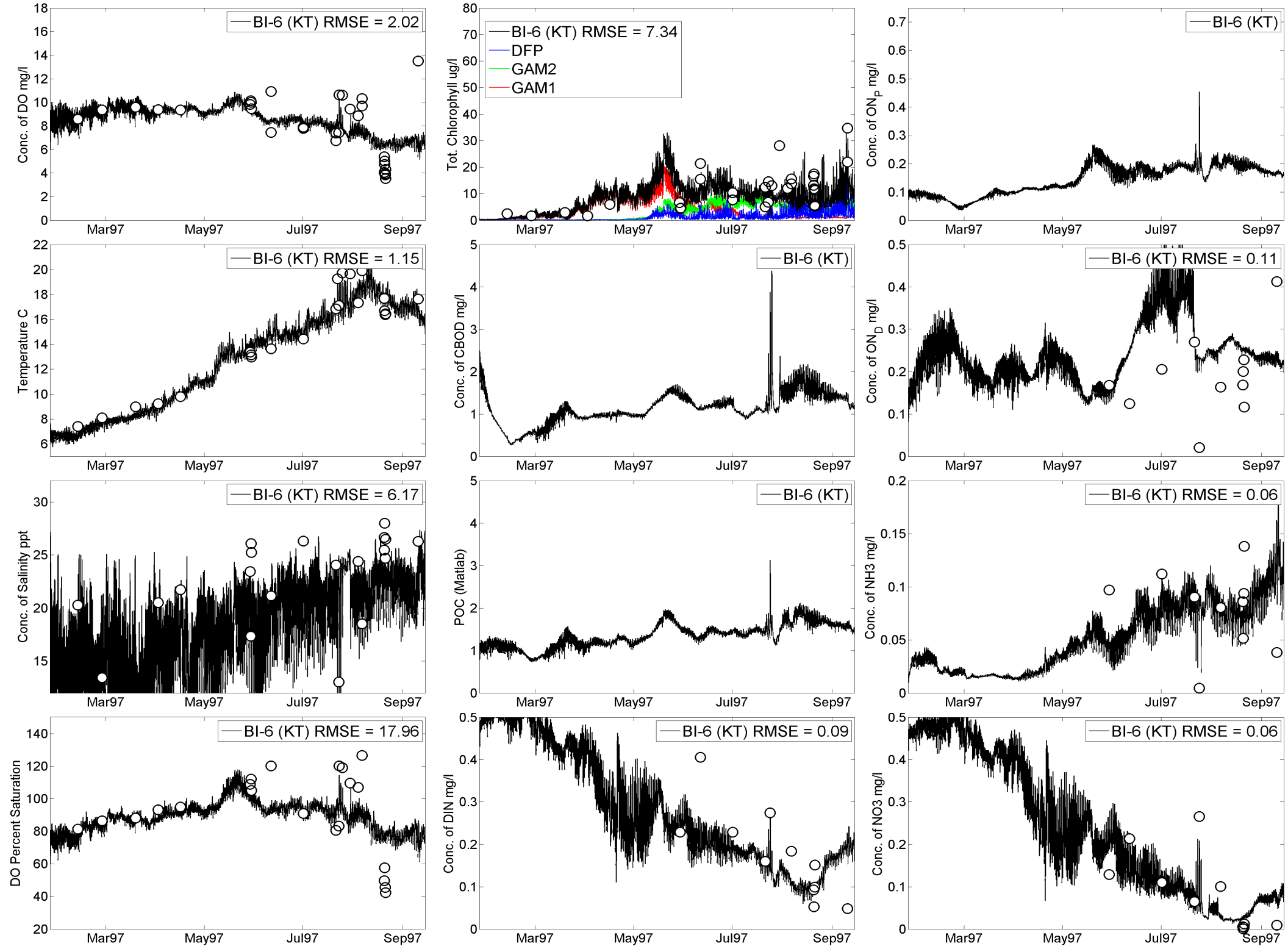

XPI_BI_GAMDFP_base016_000_newGLLVHT.nc, BI−5 (K = KB)

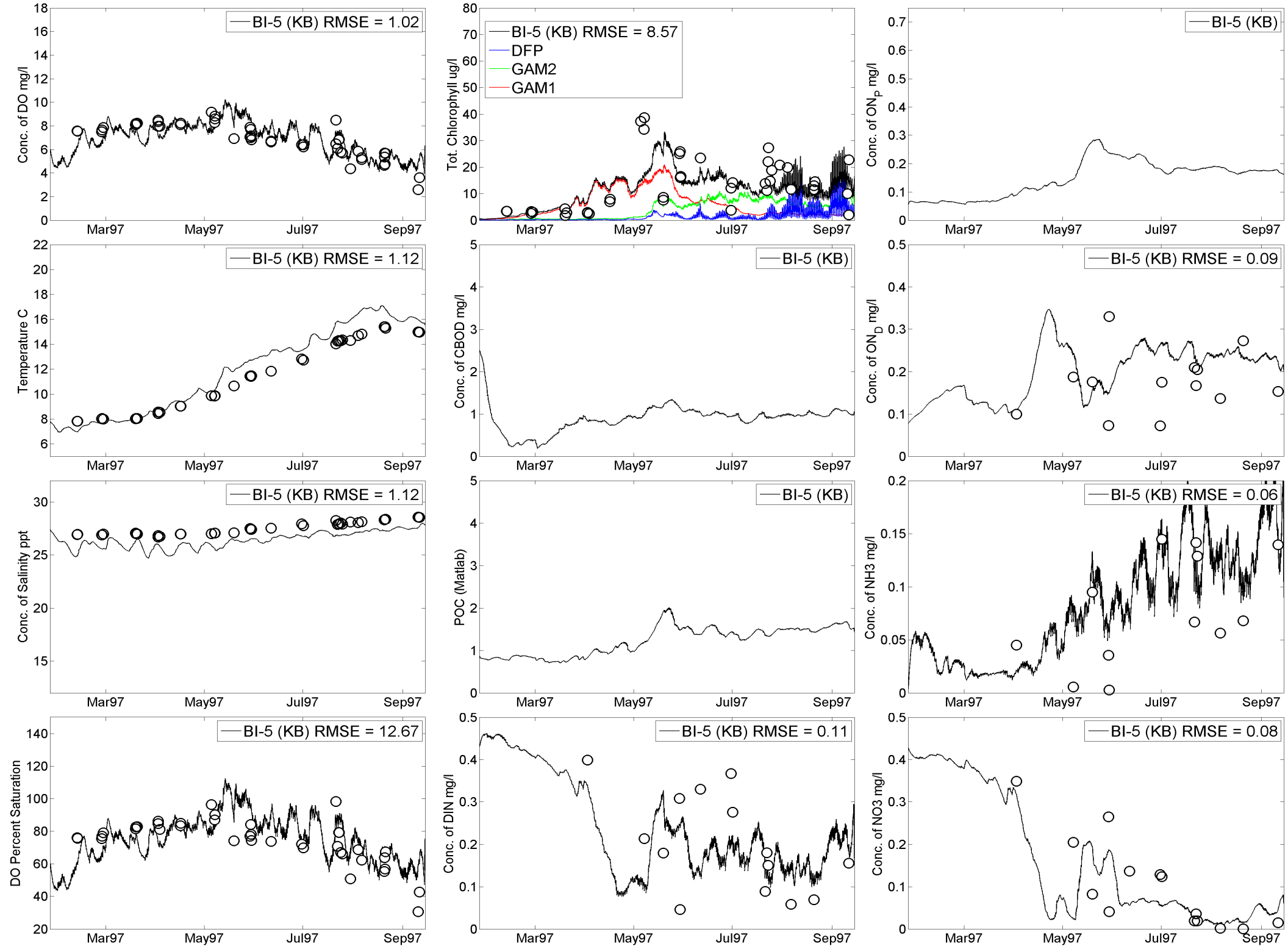

XPI_BI_GAMDFP_base016_000_newGLLVHT.nc, BI−5 (K = 10)

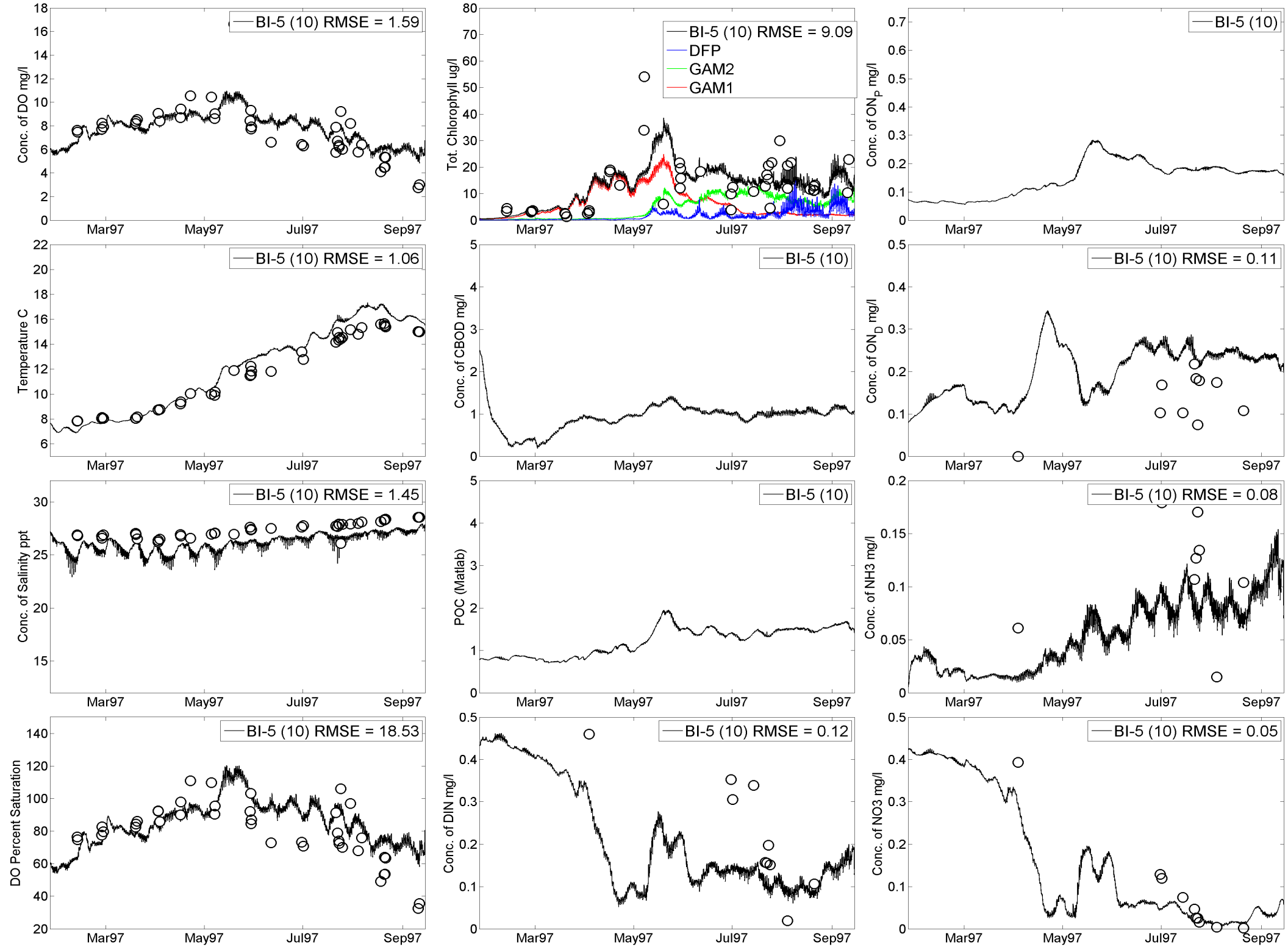

XPI_BI_GAMDFP_base016_000_newGLLVHT.nc, BI−5 (K = KT)

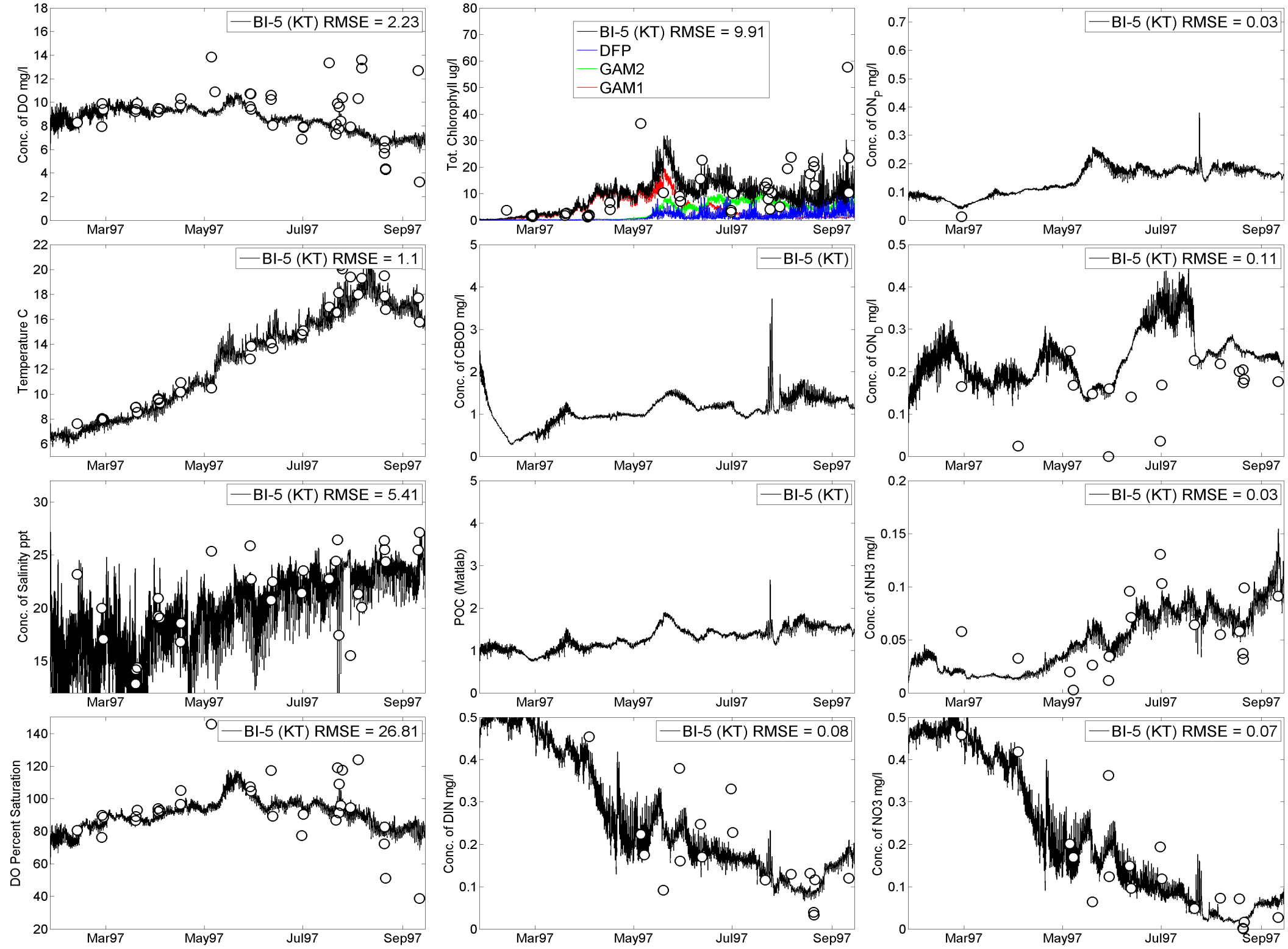

XPI_BI_GAMDFP_base016_000_newGLLVHT.nc, BI−4 (K = KB)

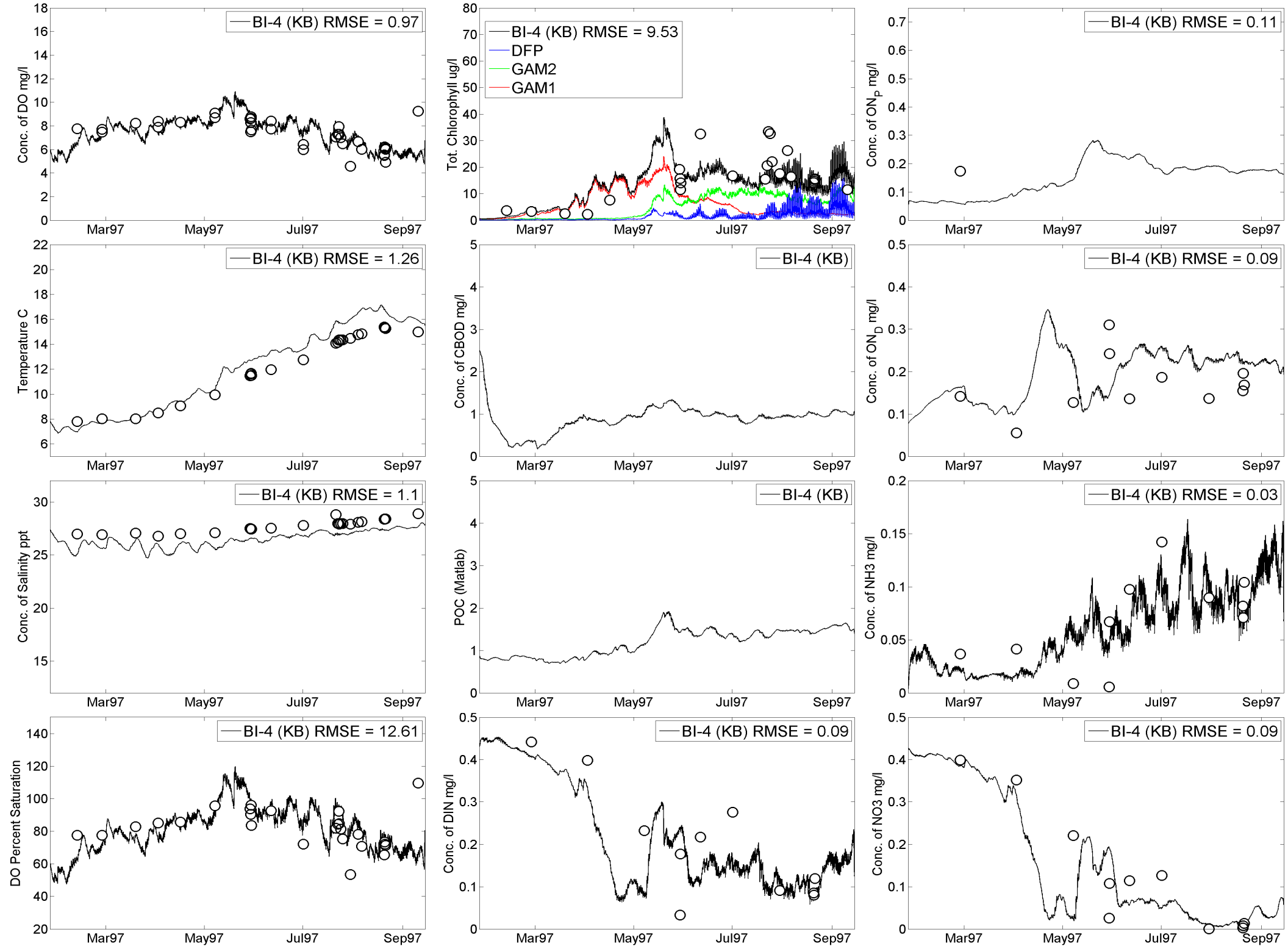

XPI_BI_GAMDFP_base016_000_newGLLVHT.nc, BI−4 (K = 10)

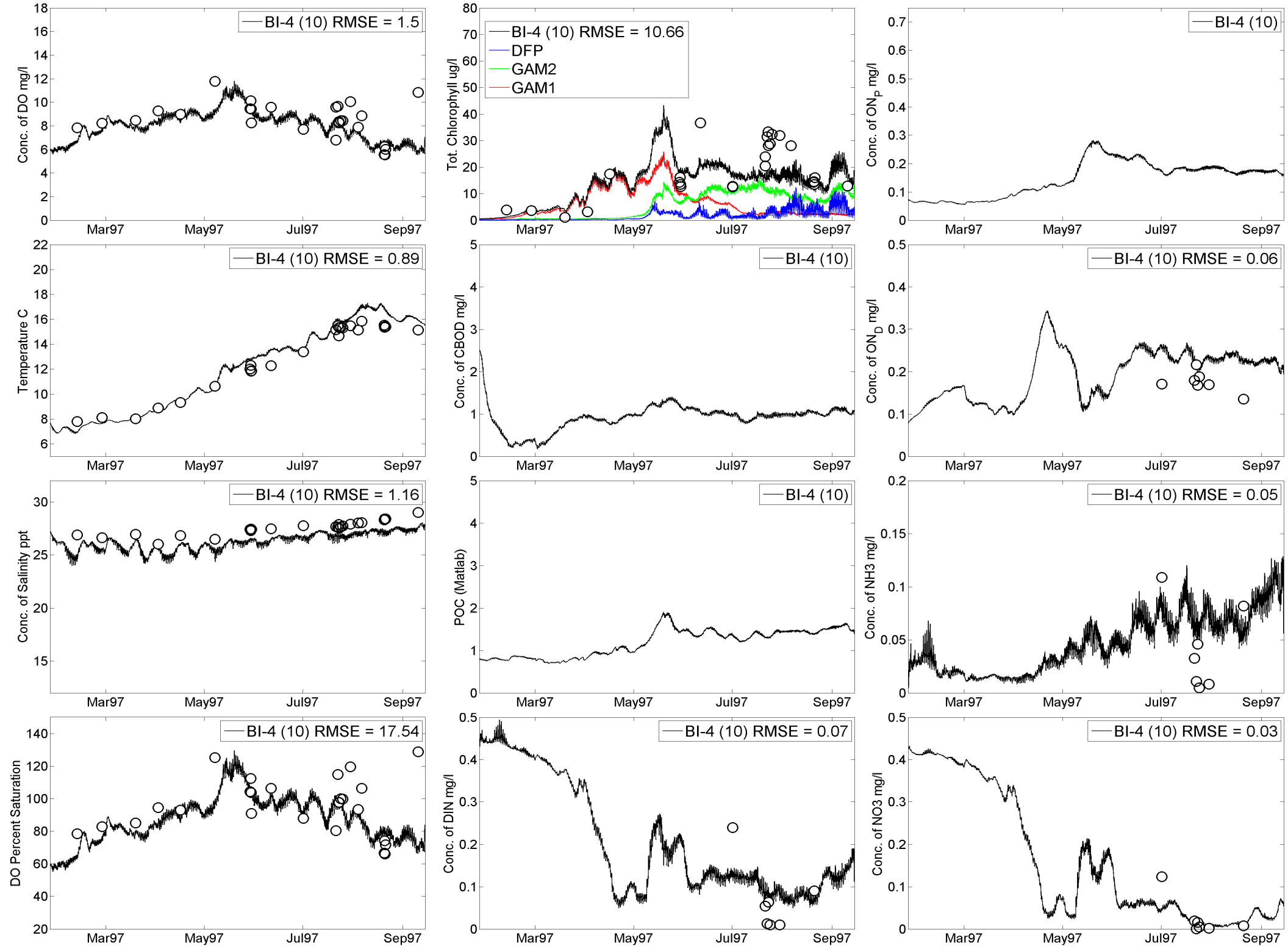

XPI_BI_GAMDFP_base016_000_newGLLVHT.nc, BI−4 (K = KT)

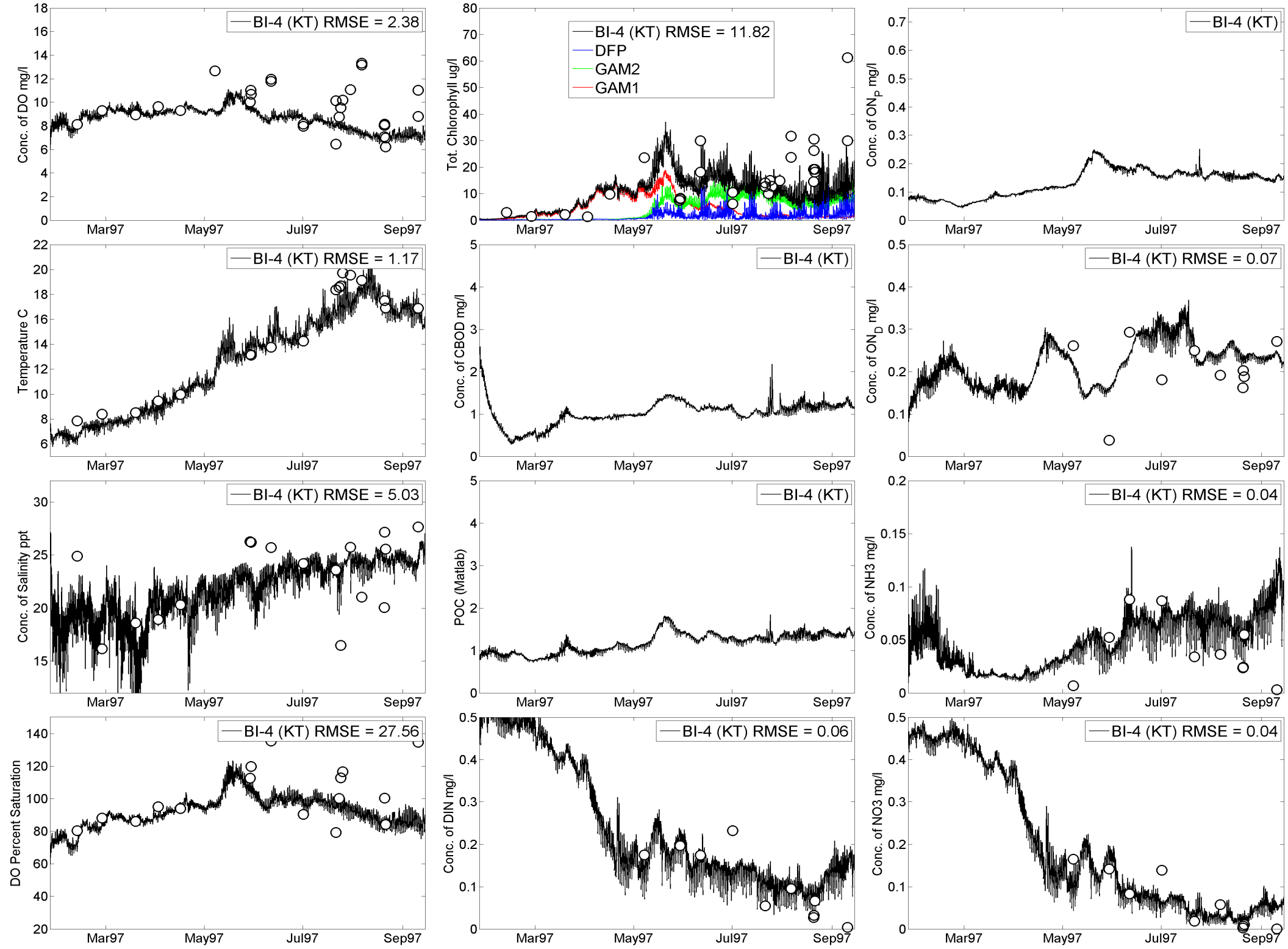

XPI_BI_GAMDFP_base016_000_newGLLVHT.nc, BI−2 (K = KB)

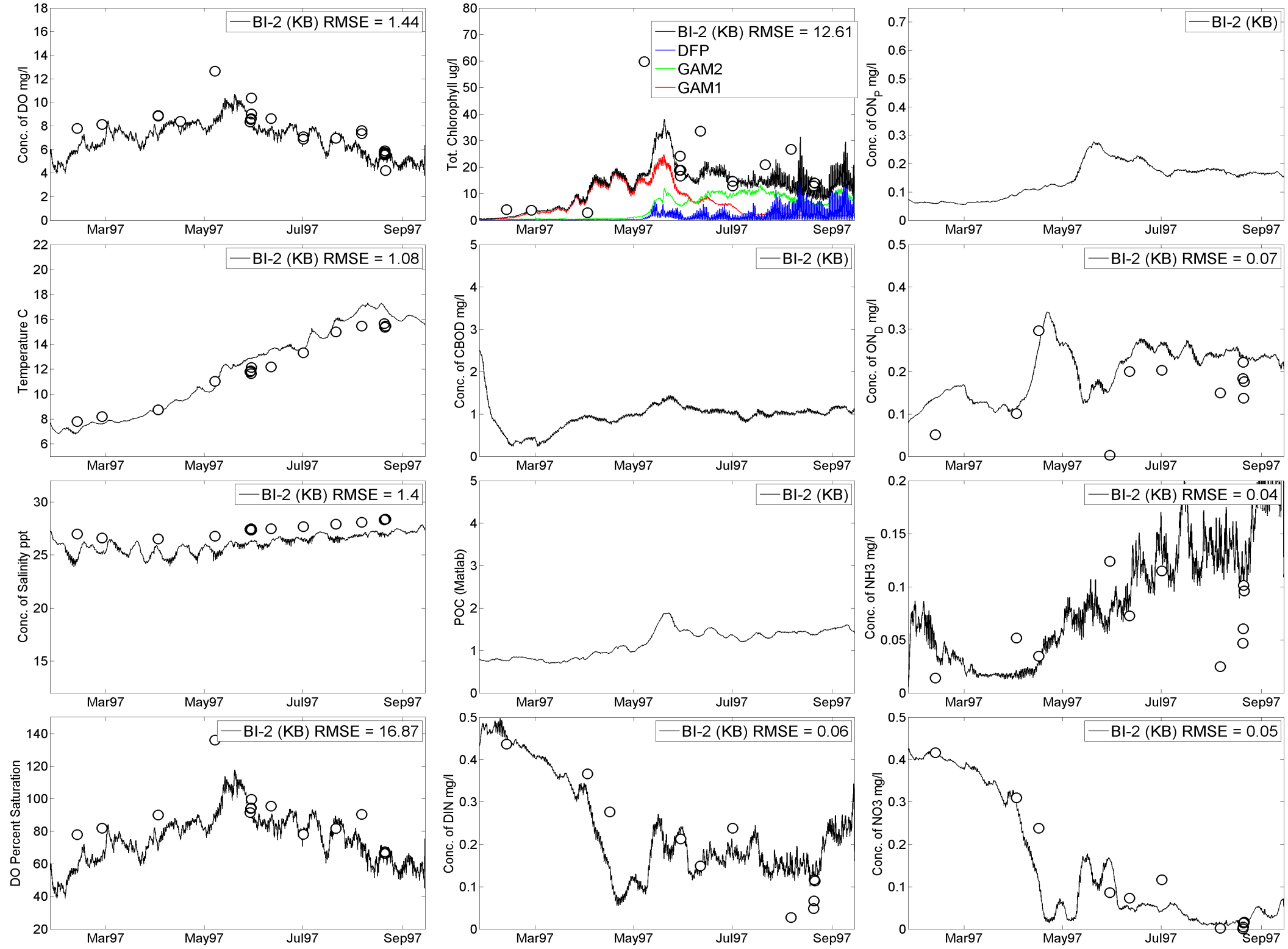

XPI_BI_GAMDFP_base016_000_newGLLVHT.nc, BI−2 (K = 9)

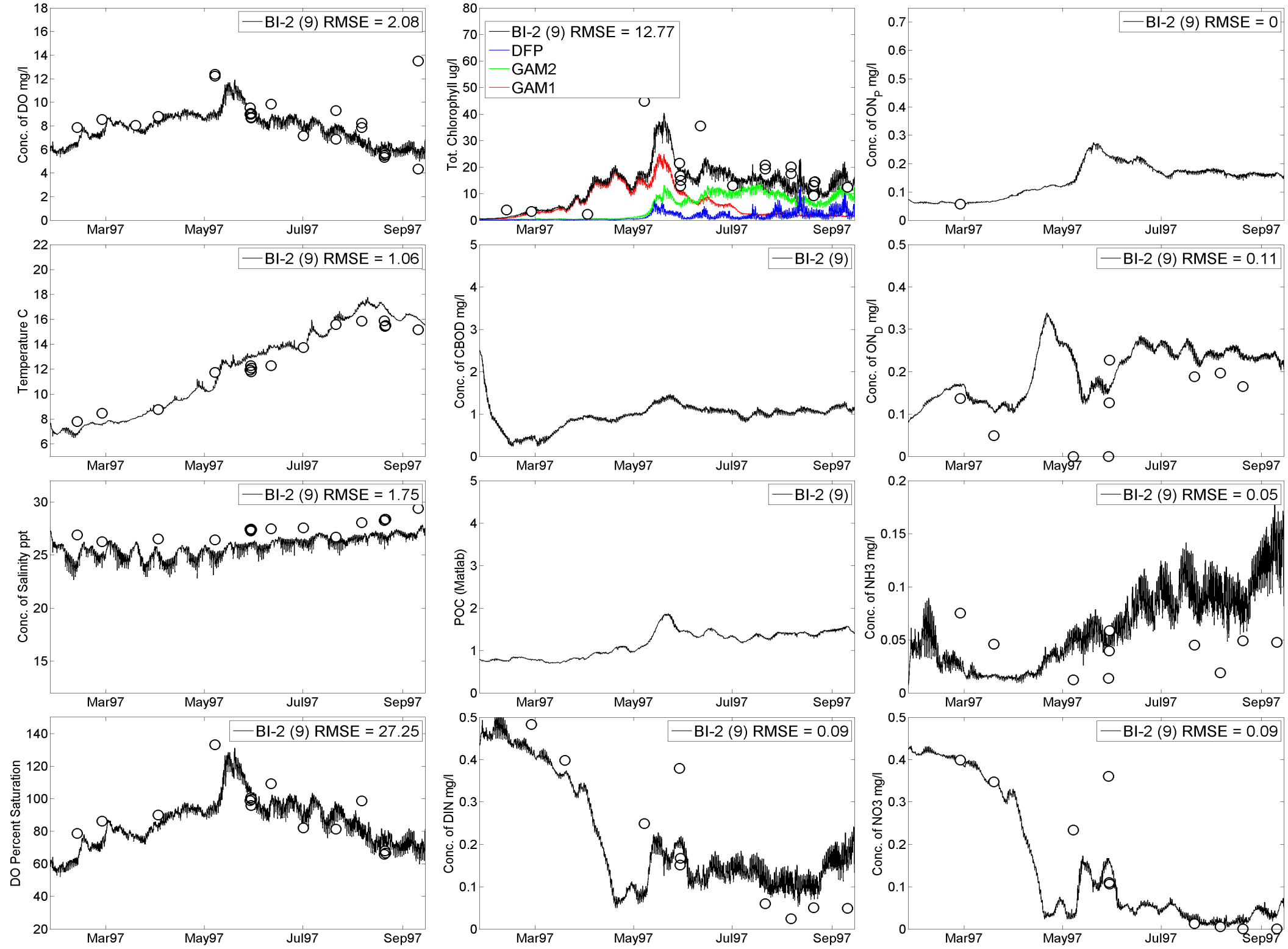

XPI_BI_GAMDFP_base016_000_newGLLVHT.nc, BI−2 (K = KT)

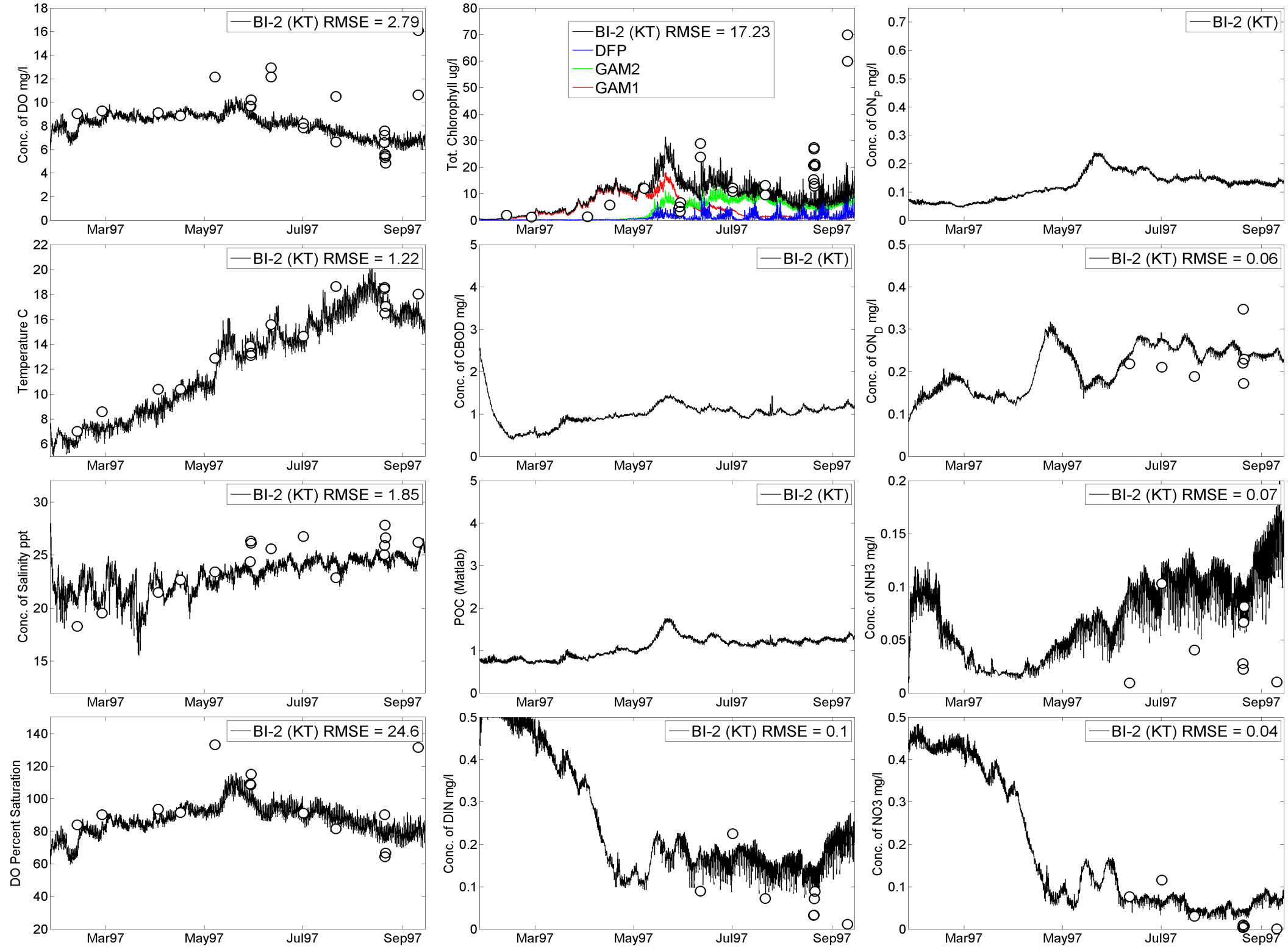

XPI_BI_GAMDFP_base016_000_newGLLVHT.nc, BI−1 (K = KB)

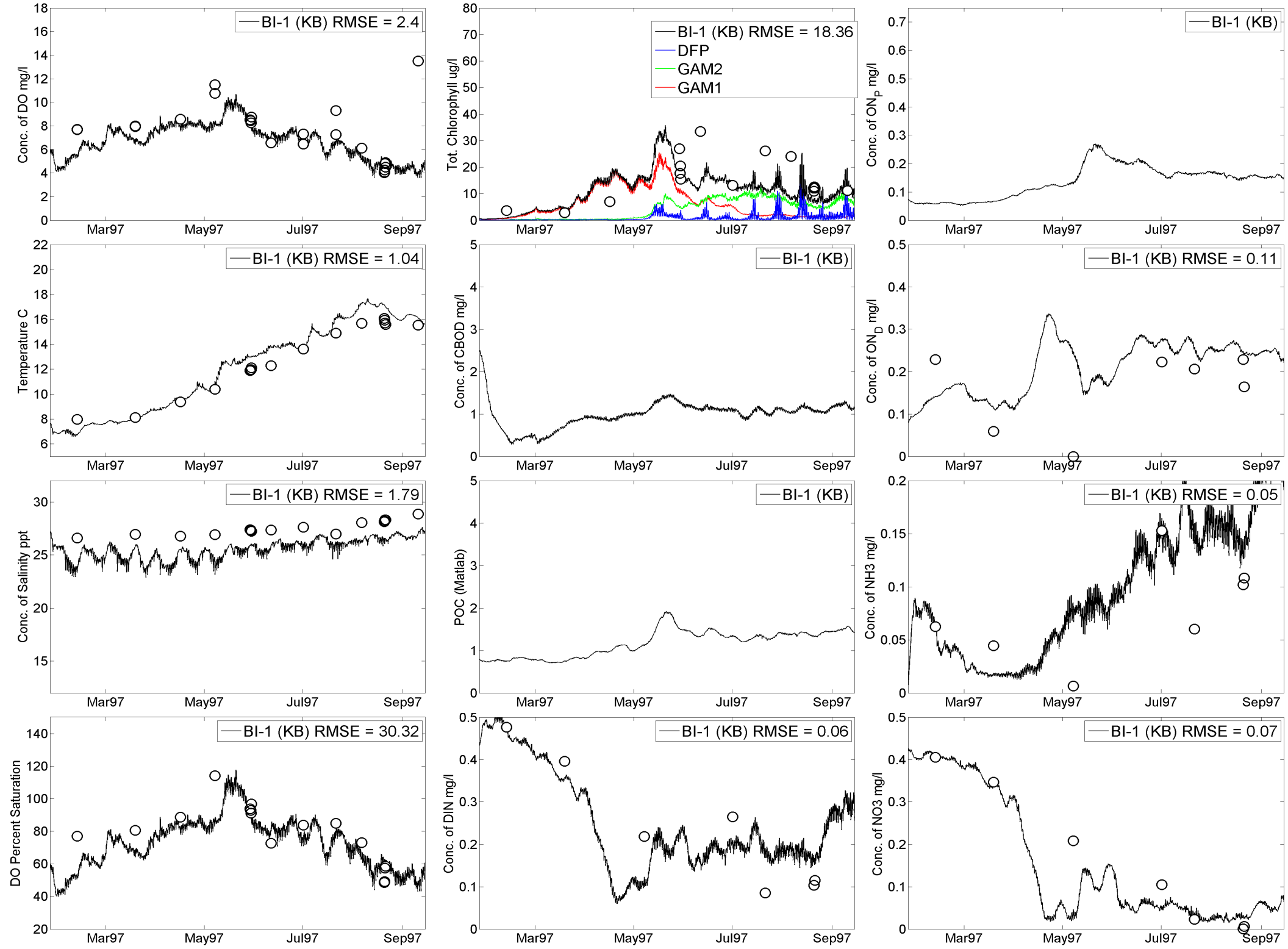

XPI_BI_GAMDFP_base016_000_newGLLVHT.nc, BI−1 (K = 8)

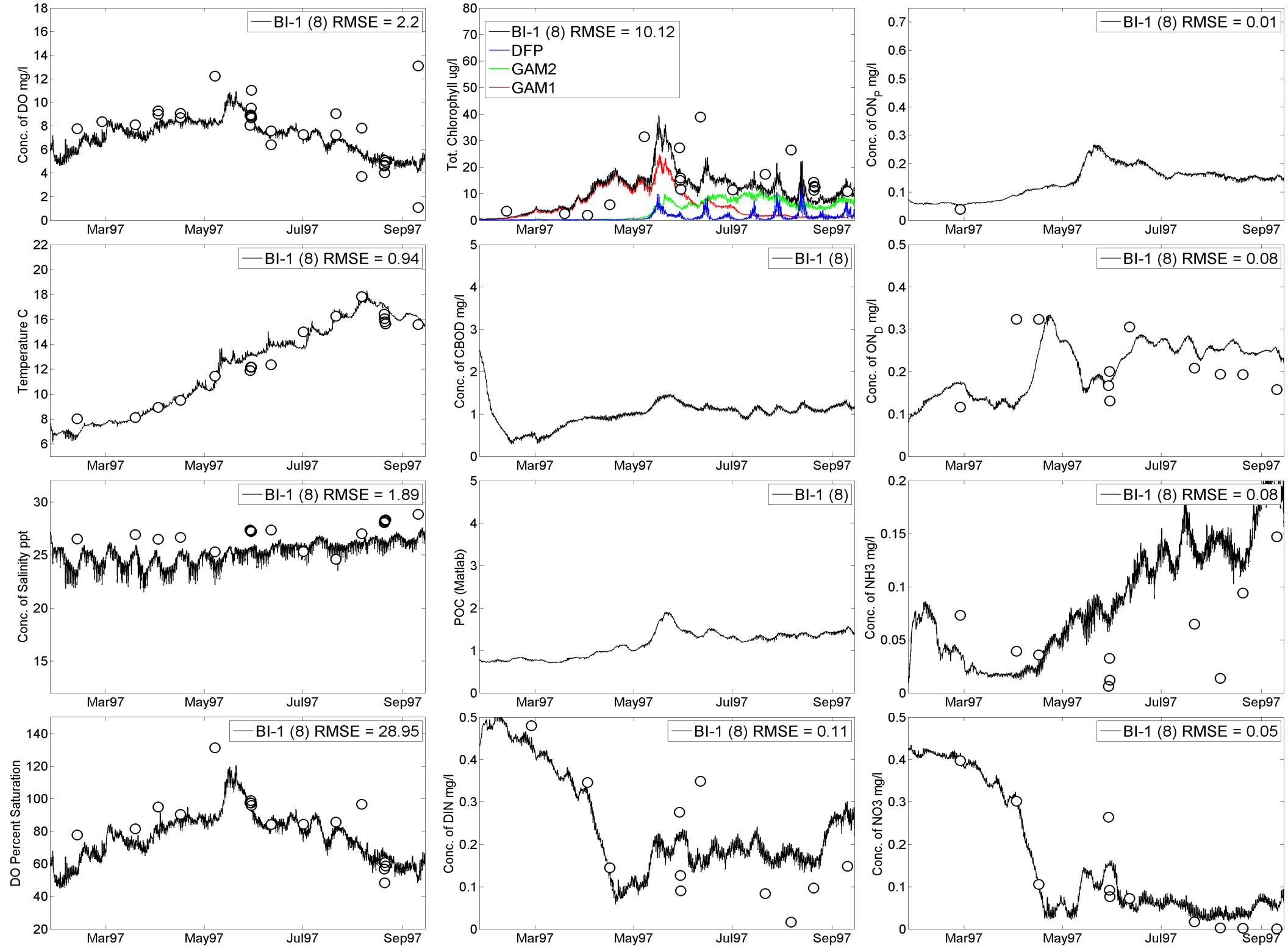

XPI_BI_GAMDFP_base016_000_newGLLVHT.nc, BI−1 (K = KT)

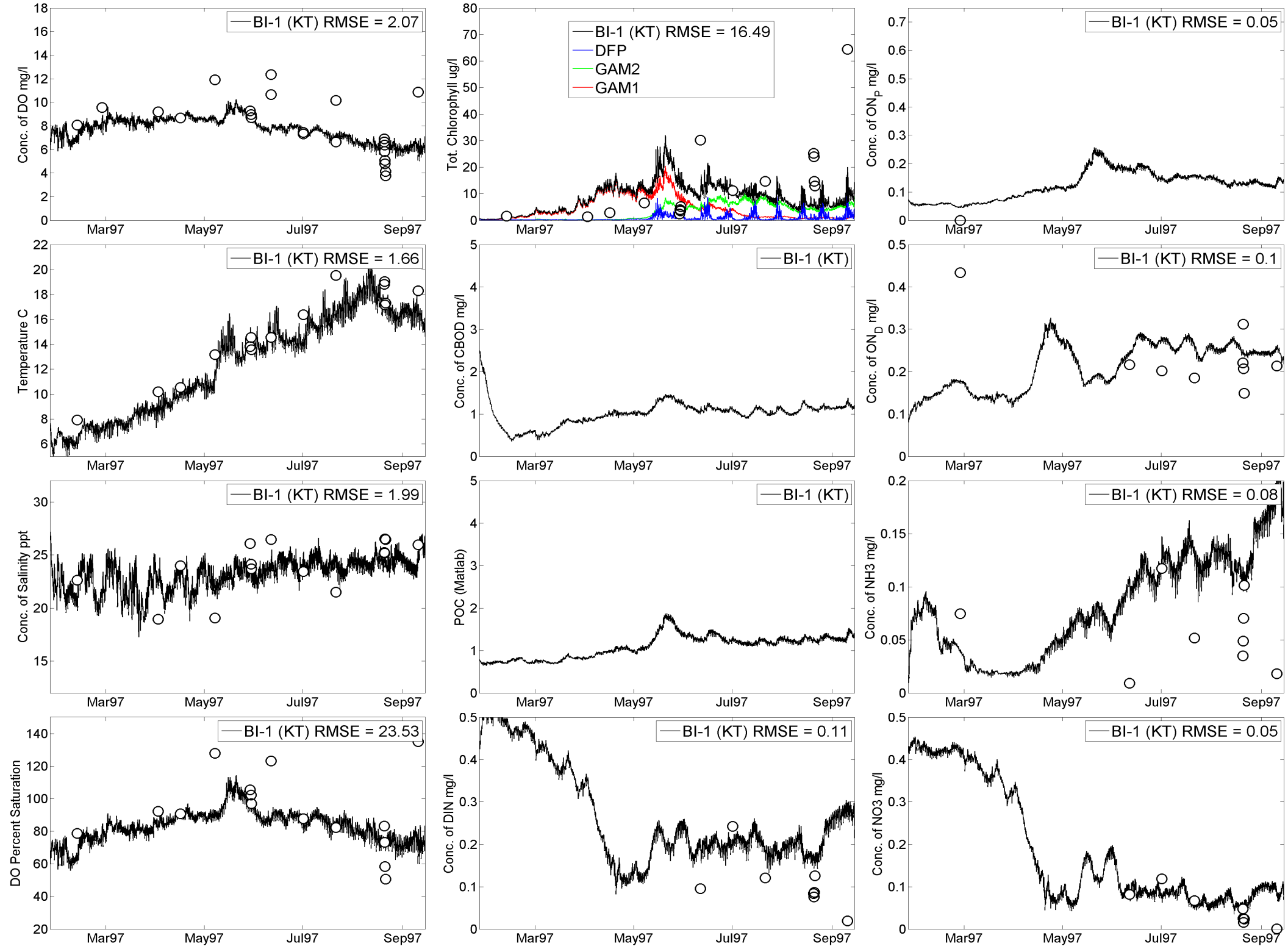

XPI_BI_GAMDFP_base016_000_newGLLVHT.nc, BA−2 (K = KB)

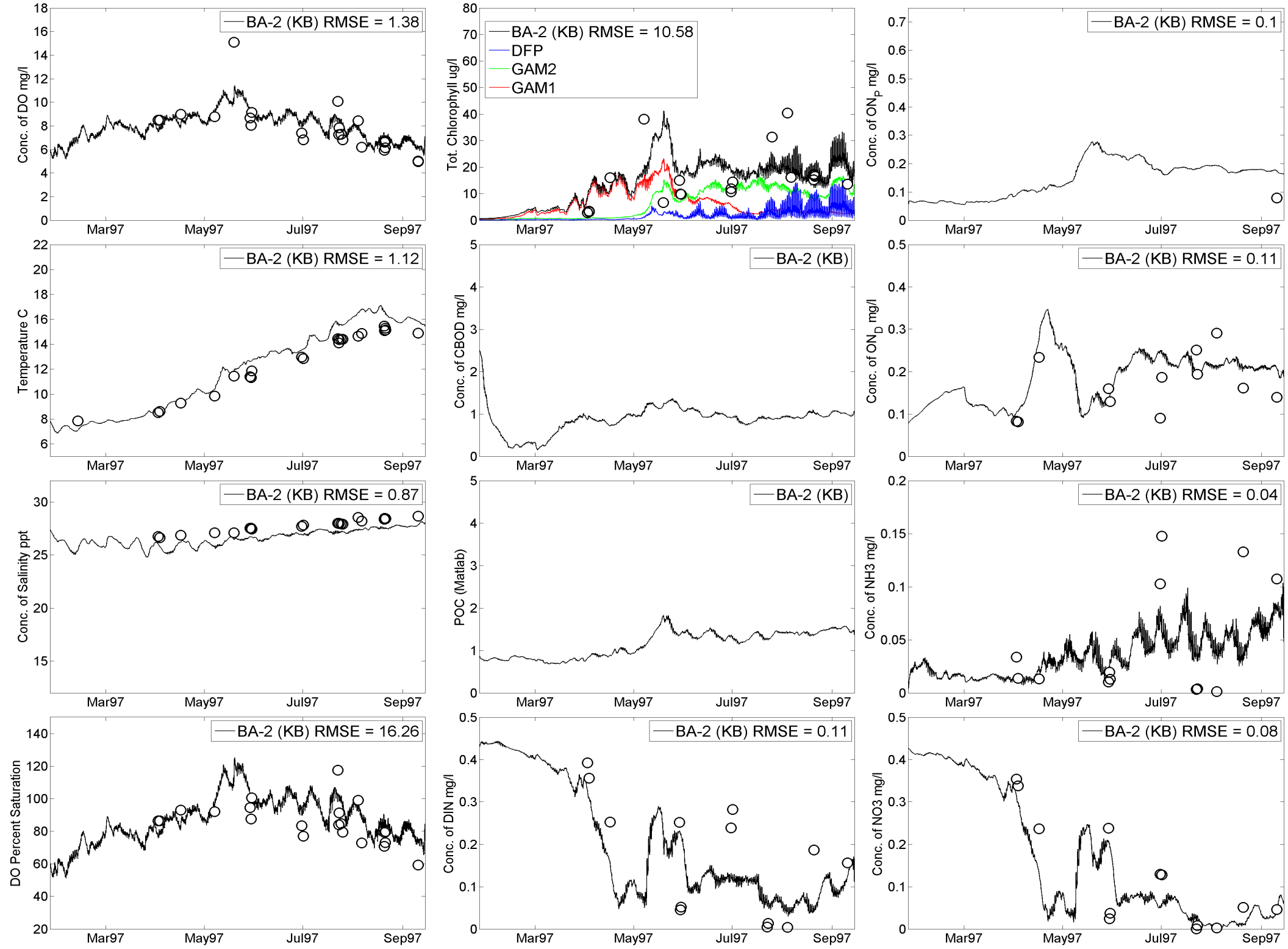

XPI_BI_GAMDFP_base016_000_newGLLVHT.nc, BA−2 (K = 9)

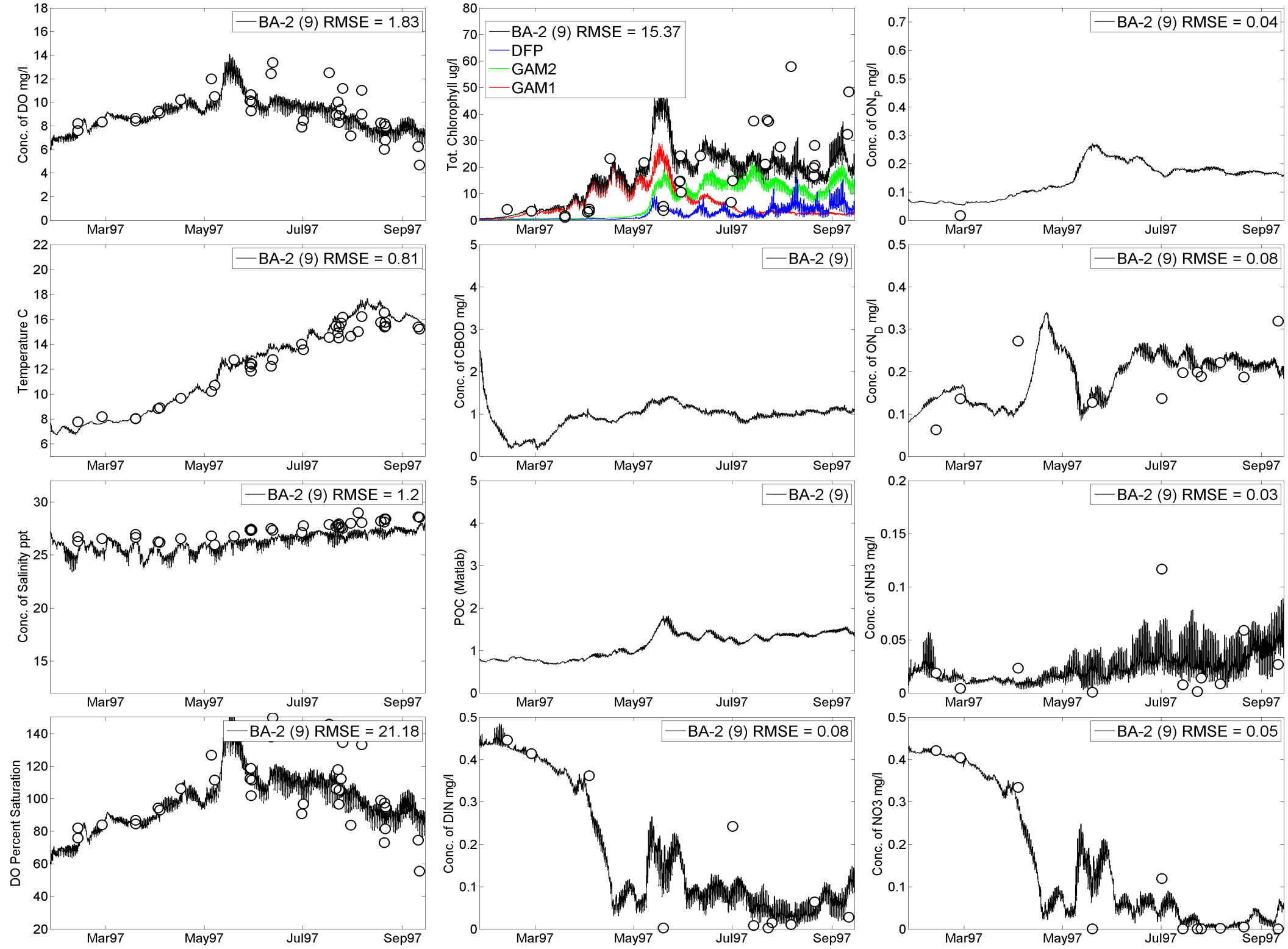

XPI_BI_GAMDFP_base016_000_newGLLVHT.nc, BA−2 (K = KT)

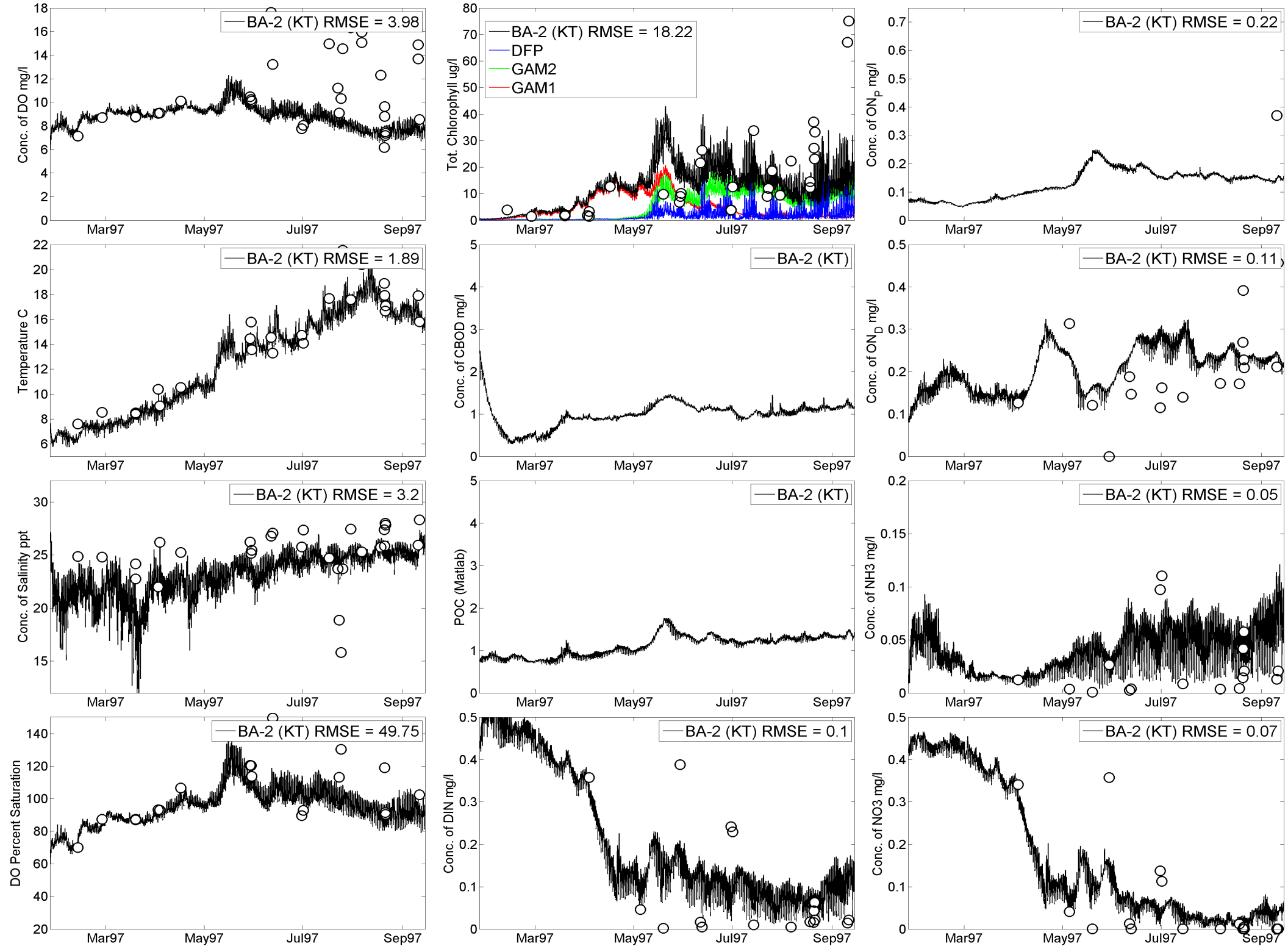

XPI_BI_GAMDFP_base016_000_newGLLVHT.nc, BB−2 (K = KB)

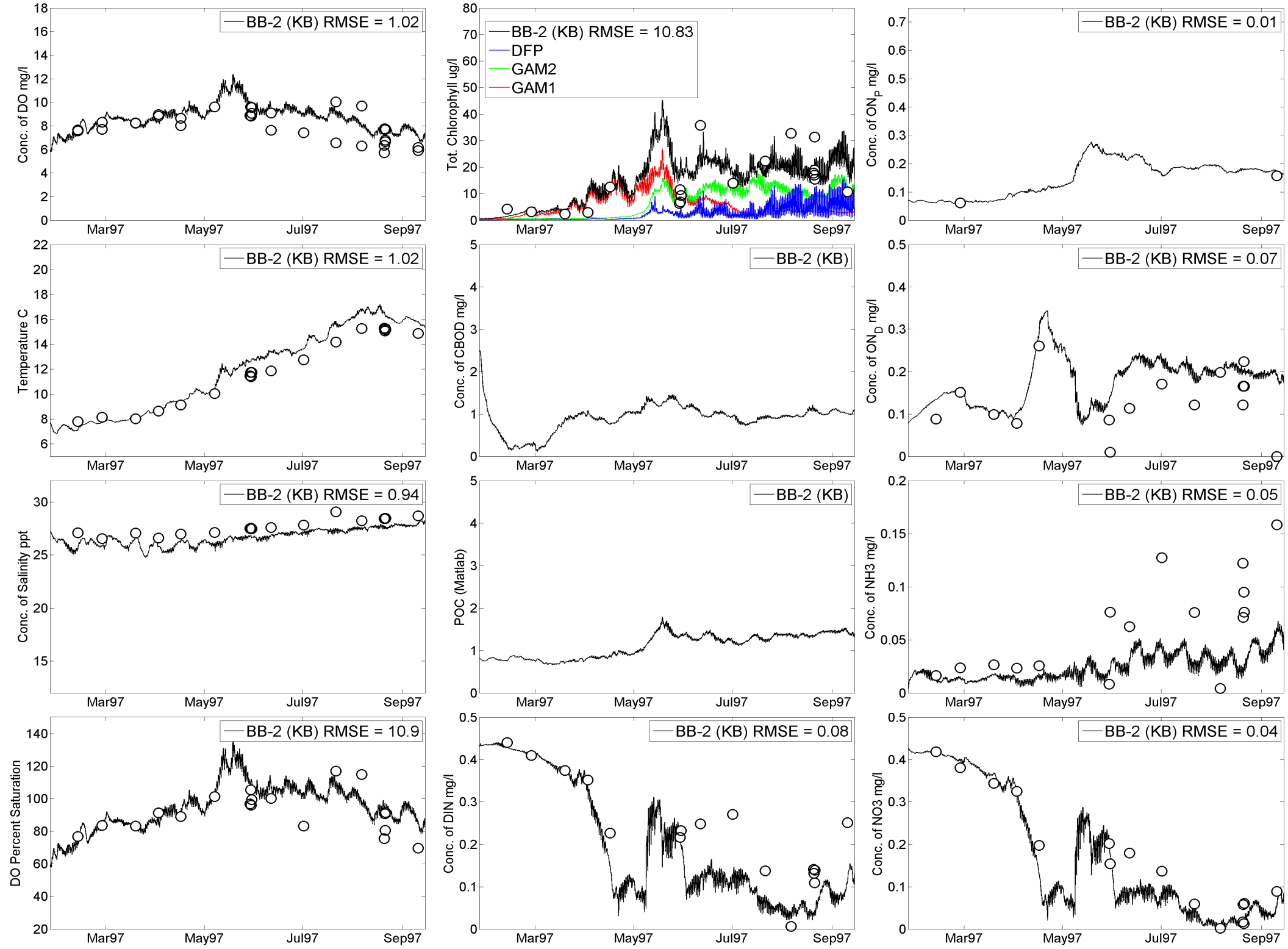

XPI_BI_GAMDFP_base016_000_newGLLVHT.nc, BB−2 (K = 9)

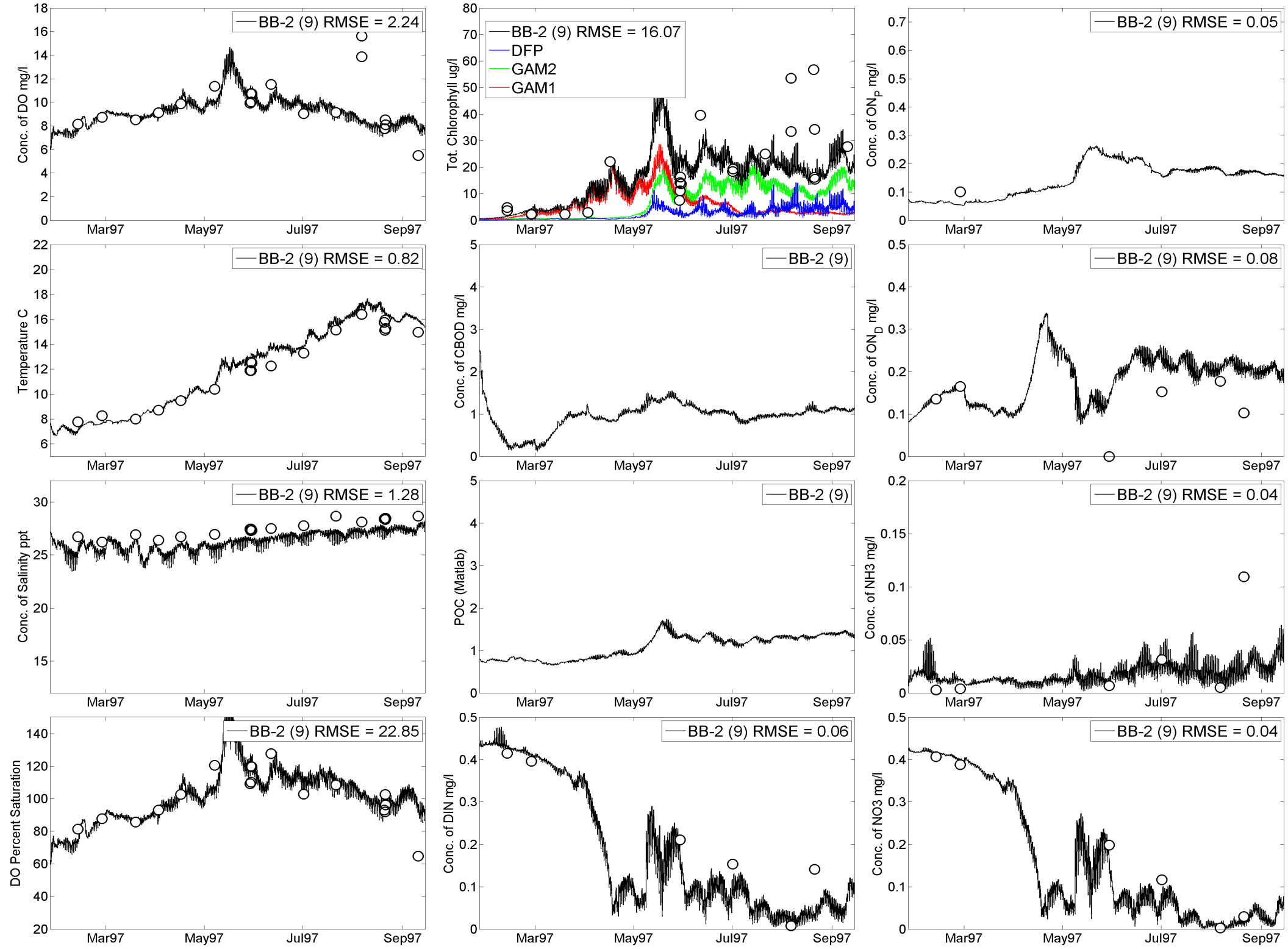

XPI_BI_GAMDFP_base016_000_newGLLVHT.nc, BB−2 (K = KT)

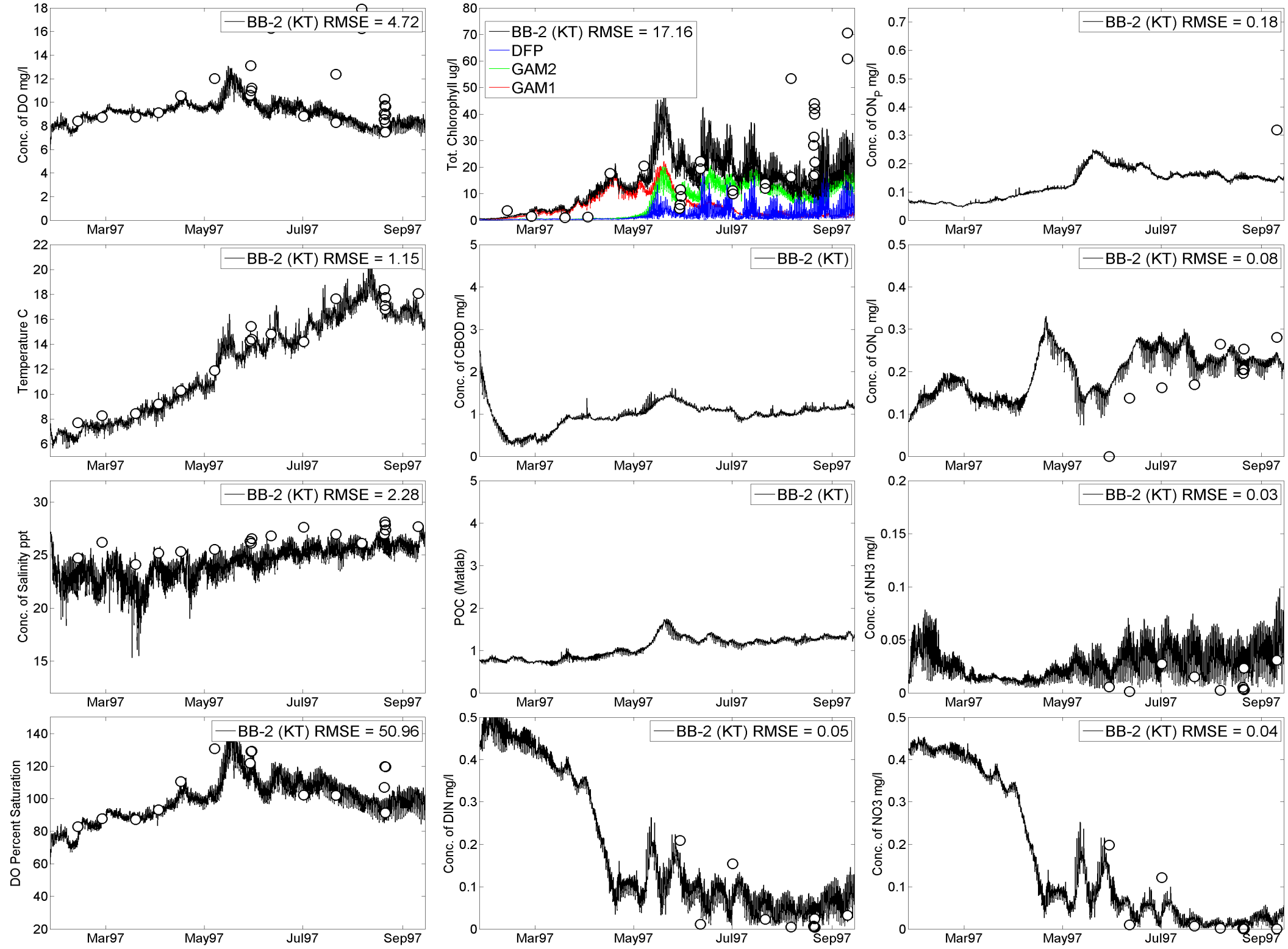

XPI_BI_GAMDFP_base016_000_newGLLVHT.nc, LOON1 (K = KB)

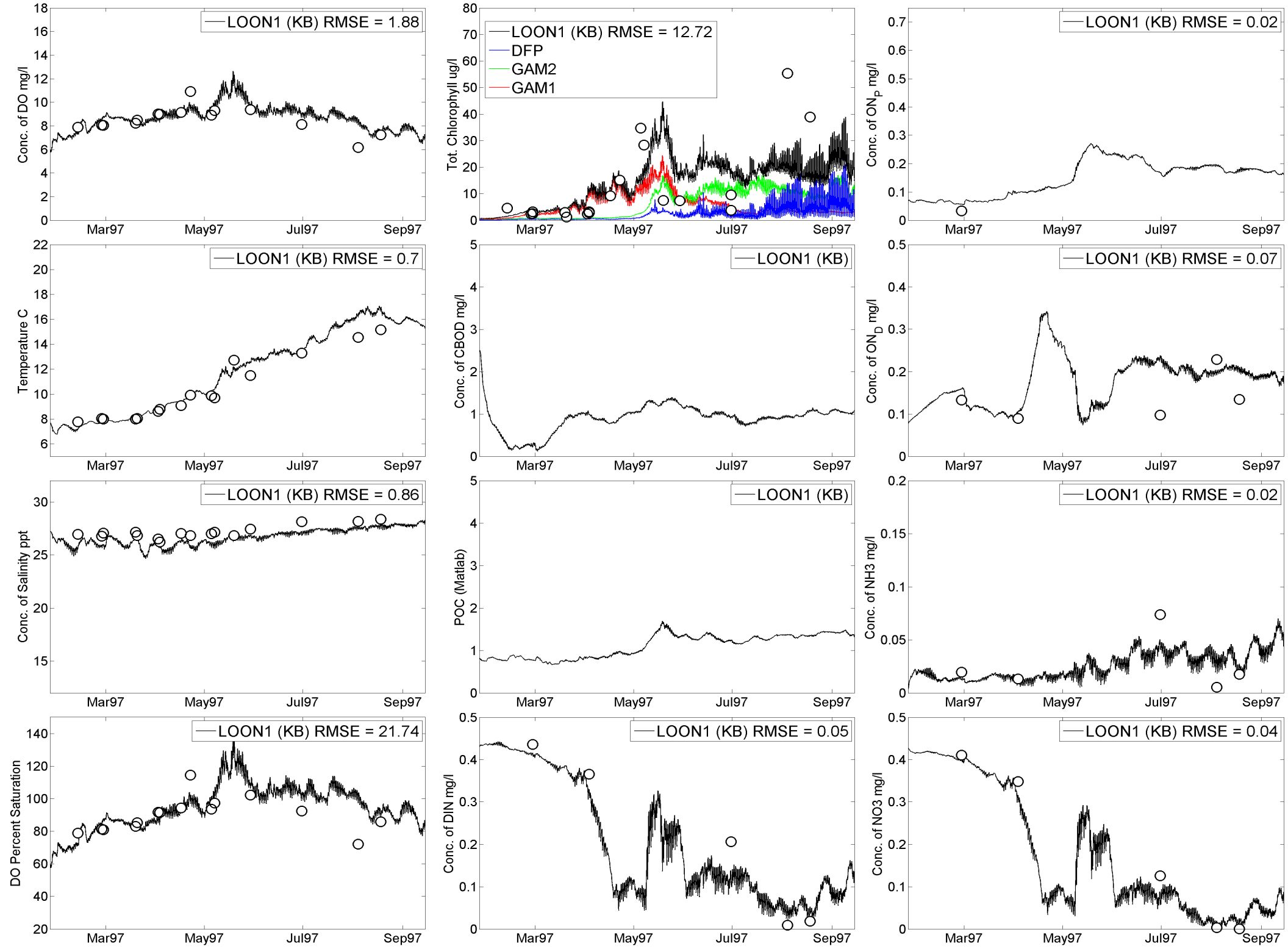

XPI_BI_GAMDFP_base016_000_newGLLVHT.nc, LOON1 (K = 9)

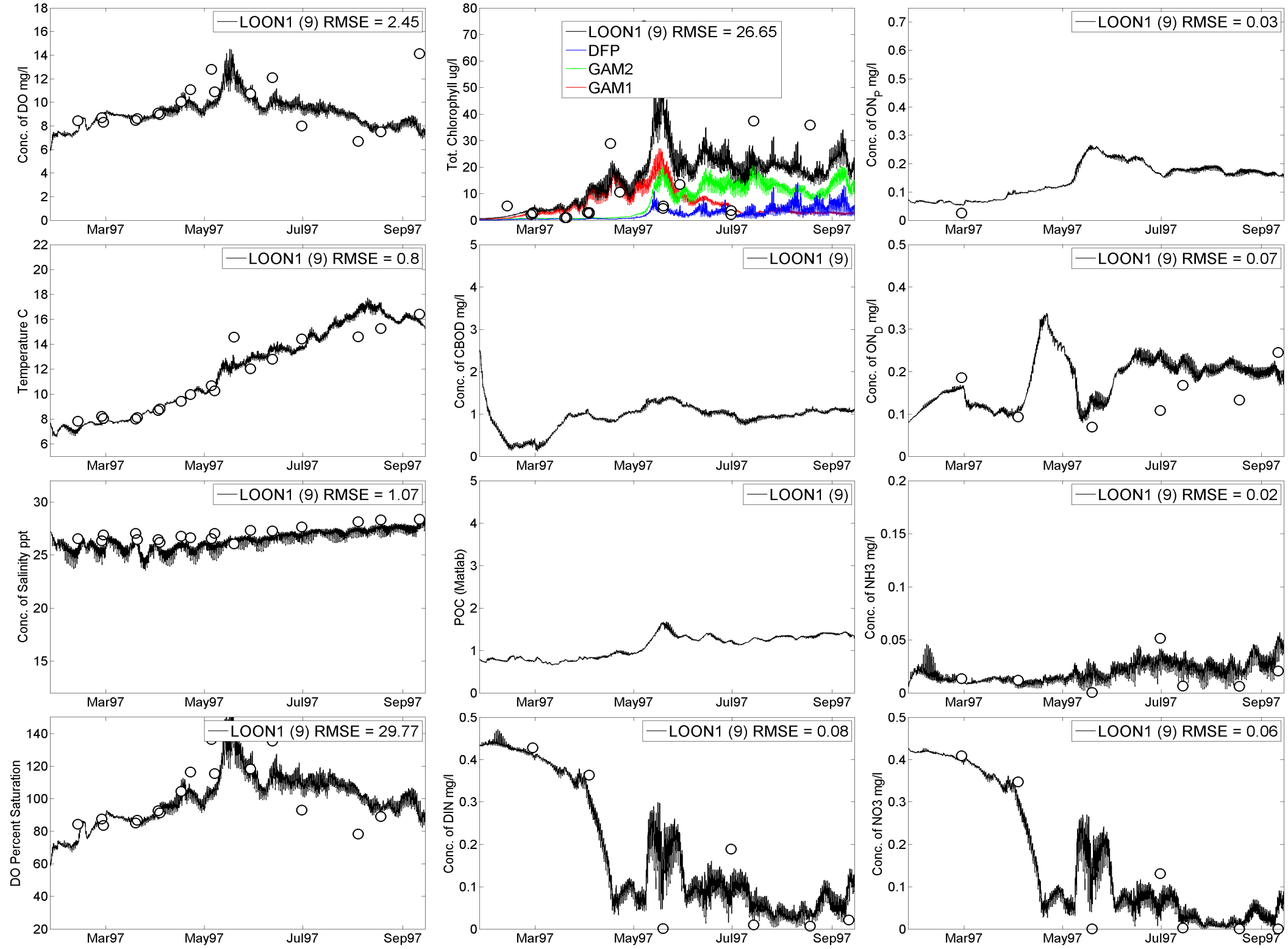

XPI_BI_GAMDFP_base016_000_newGLLVHT.nc, LOON1 (K = KT)

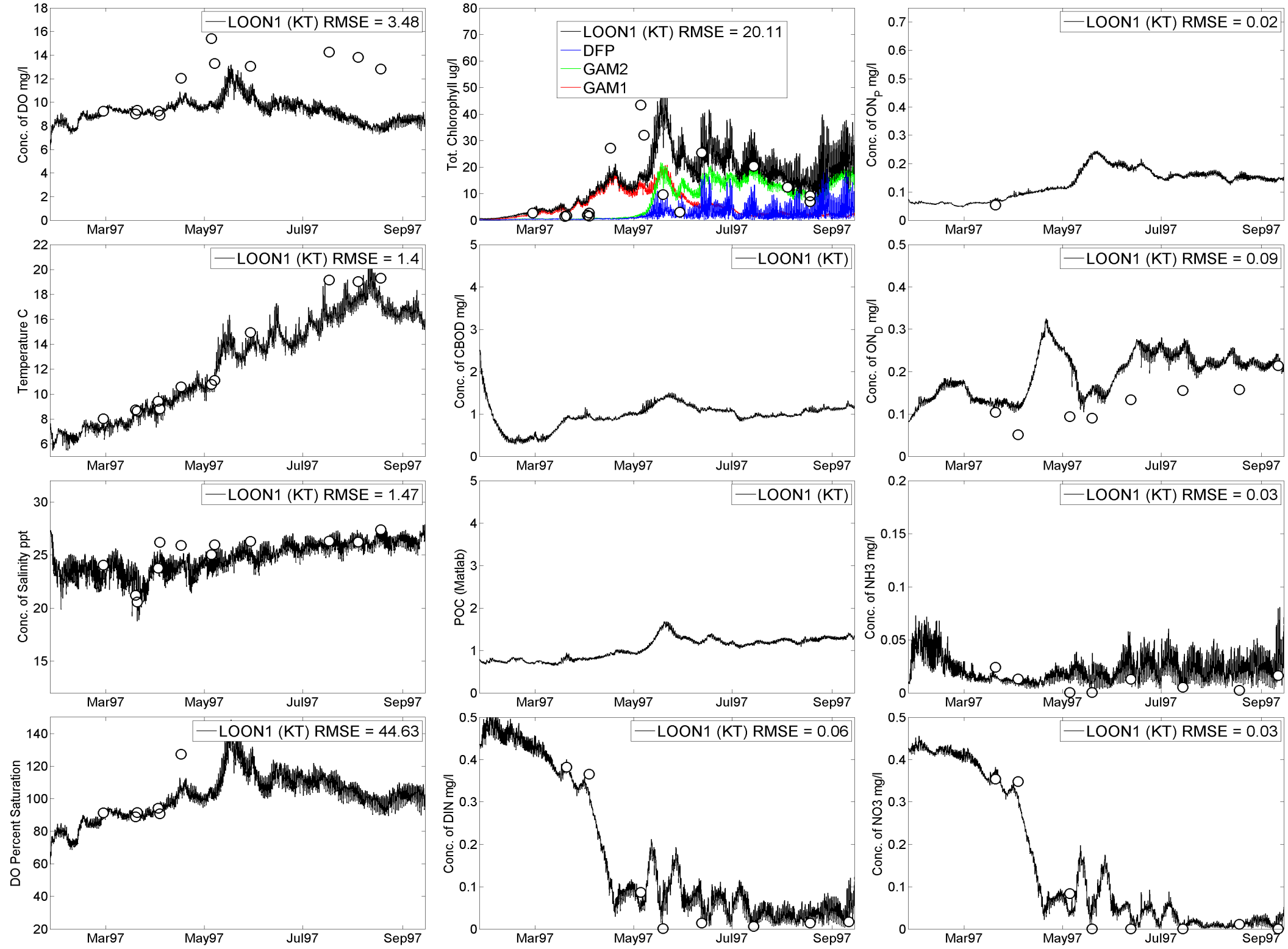

XPI_BI_GAMDFP_base016_000_newGLLVHT.nc, BC−2 (K = KB)

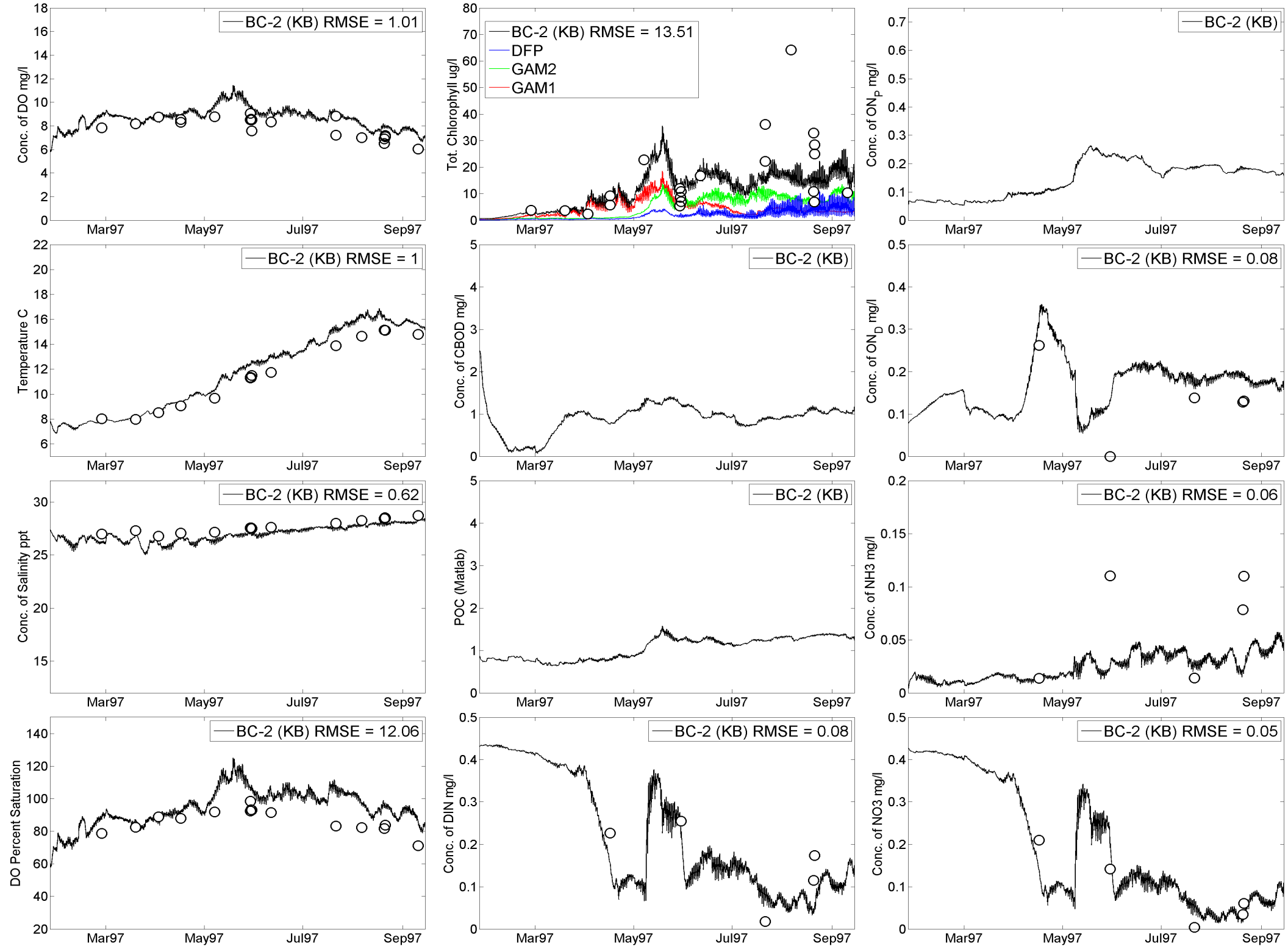

XPI_BI_GAMDFP_base016_000_newGLLVHT.nc, BC−2 (K = 9)

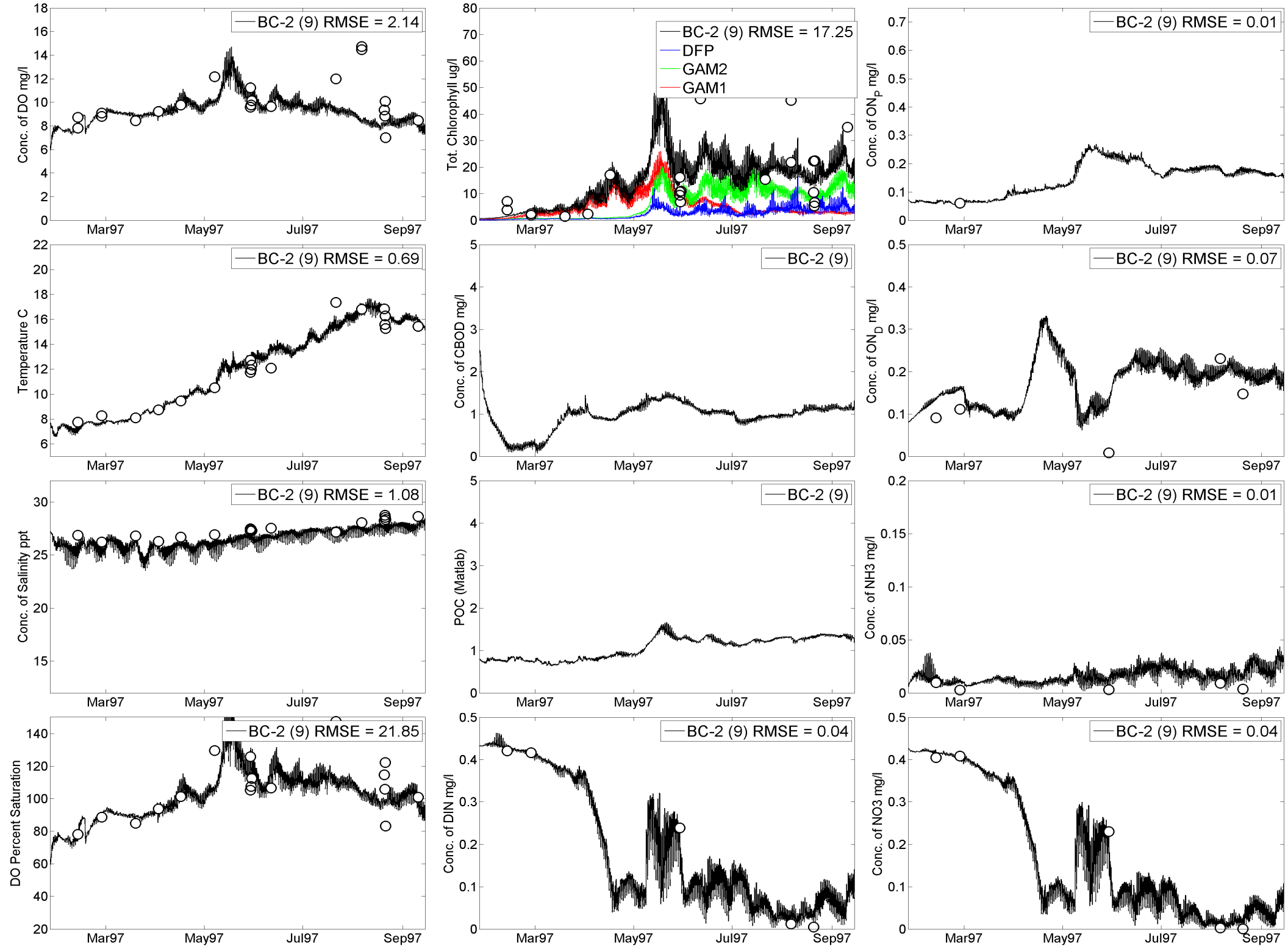

XPI_BI_GAMDFP_base016_000_newGLLVHT.nc, BC−2 (K = KT)

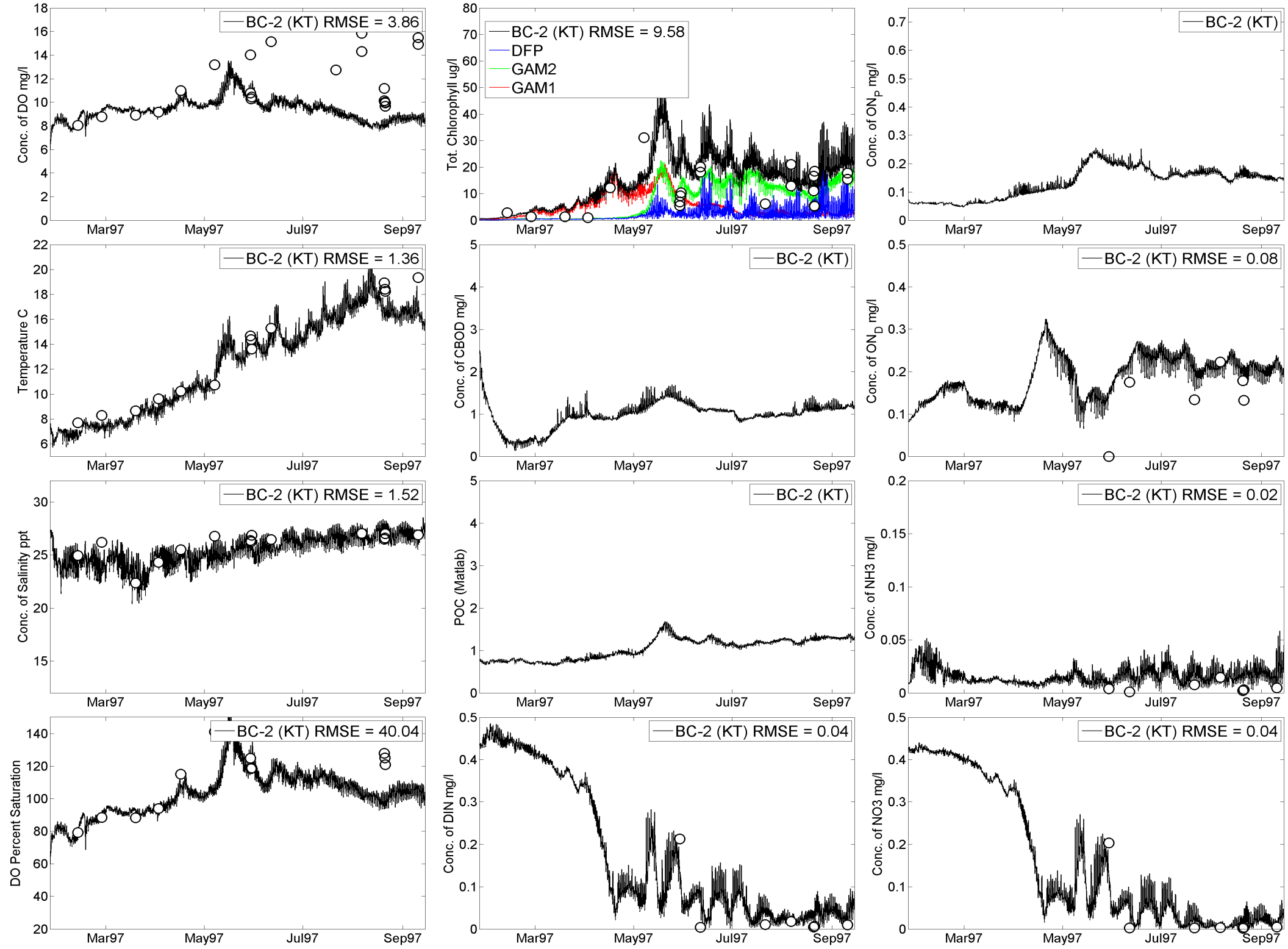

XPI_BI_GAMDFP_base016_000_newGLLVHT.nc, BD−2 (K = KB)

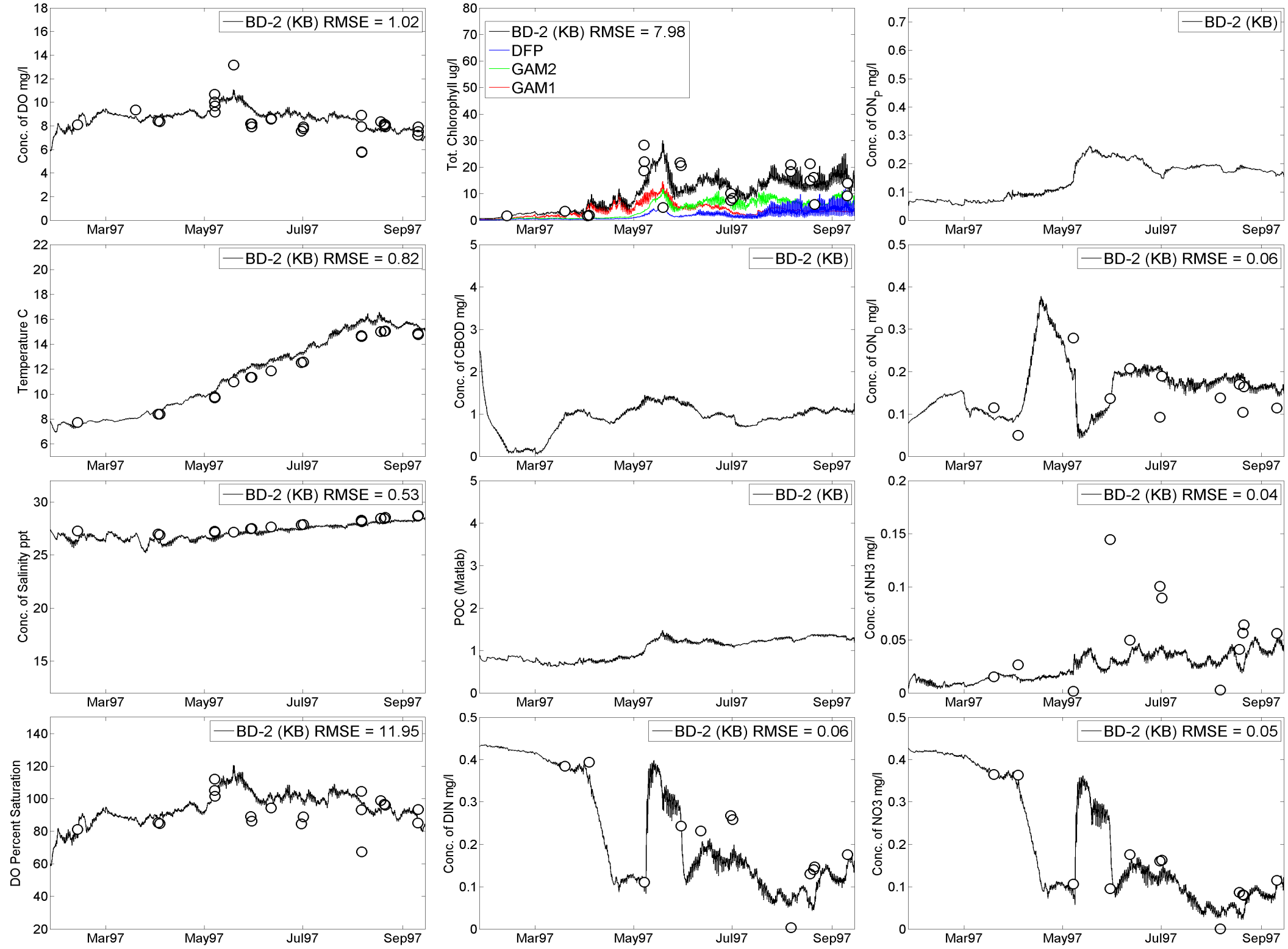

XPI_BI_GAMDFP_base016_000_newGLLVHT.nc, BD−2 (K = 11)

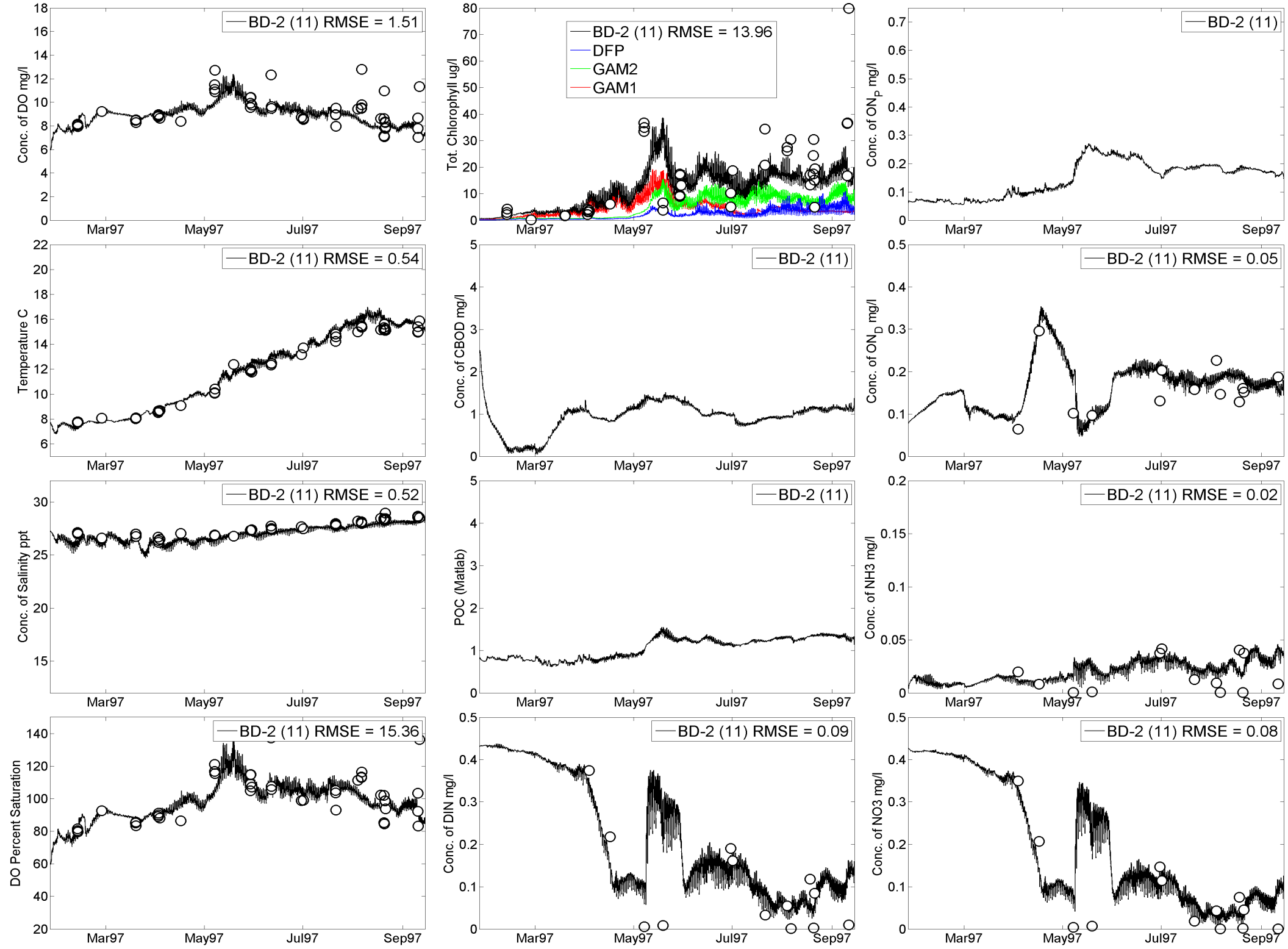

XPI_BI_GAMDFP_base016_000_newGLLVHT.nc, BD−2 (K = KT)

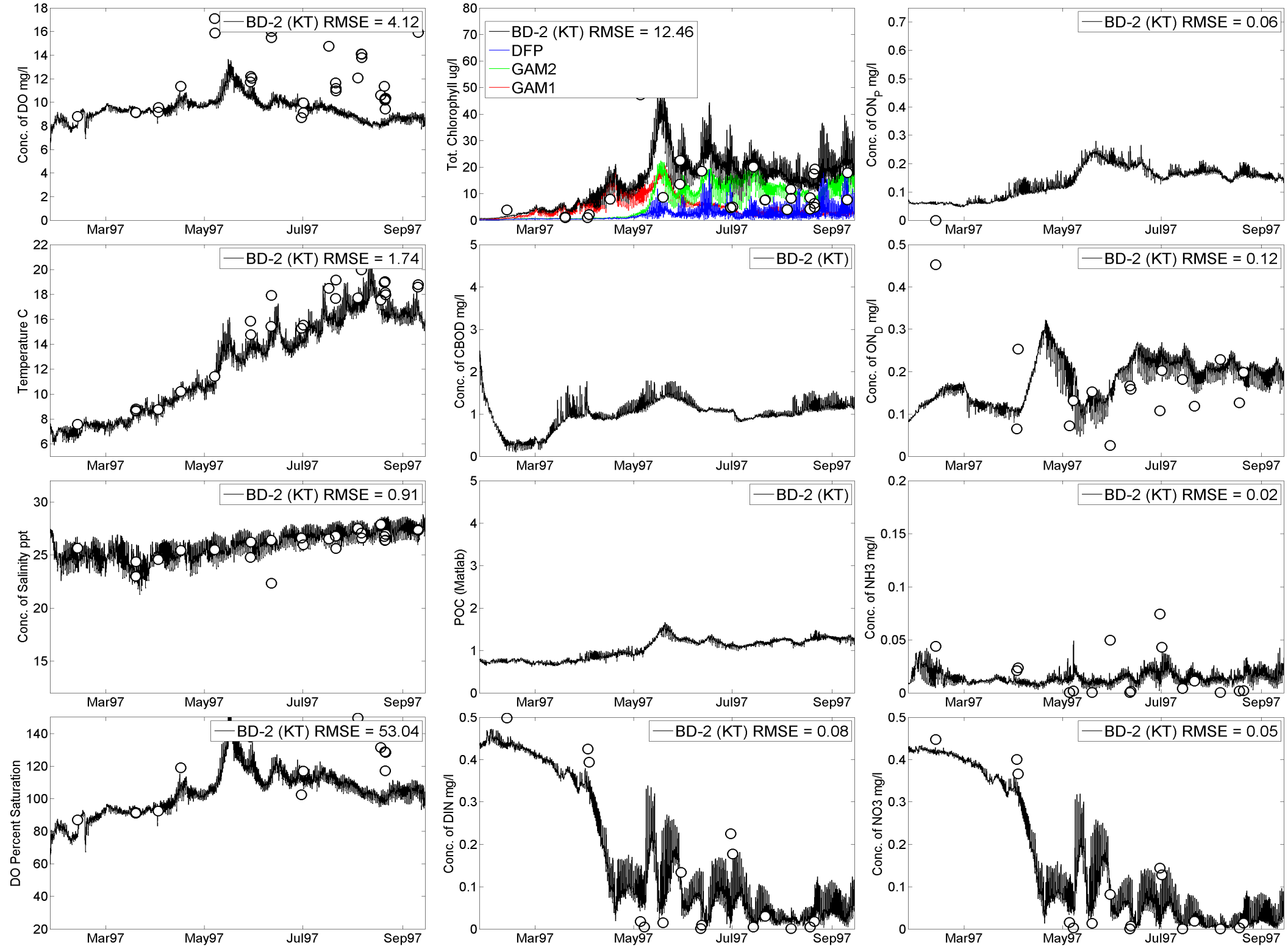

XPI_BI_GAMDFP_base016_000_newGLLVHT.nc, BE−2 (K = KB)

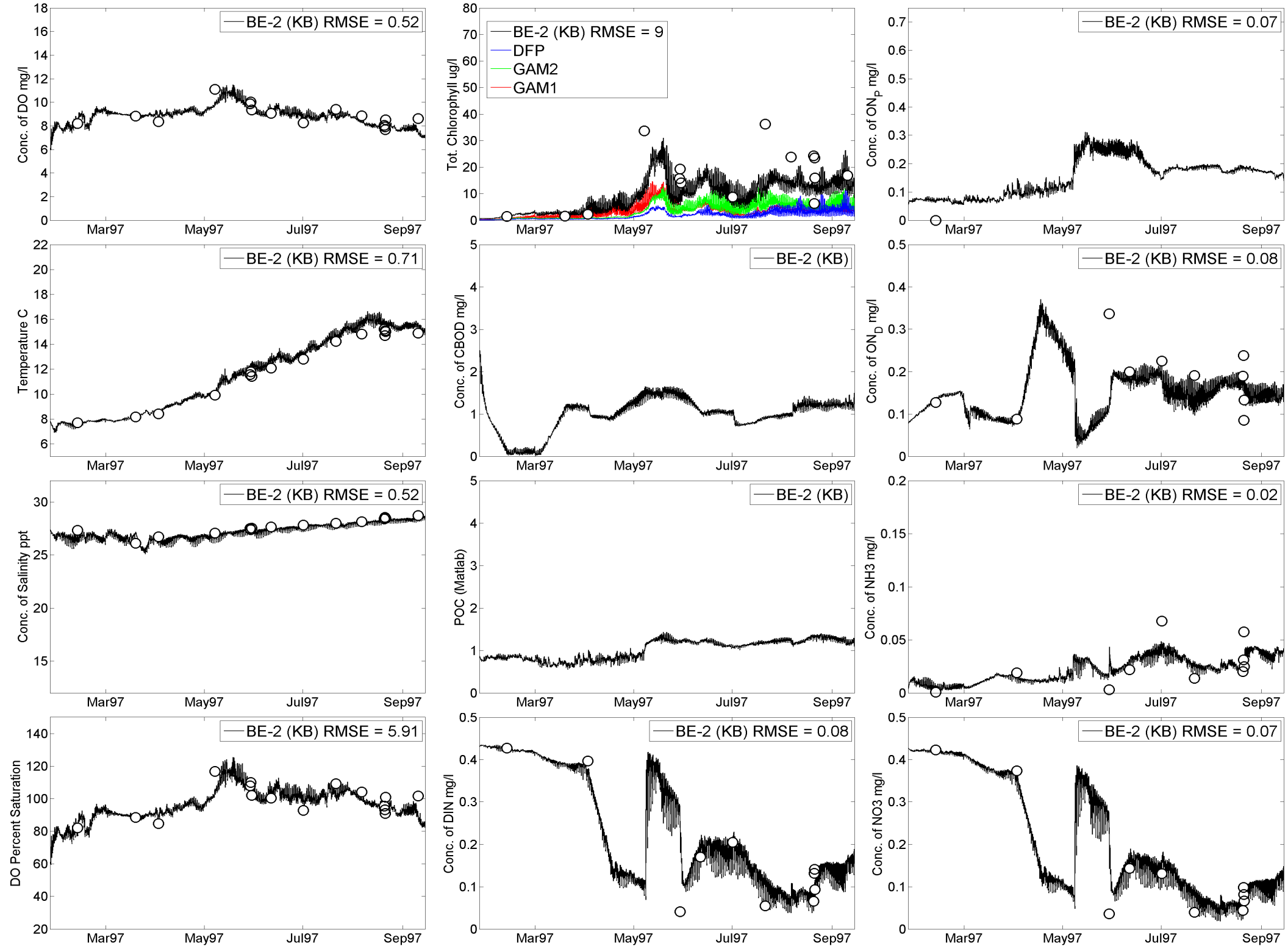

XPI_BI_GAMDFP_base016_000_newGLLVHT.nc, BE−2 (K = 9)

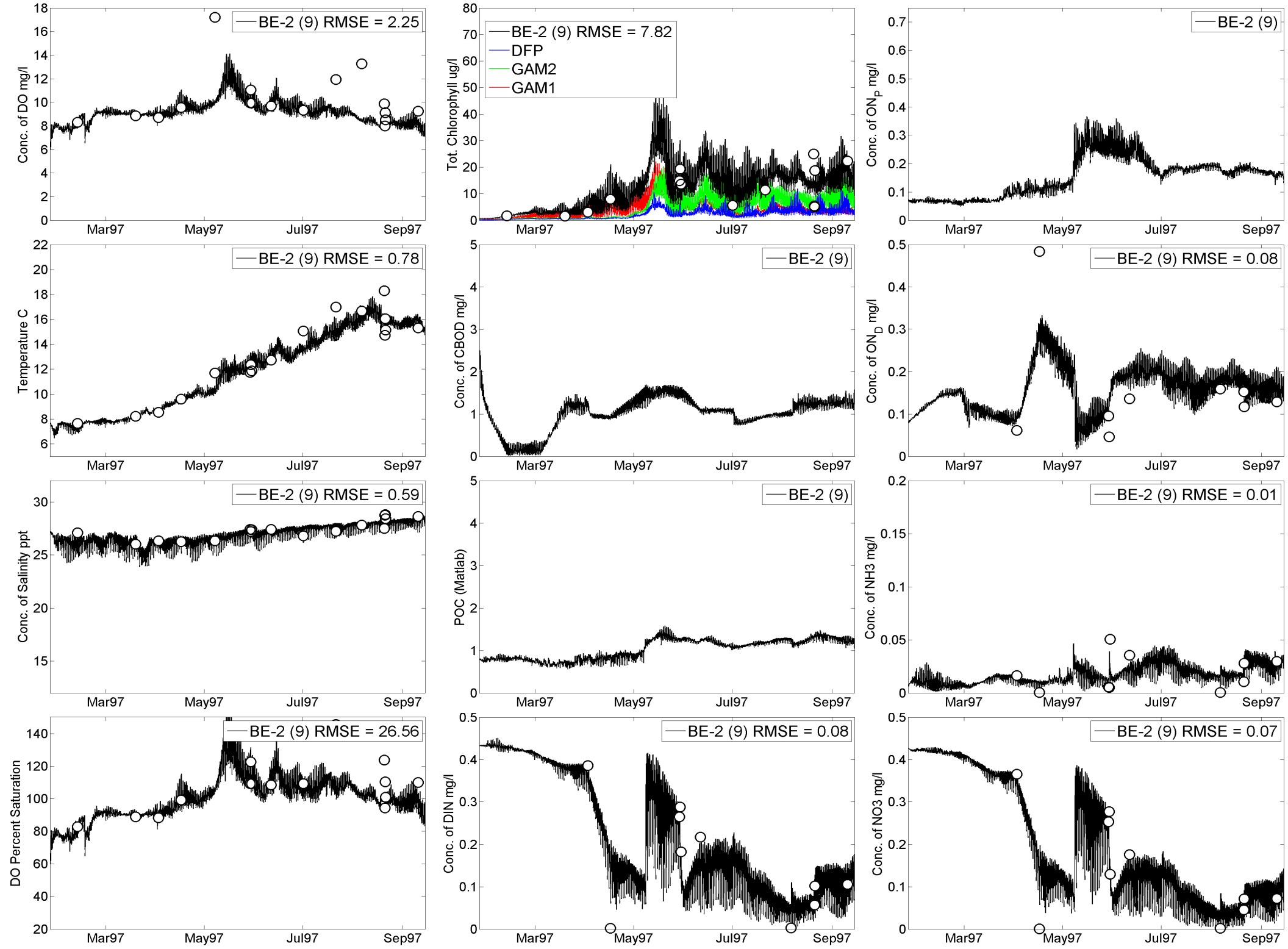

XPI_BI_GAMDFP_base016_000_newGLLVHT.nc, BE−2 (K = KT)

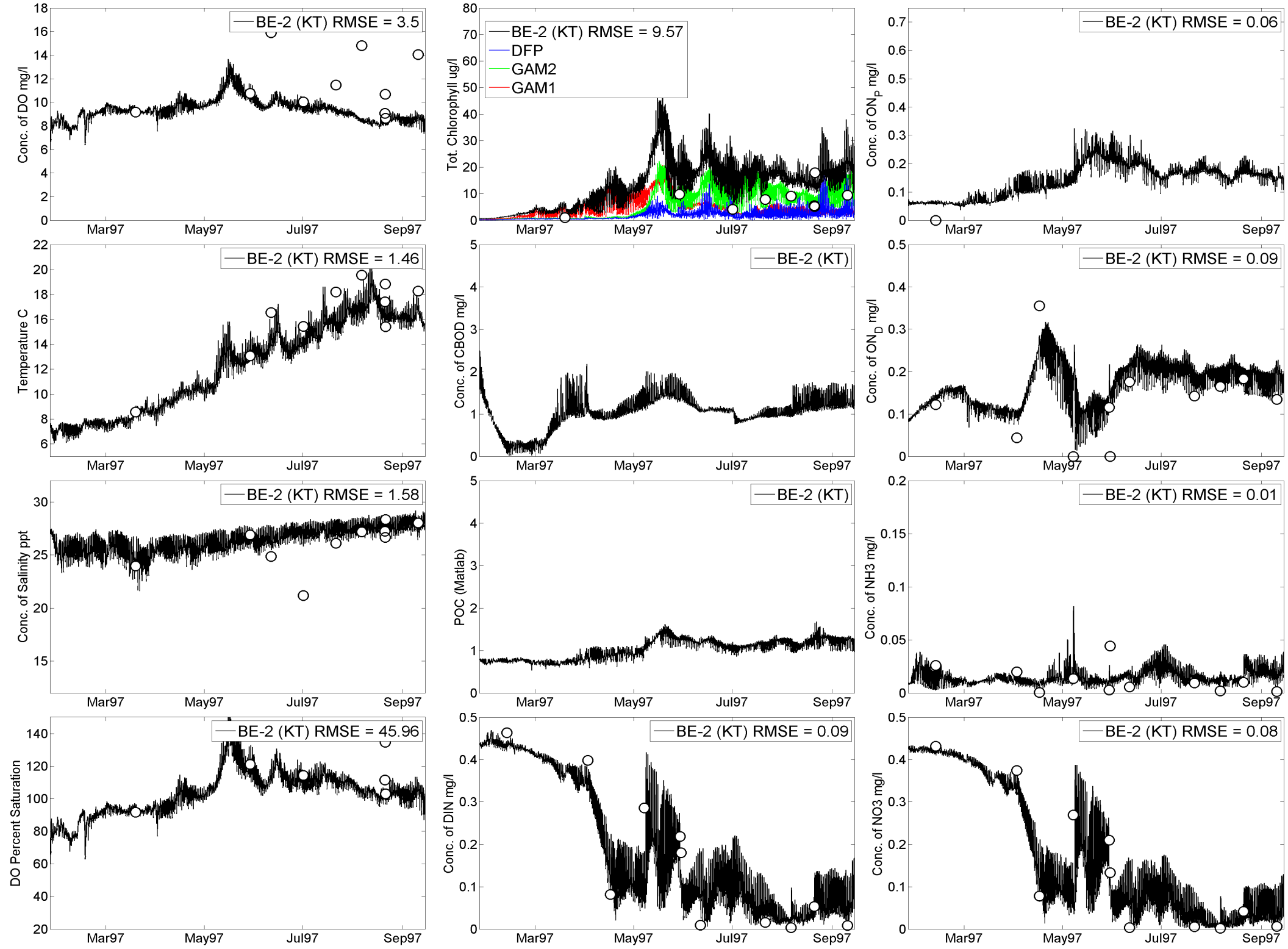

XPI_BI_GAMDFP_base016_000_newGLLVHT.nc, BF−3 (K = KB)

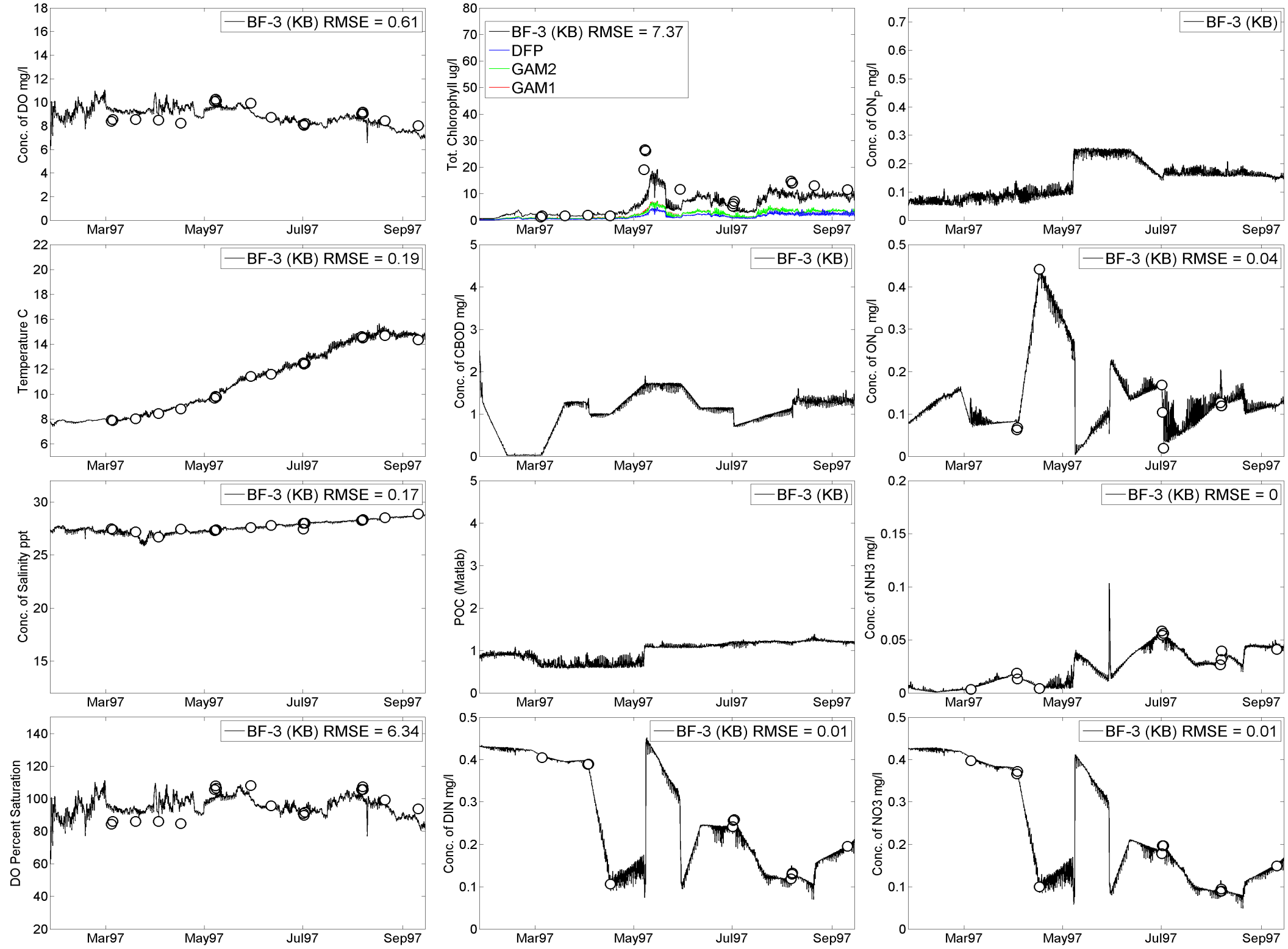

XPI_BI_GAMDFP_base016_000_newGLLVHT.nc, BF−3 (K = 12)

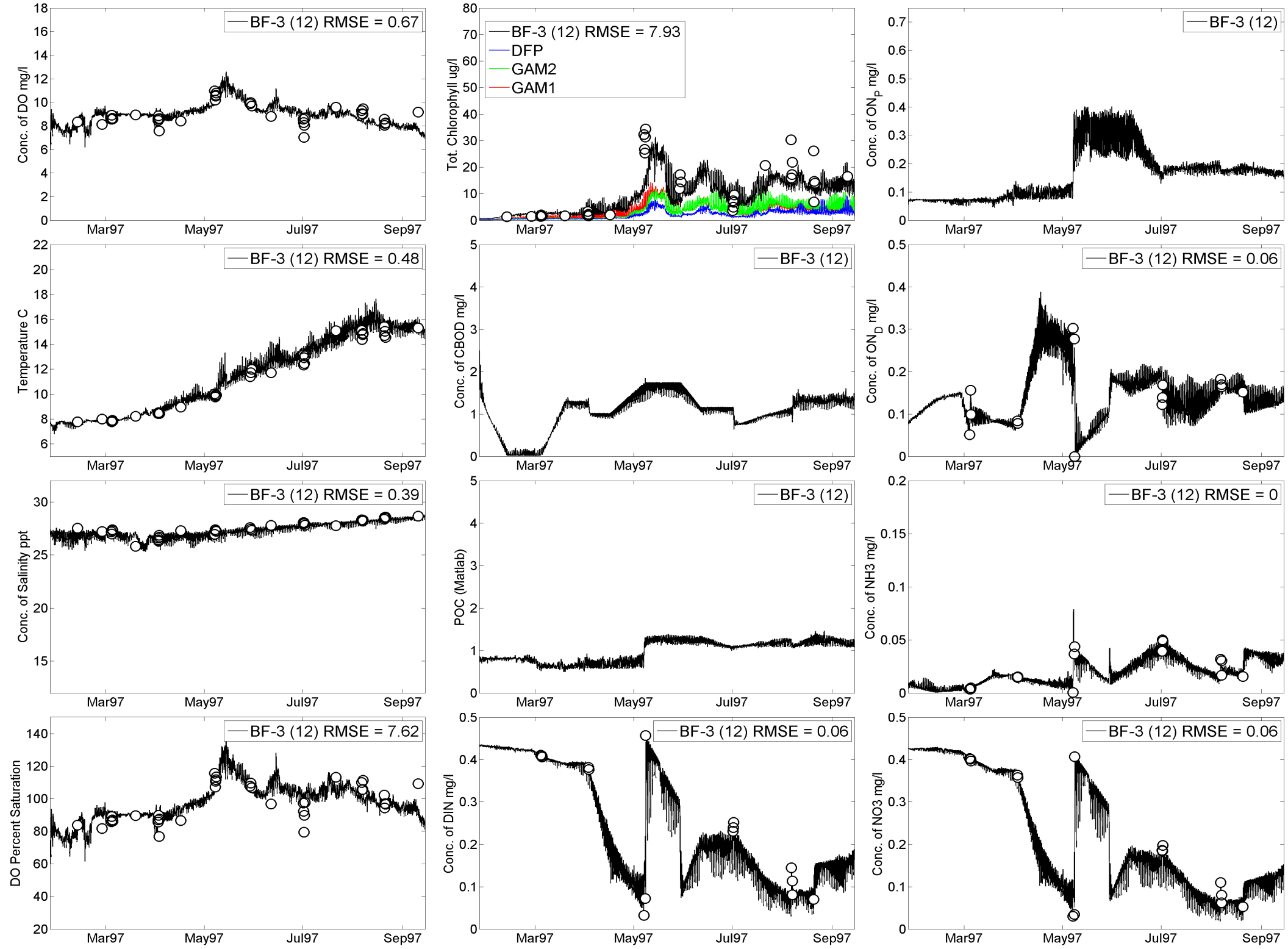

XPI_BI_GAMDFP_base016_000_newGLLVHT.nc, BF−3 (K = KT)

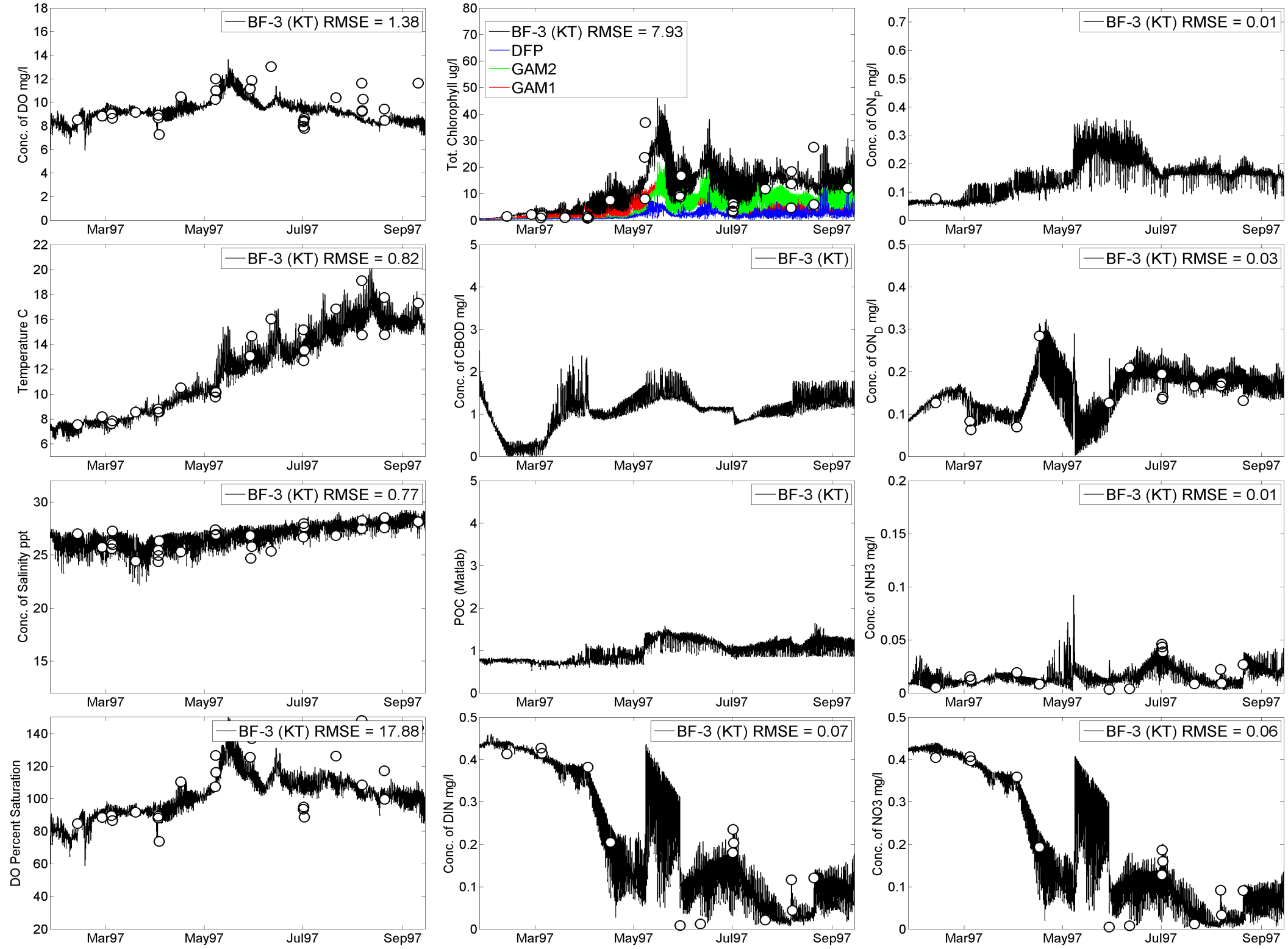

Appendix G.3. Budd Inlet Model: Water Quality Profiles

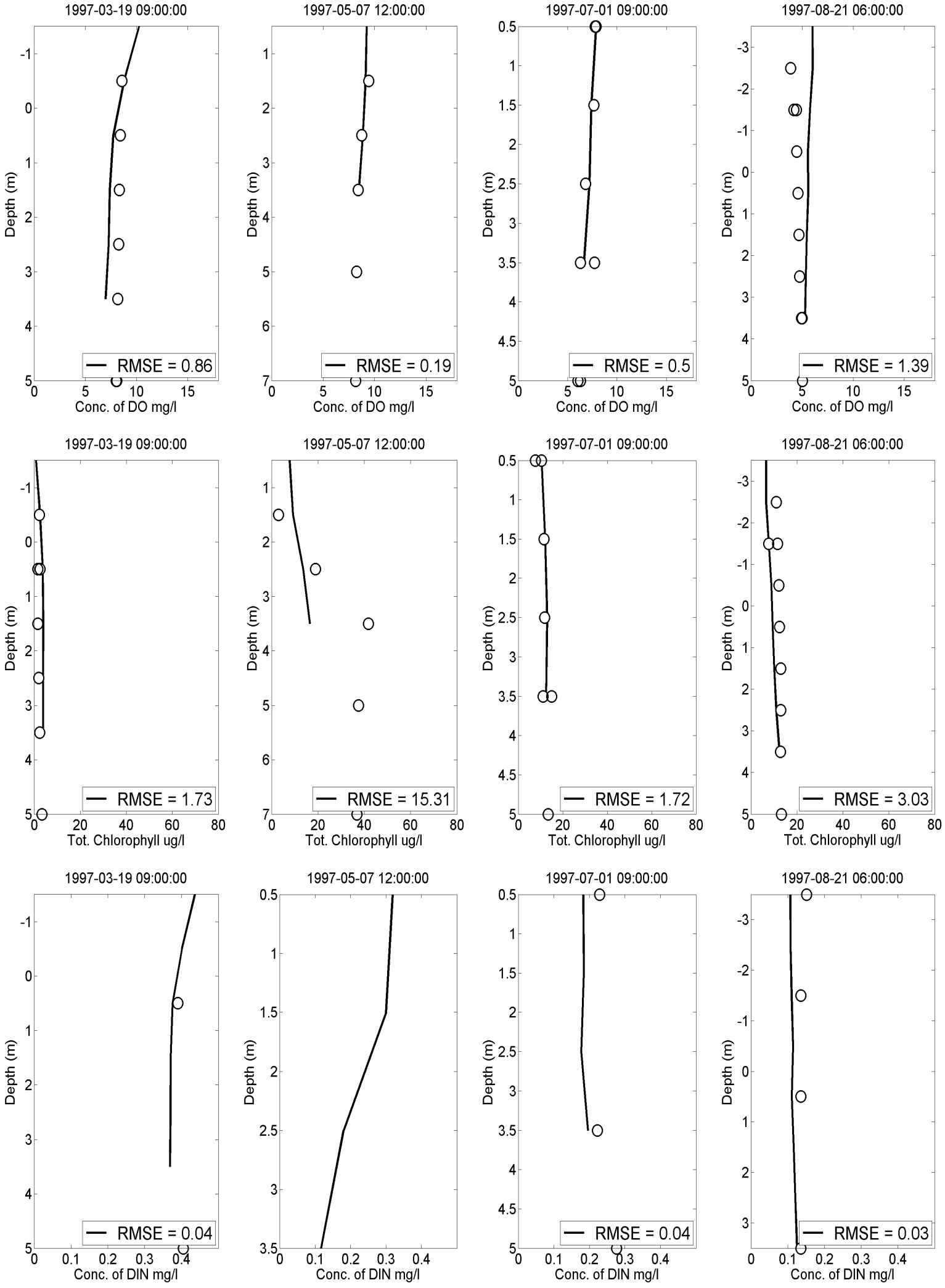

XPI_BI_GAMDFP_base016_000_newGLLVHT.nc, BI-6

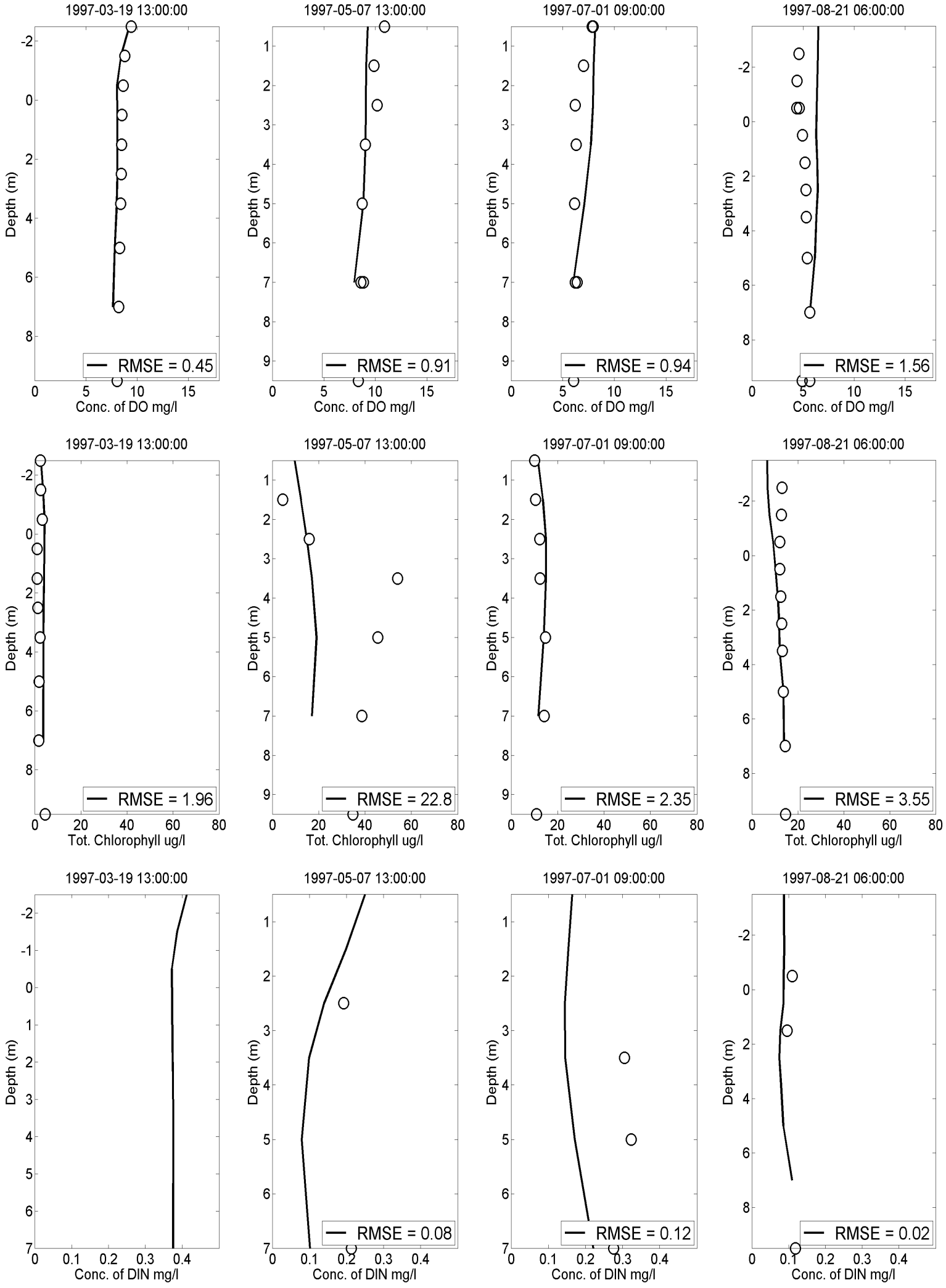
1997-03-19 13:00:00
1997-05-07 13:00:00
1997-07-01 09:00:00
1997-08-21 06:00:00
Depth (m)
RMSE = 0.45
RMSE = 0.91
RMSE = 0.94
RMSE = 1.56
Conc. of DO mg/l
RMSE = 1.96
RMSE = 22.8
RMSE = 2.35
RMSE = 3.55
Tot. Chlorophyll ug/l
RMSE = 0.08
RMSE = 0.12
RMSE = 0.02
Conc. of DIN mg/l
XPI_BI_GAMDFP_base016_000_newGLLVHT.nc, BI-5

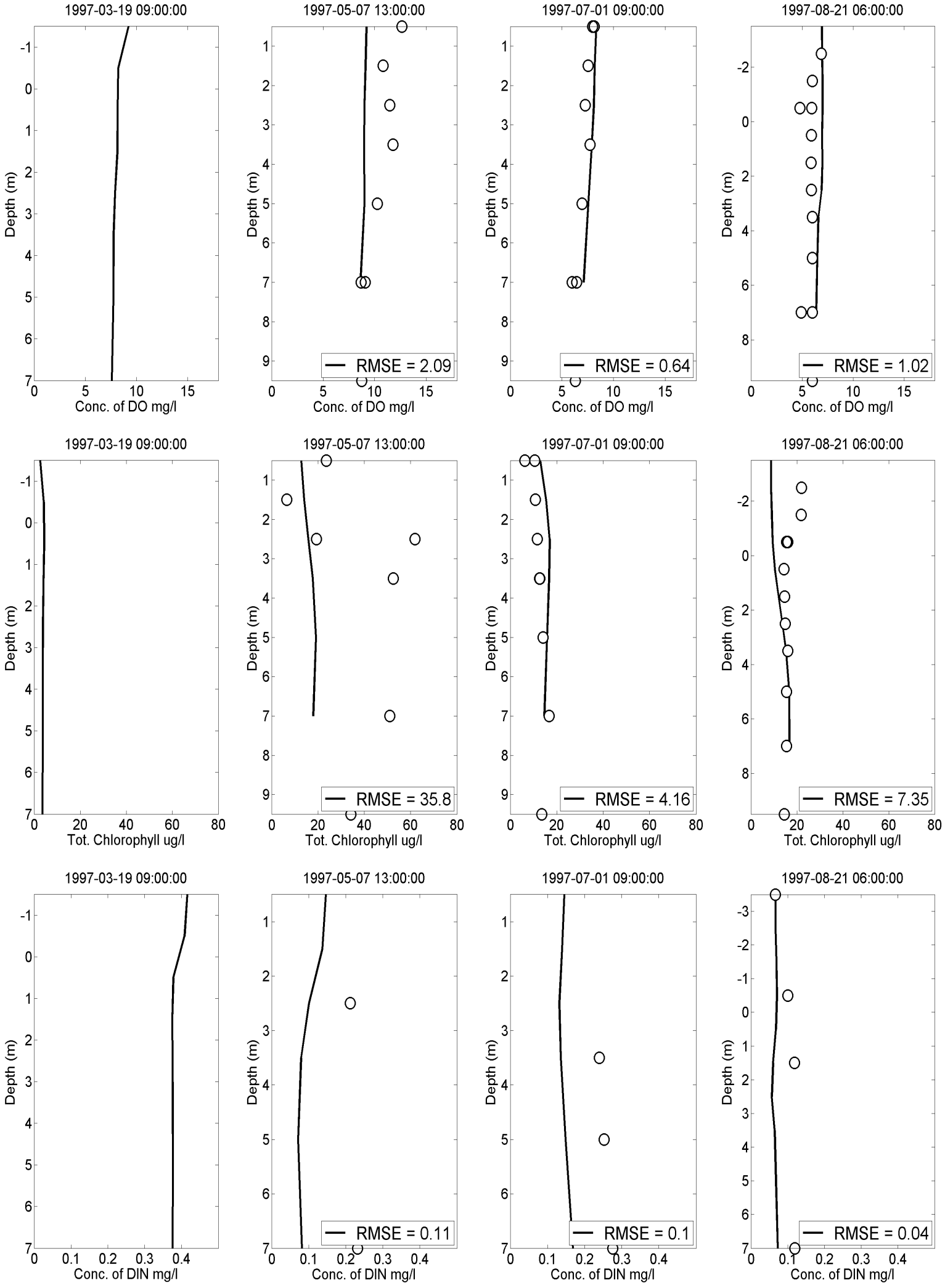
1997-03-19 09:00:00
1997-05-07 13:00:00
1997-07-01 09:00:00
1997-08-21 06:00:00
Depth (m)
Conc. of DO mg/l
RMSE = 2.09
RMSE = 0.64
RMSE = 1.02
Tot. Chlorophyll ug/l
RMSE = 35.8
RMSE = 4.16
RMSE = 7.35
Conc. of DIN mg/l
RMSE = 0.11
RMSE = 0.1
RMSE = 0.04
XPI_BI_GAMDFP_base016_000_newGLLVHT.nc, BI-4

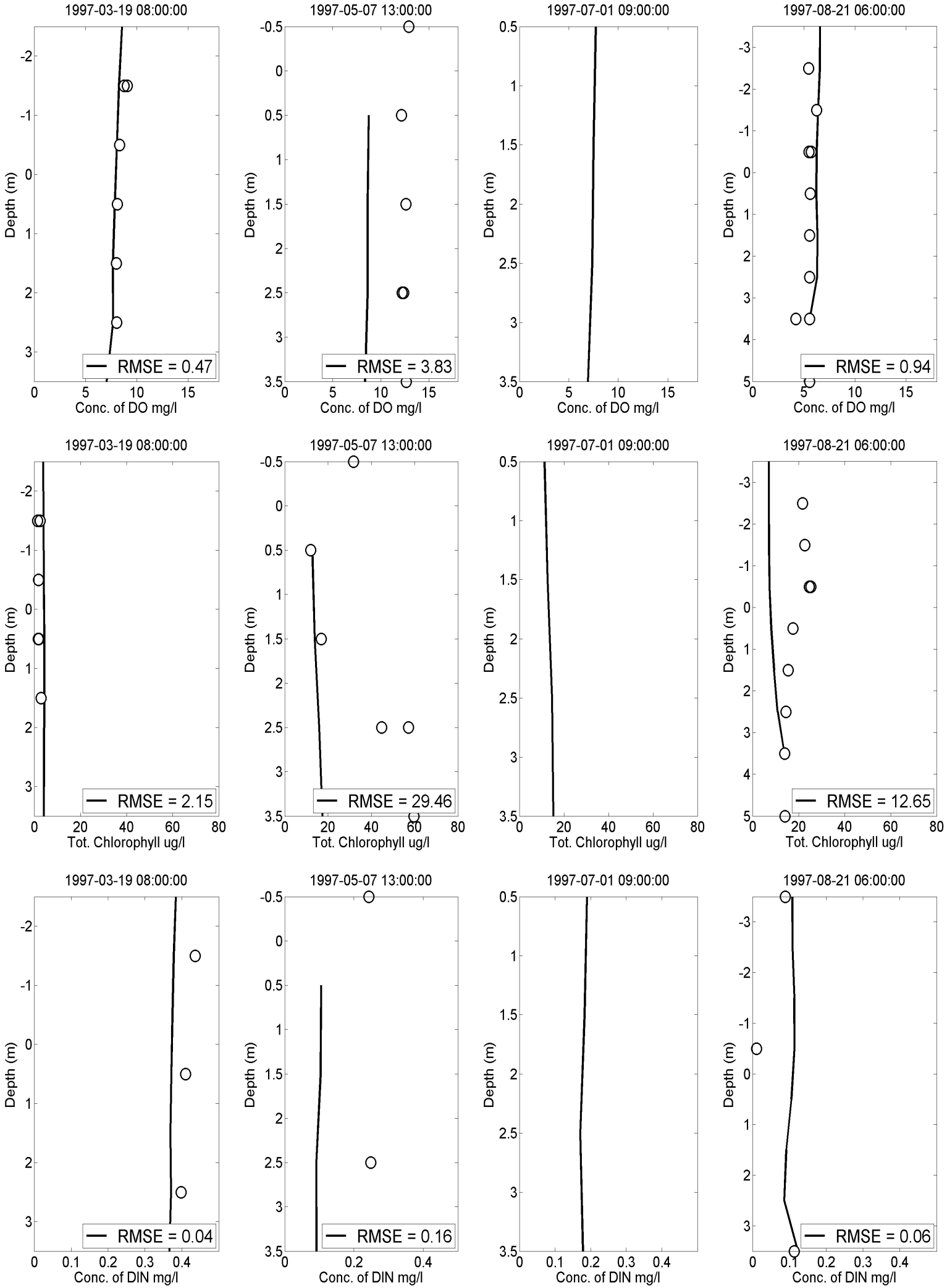

XPI_BI_GAMDFP_base016_000_newGLLVHT.nc, BI-2

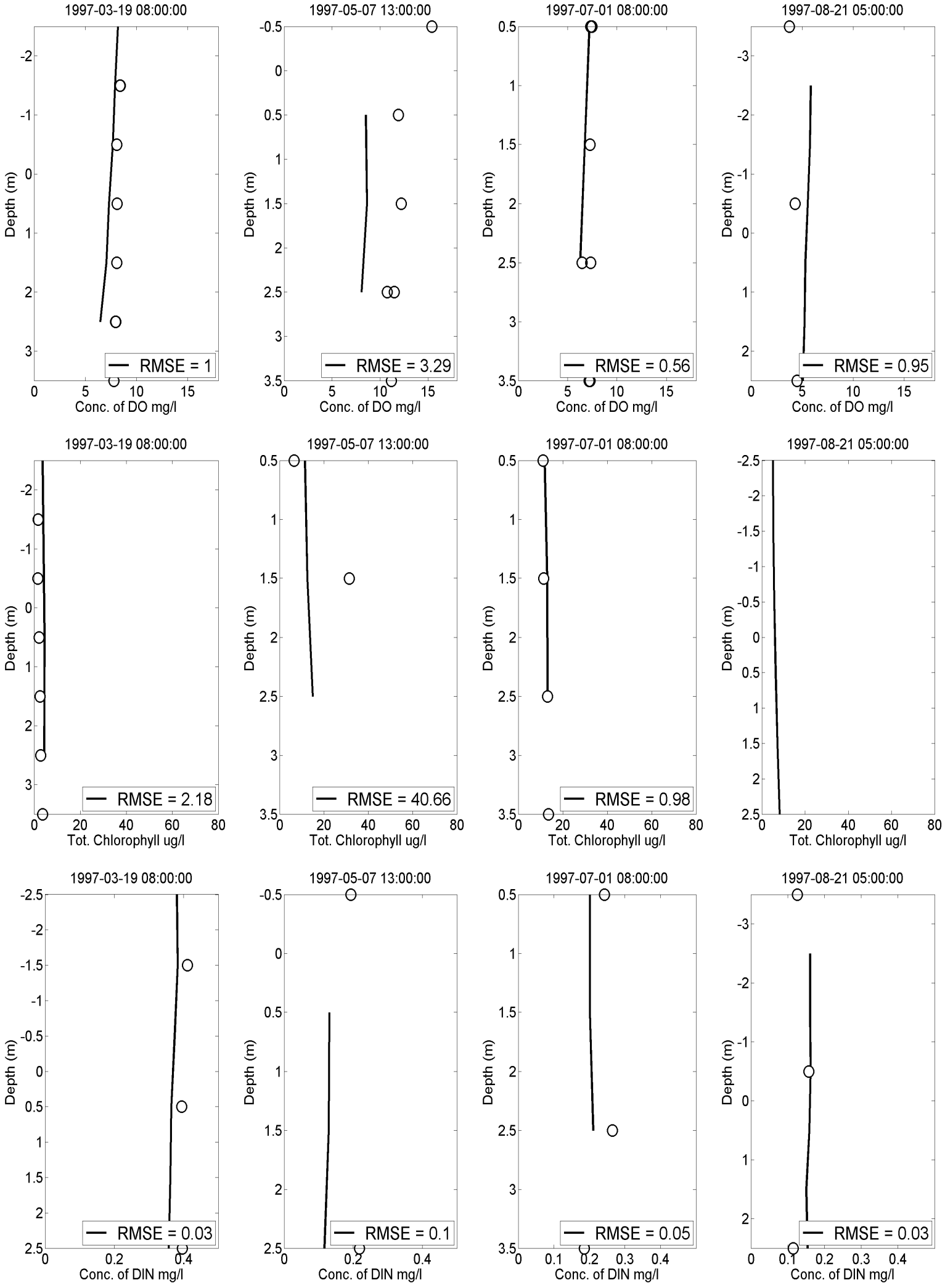
1997-03-19 08:00:00
1997-05-07 13:00:00
1997-07-01 08:00:00
1997-08-21 05:00:00
Depth (m)
Conc. of DO mg/l
RMSE = 1
RMSE = 3.29
RMSE = 0.56
RMSE = 0.95
1997-03-19 08:00:00
1997-05-07 13:00:00
1997-07-01 08:00:00
1997-08-21 05:00:00
Depth (m)
Tot. Chlorophyll ug/l
RMSE = 2.18
RMSE = 40.66
RMSE = 0.98
1997-03-19 08:00:00
1997-05-07 13:00:00
1997-07-01 08:00:00
1997-08-21 05:00:00
Depth (m)
Conc. of DIN mg/l
RMSE = 0.03
RMSE = 0.1
RMSE = 0.05
RMSE = 0.03
XPI_BI_GAMDFP_base016_000_newGLLVHT.nc, BI−1

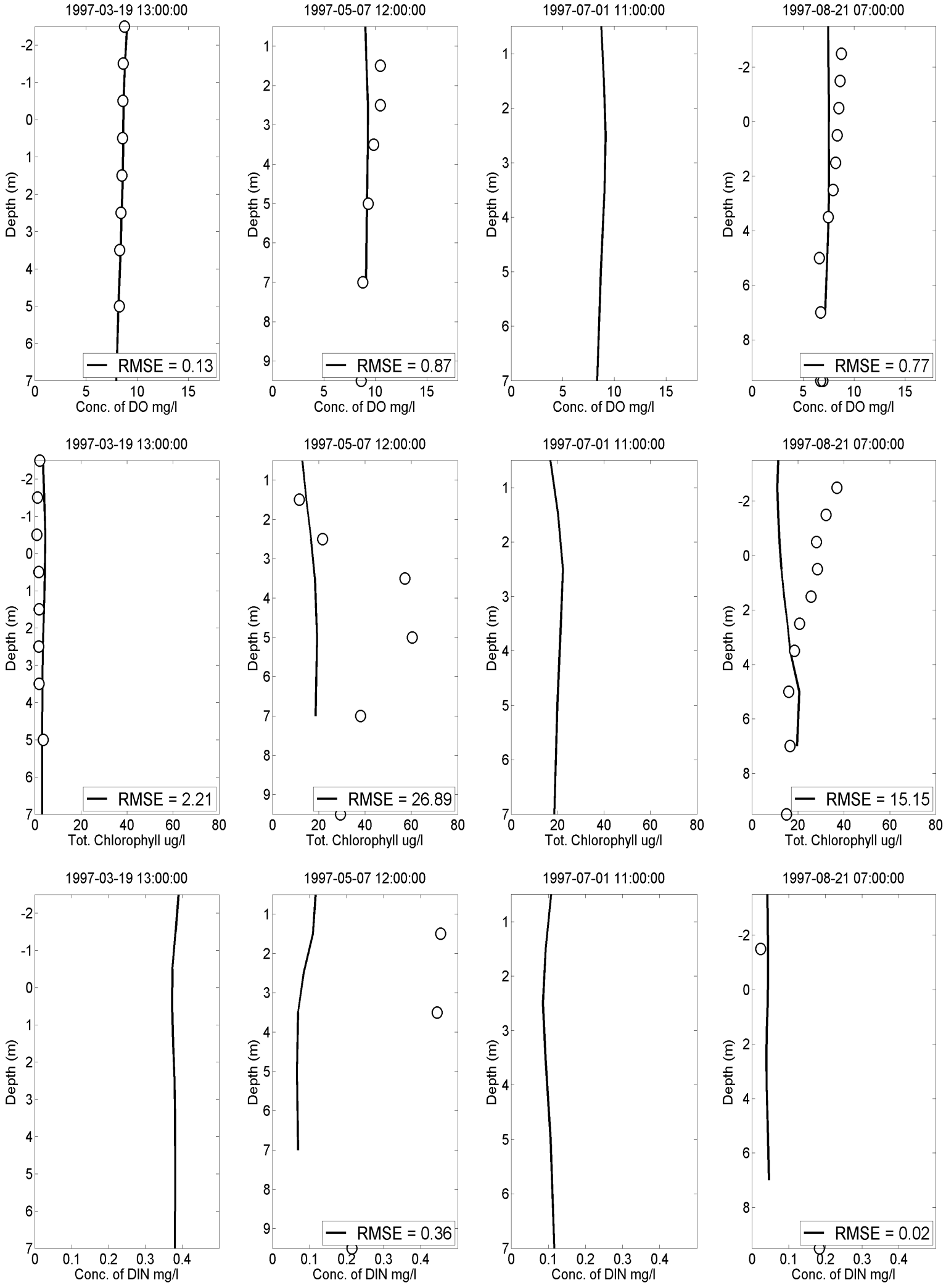
1997-03-19 13:00:00
1997-05-07 12:00:00
1997-07-01 11:00:00
1997-08-21 07:00:00
Depth (m)
Conc. of DO mg/l
RMSE = 0.13
RMSE = 0.87
RMSE = 0.77
1997-03-19 13:00:00
1997-05-07 12:00:00
1997-07-01 11:00:00
1997-08-21 07:00:00
Depth (m)
Tot. Chlorophyll ug/l
RMSE = 2.21
RMSE = 26.89
RMSE = 15.15
1997-03-19 13:00:00
1997-05-07 12:00:00
1997-07-01 11:00:00
1997-08-21 07:00:00
Depth (m)
Conc. of DIN mg/l
RMSE = 0.36
RMSE = 0.02
XPI_BI_GAMDFP_base016_000_newGLLVHT.nc, BA-2

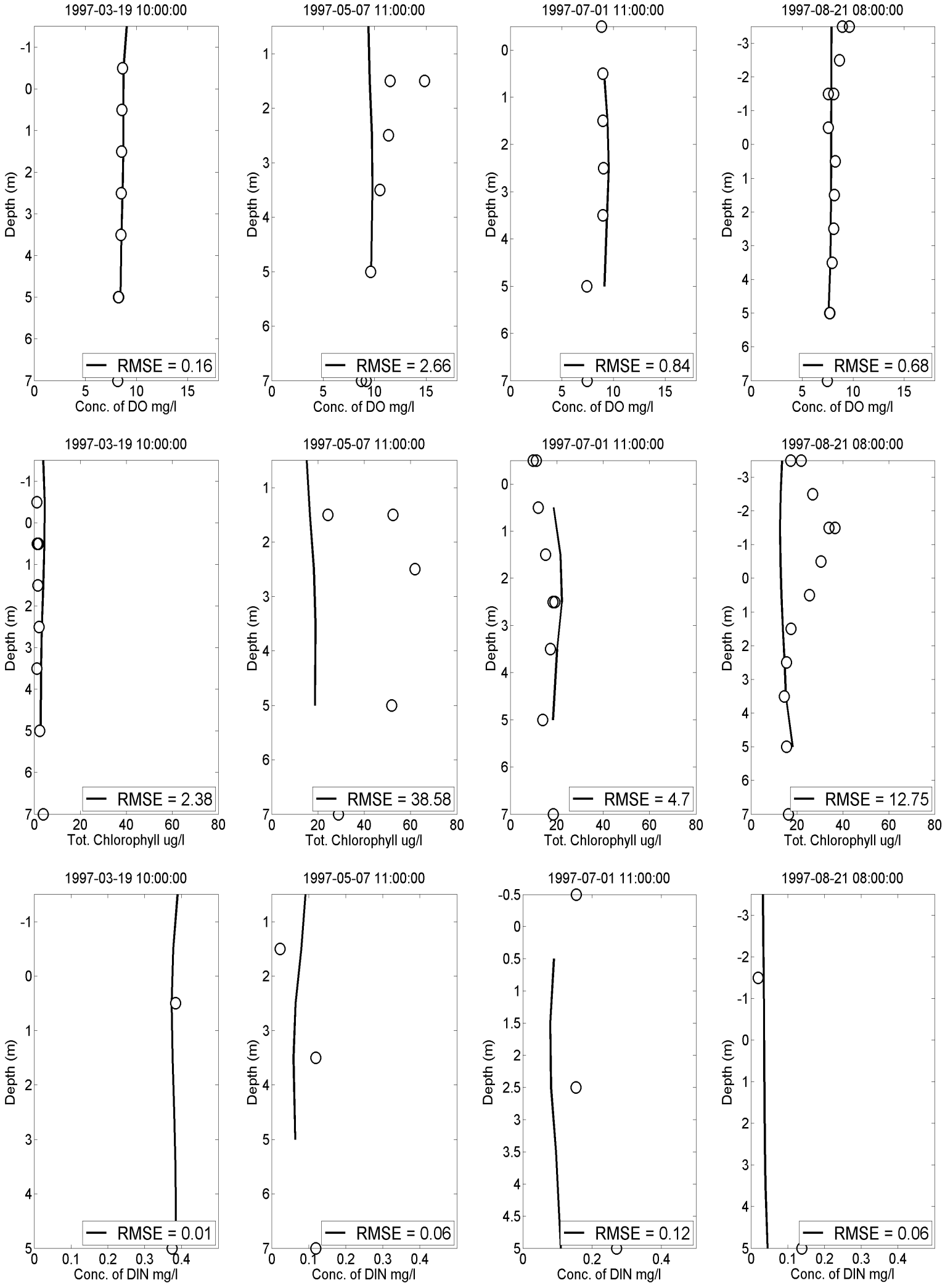
1997-03-19 10:00:00
1997-05-07 11:00:00
1997-07-01 11:00:00
1997-08-21 08:00:00
Depth (m)
Conc. of DO mg/l
RMSE = 0.16
RMSE = 2.66
RMSE = 0.84
RMSE = 0.68
1997-03-19 10:00:00
1997-05-07 11:00:00
1997-07-01 11:00:00
1997-08-21 08:00:00
Depth (m)
Tot. Chlorophyll ug/l
RMSE = 2.38
RMSE = 38.58
RMSE = 4.7
RMSE = 12.75
1997-03-19 10:00:00
1997-05-07 11:00:00
1997-07-01 11:00:00
1997-08-21 08:00:00
Depth (m)
Conc. of DIN mg/l
RMSE = 0.01
RMSE = 0.06
RMSE = 0.12
RMSE = 0.06
XPI_BI_GAMDFP_base016_000_newGLLVHT.nc, BB-2

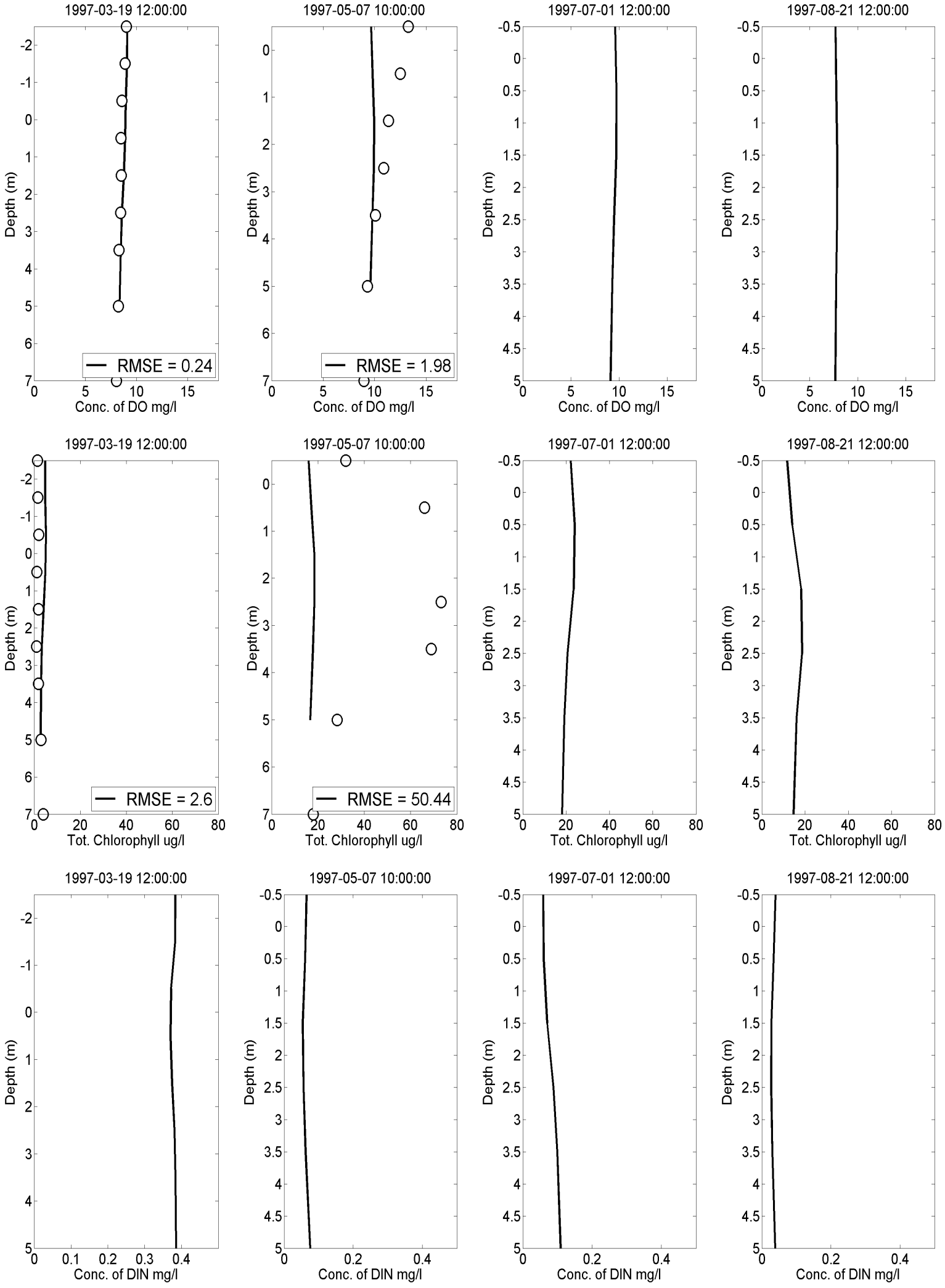
1997-03-19 12:00:00
1997-05-07 10:00:00
1997-07-01 12:00:00
1997-08-21 12:00:00
Depth (m)
RMSE = 0.24
RMSE = 1.98
Conc. of DO mg/l
RMSE = 2.6
RMSE = 50.44
Tot. Chlorophyll ug/l
Conc. of DIN mg/l
XPI_BI_GAMDFP_base016_000_newGLLVHT.nc, LOON1

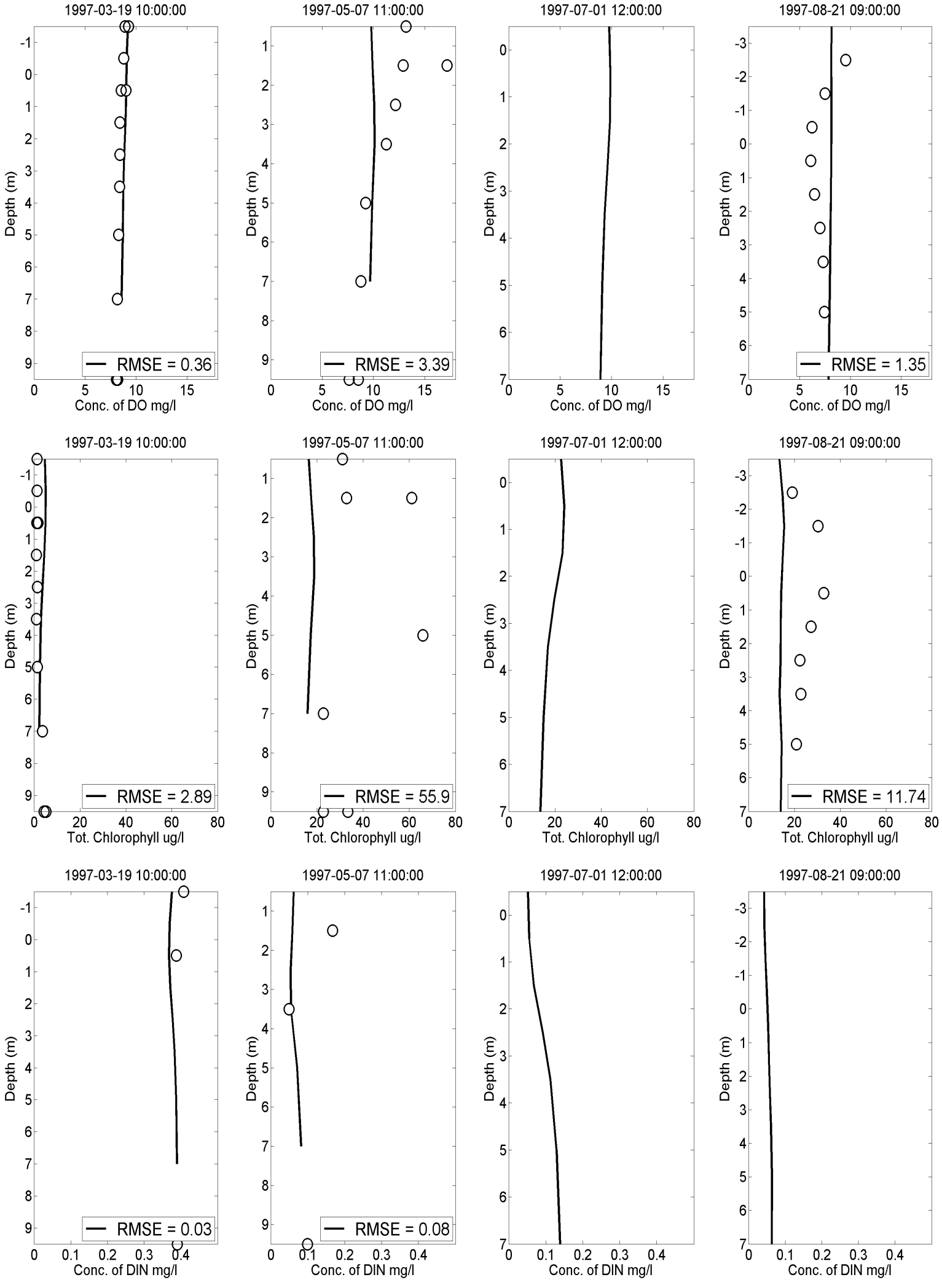

XPI_BI_GAMDFP_base016_000_newGLLVHT.nc, BC−2

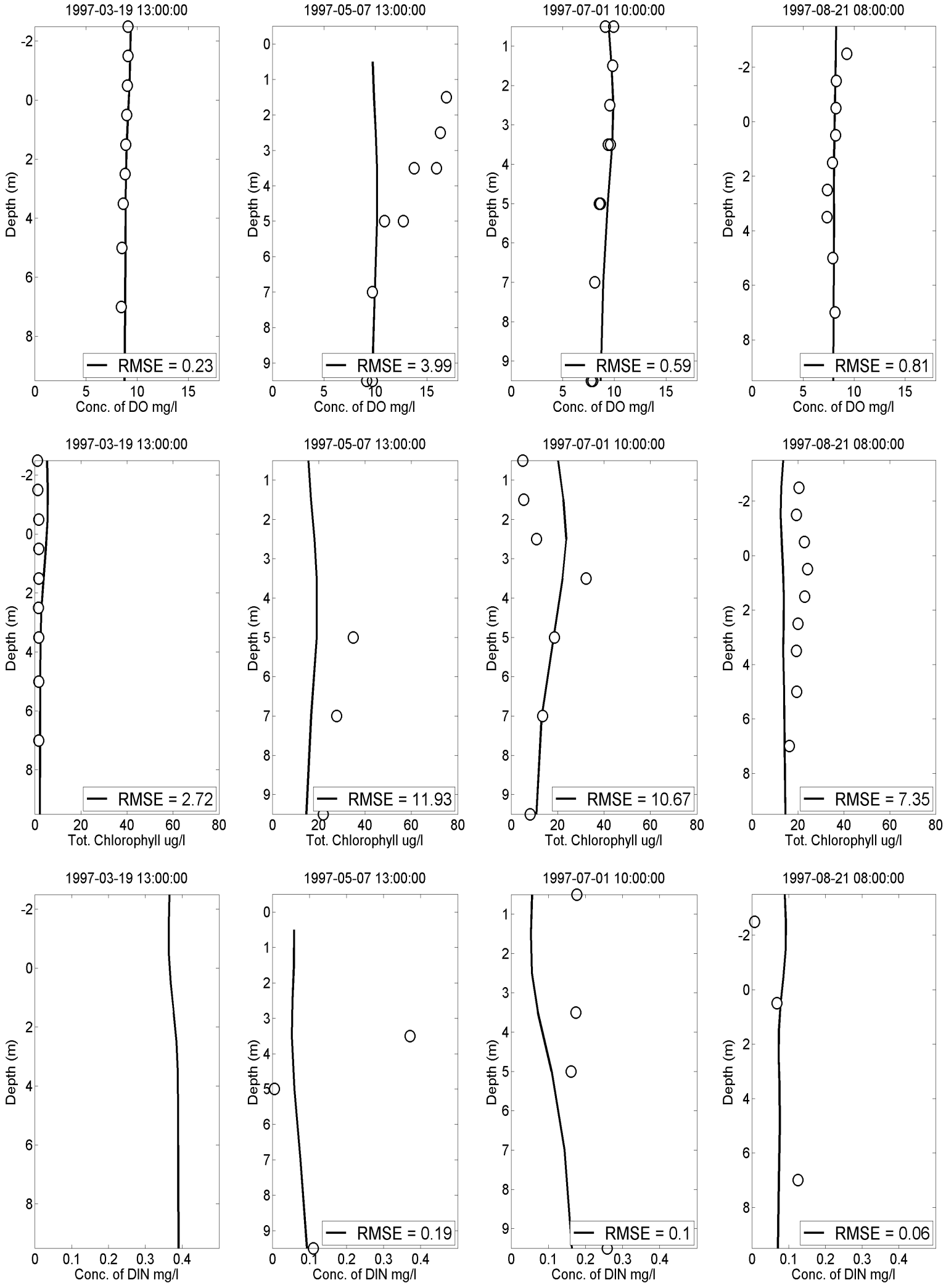
1997-03-19 13:00:00
1997-05-07 13:00:00
1997-07-01 10:00:00
1997-08-21 08:00:00
Depth (m)
RMSE = 0.23
RMSE = 3.99
RMSE = 0.59
RMSE = 0.81
Conc. of DO mg/l
RMSE = 2.72
RMSE = 11.93
RMSE = 10.67
RMSE = 7.35
Tot. Chlorophyll ug/l
RMSE = 0.19
RMSE = 0.1
RMSE = 0.06
Conc. of DIN mg/l
XPI_BI_GAMDFP_base016_000_newGLLVHT.nc, BD-2

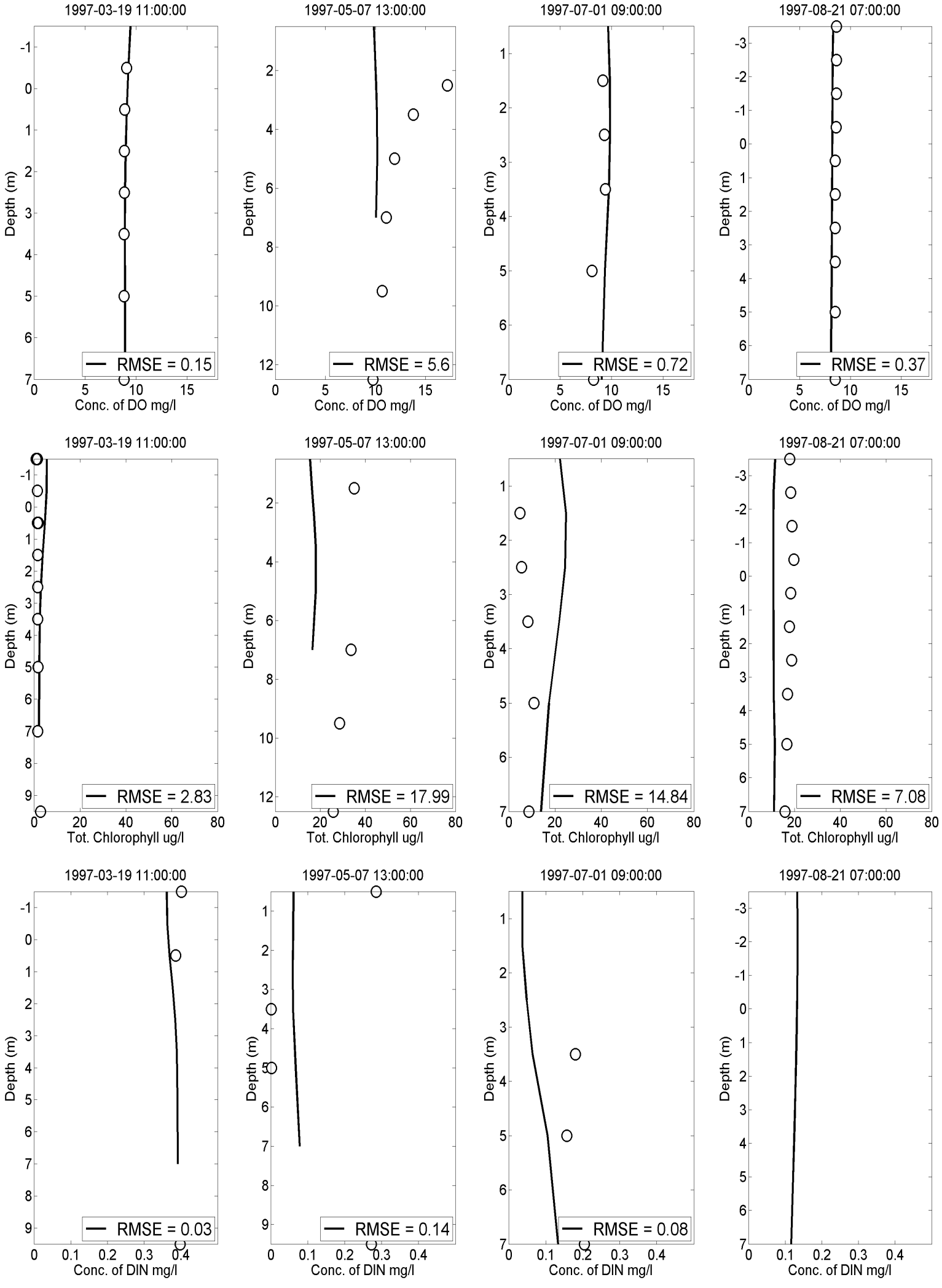
1997-03-19 11:00:00
1997-05-07 13:00:00
1997-07-01 09:00:00
1997-08-21 07:00:00
Depth (m)
RMSE = 0.15
RMSE = 5.6
RMSE = 0.72
RMSE = 0.37
Conc. of DO mg/l
RMSE = 2.83
RMSE = 17.99
RMSE = 14.84
RMSE = 7.08
Tot. Chlorophyll ug/l
RMSE = 0.03
RMSE = 0.14
RMSE = 0.08
Conc. of DIN mg/l
XPI_BI_GAMDFP_base016_000_newGLLVHT.nc, BE−2

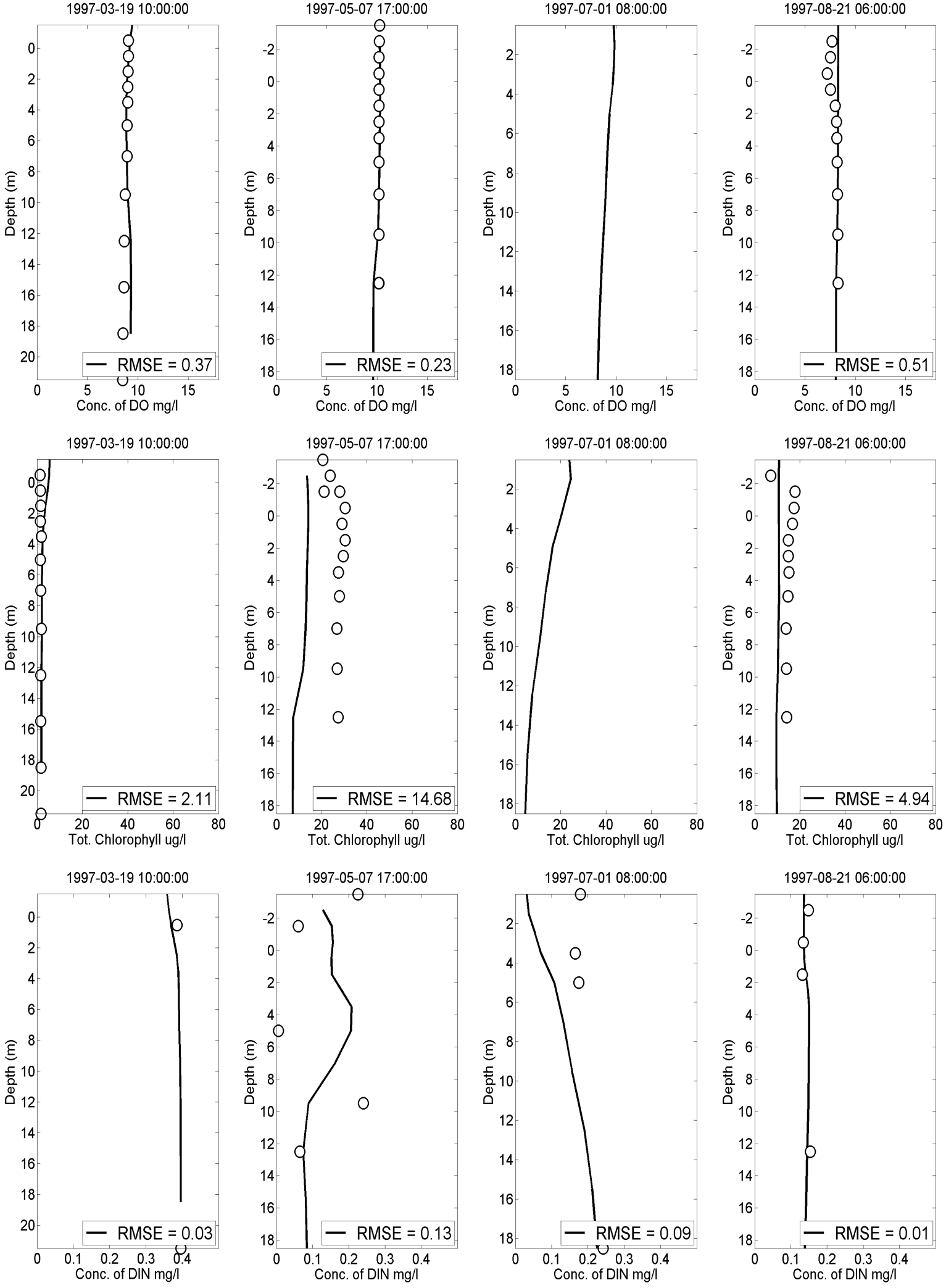

XPI_BI_GAMDFP_base016_000_newGLLVHT.nc, BF-3